Applied Physics Reviews REVIEW pubs.aip.org/aip/are

Advances in ultrafast plasmonics

Cite as: Appl. Phys. Rev. **10**, 021318 (2023); doi: 10.1063/5.0134993
Submitted: 15 November 2022 · Accepted: 1 May 2023 ·
Published Online: 20 June 2023

Alemayehu Nana Koya,[1,2] Marco Romanelli,[3] Joel Kuttruff,[4] Nils Henriksson,[5] Andrei Stefancu,[6] Gustavo Grinblat,[7] Aitor De Andres,[5] Fritz Schnur,[5] Mirko Vanzan,[3] Margherita Marsili,[3,8] Mahfujur Rahaman,[9] Alba Viejo Rodríguez,[10] Tlek Tapani,[5] Haifeng Lin,[5] Bereket Dalga Dana,[11] Jingquan Lin,[12] Grégory Barbillon,[13] Remo Proietti Zaccaria,[14] Daniele Brida,[10] Deep Jariwala,[9] László Veisz,[5] Emiliano Cortés,[6] Stefano Corni,[3,15] Denis Garoli,[14,a)] and Nicolò Maccaferri[5,10,a)]

AFFILIATIONS

[1]GPL Photonics Laboratory, State Key Laboratory of Luminescence and Applications, Changchun Institute of Optics, Fine Mechanics and Physics, Chinese Academy of Sciences, Changchun, Jilin 130033, People's Republic of China
[2]Department of Physics, College of Natural and Computational Sciences, Wolaita Sodo University, P. O. Box 138, Wolaita Sodo, Ethiopia
[3]Department of Chemical Sciences, University of Padova, via Marzolo 1, 35122 Padova, Italy
[4]Department of Physics, University of Konstanz, Universitaetsstrasse 10, 78464 Konstanz, Germany
[5]Department of Physics, Umeå University, Linnaeus väg 24, SE-90187 Umeå, Sweden
[6]Nanoinstitut München, Fakultät für Physik, Ludwig-Maximilians-Universität München, 80539 München, Germany
[7]Departamento de Física, FCEN, IFIBA-CONICET, Universidad de Buenos Aires, C1428EGA Buenos Aires, Argentina
[8]Department of Physics and Astronomy, University of Bologna, 40127 Bologna, Italy
[9]Department of Electrical and Systems Engineering, University of Pennsylvania, Philadelphia, Pennsylvania 19104, USA
[10]Department of Physics and Materials Science, University of Luxembourg, 162a avenue de la Faïencerie, 1511 Luxembourg, Luxembourg
[11]Department of Physics, College of Natural and Computational Sciences, Jinka University, P. O. Box 165, Jinka, Ethiopia
[12]School of Science, Changchun University of Science and Technology, Changchun 130022, China
[13]EPF-Ecole d'Ingénieurs, 55 Avenue du Président Wilson, 94230 Cachan, France
[14]Istituto Italiano di Tecnologia, Via Morego 30, 16163 Genova, Italy
[15]CNR-NANO Istituto Nanoscience, Via Campi, 213/a, 41125 Modena, Italy

[a)]**Authors to whom correspondence should be addressed:** denis.garoli@iit.it and nicolo.maccaferri@umu.se

ABSTRACT

In the past 20 years, we have reached a broad understanding of many light-driven phenomena in nanoscale systems. The temporal dynamics of the excited states are instead quite challenging to explore, and, at the same time, crucial to study for understanding the origin of fundamental physical and chemical processes. In this review, we examine the current state and prospects of ultrafast phenomena driven by plasmons both from a fundamental and applied point of view. This research area is referred to as ultrafast plasmonics and represents an outstanding playground to tailor and control fast optical and electronic processes at the nanoscale, such as ultrafast optical switching, single photon emission, and strong coupling interactions to tailor photochemical reactions. Here, we provide an overview of the field and describe the methodologies to monitor and control nanoscale phenomena with plasmons at ultrafast timescales in terms of both modeling and experimental characterization. Various directions are showcased, among others recent advances in ultrafast plasmon-driven chemistry and multi-functional plasmonics, in which charge, spin, and lattice degrees of freedom are exploited to provide active control of the optical and electronic properties of nanoscale materials. As the focus shifts to the development of practical devices, such as all-optical transistors, we also emphasize new materials and applications in ultrafast plasmonics and highlight recent development in the relativistic realm. The latter is a promising research field with potential applications in fusion research or particle and light sources providing properties such as attosecond duration.

TABLE OF CONTENTS

I. INTRODUCTION: TAMING THE NANOSCALE WITH ULTRAFAST PLASMONICS

Surface plasmons, both propagating and localized (SPPs and LSPs, respectively), are light-driven collective oscillations of free electrons at the interface between a conducting material and the dielectric environment. They are known for their unique feature to concentrate light into deep sub-wavelength volumes well-beyond the diffraction limit, thus providing unprecedented opportunities to control and manipulate light at the nanoscale.[1–12] The knowledge of both the spatial and temporal structure of plasmonic fields can enable a wider understanding and control of light–matter interactions at the nanoscale. This allows, for example, to realize energy-efficient and faster all-optical information processing or develop novel toolboxes for tailored nanoscale photochemistry. In this context, recent advances in coherent light sources, time-resolved optical measurements, nanotechnology, materials science, and nanoengineering, as well as numerical simulations have offered great opportunities to explore the interaction of ultrashort femtosecond (fs) light pulses and plasmonic structures with the highest possible precision and resolution, giving rise to the emergence of *ultrafast plasmonics*.[13–18] This thriving research field aims at the development of compact optical devices that can generate, control, modulate, sense, and process ultrafast optical and electronic excitations at the nanoscale.[19–24] Furthermore, the unique potential of all dielectric photonic materials or 2D materials, such as transition metal dichalcogenides (TMDCs), has lately been recognized by the ultrafast plasmonics community.[25] As a result, in the past decade, the field of ultrafast plasmonics has become a rapidly growing field of study with plenty of opportunities in fundamental science and practical applications.

In general, ultrafast optical techniques are used to explore the physical and chemical phenomena below 1 picosecond (ps) using ultrashort light pulses, which are obtained with mode-locking techniques and can reach attosecond (as) time duration.[26] Such ultrashort pulses allow to measure in real-time the fastest, including sub-fs, processes taking place during chemical reactions as well as collective electron dynamics in atoms, molecules, and solids, allowing precise spectroscopy and nanoscale metrology. Specifically, the interaction of ultrafast pulses with solid-state nanostructures made of metallic materials or heavily doped semiconductors allows us to control the spatial and temporal evolution of the optical near field associated with the excitation of plasmons and their nonlinear optical properties.[27–37] In general, the excitation of a plasmon is one of the fastest processes in condensed matter physics. In fact, the timeframe of the plasmon excitation, usually defined by the inverse of the plasmonic resonance spectral width, is on the order of 100 as.[38] The plasmon relaxation time, the so-called plasmon dephasing process, is also ultrashort, in the 10 fs–1 ps range, where the main physical process involved is the electron–electron (e–e) and electron–surface scattering [see Fig. 1(a)]. Subsequently, energy is dissipated via electron–phonon (e–ph) relaxation (1–100 ps) and phonon–phonon (ph–ph) (100 ps–10 ns) scattering.[39–41] In more detail, during the first 100 fs following Landau damping (exponential decrease as a function of time of charge waves in plasma or a similar environment),[42] the non-thermal distribution of electron–hole pairs decays either through re-emission of photons (radiative decay) or through carrier multiplication caused by e–e interactions (non-radiative decay). During this very short time interval τ_{nth}, the hot carrier distribution is highly non-thermal. The hot carriers, which are electrons having energies larger than those of thermally excited electrons at room temperature, will redistribute their energy by e–e and e–ph scattering processes on a timescale τ_{el} ranging from 10 fs to 100 ps. Finally, the heat is transferred to the surroundings of the metallic structure on a longer timescale τ_{ph} ranging from 100 ps to 10 ns, via thermal conduction.[43] Such ultrafast dynamics make plasmonic nanostructures promising for various applications, especially for enhanced spectroscopy, photocatalysis, information processing, and quantum technologies.

These and many other applications require precise spatial and temporal control over the optical responses of nanostructured materials on both the fs and nm scales. To meet this requirement and to have a detailed insight into the physical mechanisms involved, a number of theoretical models,[44,45] in particular finite element method (FEM), finite-difference time domain (FDTD) method and time-dependent density functional theory (TDDFT), have been developed.[46–52] As well, experimental techniques, such as time-resolved photo-emission electron microscopy (TR-PEEM) or photo-induced near-field electron microscopy (PINEM), both fulfilling spatial and temporal resolution requirements,[53–60] have been widely employed to investigate, and even shape, the ultrafast optical near-field dynamics of plasmonic nanostructures.[61–63] From an experimental point of view, it is also common to employ optical pump–probe schemes, including x-ray free electron lasers (XFELs), to study the ultrafast charge and spin dynamics in plasmonic nanostructures, in particular those displaying magnetic properties.[64–69] Full-field-resolved detection of the temporal response of plasmonic nanostructures, as well as their nonlinear optical properties, in the mid-infrared regime has also been carried out recently by employing time-resolved spectroscopy implementing electro-optical sampling (EOS) detection scheme.[70] Together, recent efforts in active manipulation of the optical response of nanostructured materials, rational design of the nanostructures and nanoscale engineering of their environment, as well as material composition, offer an exciting opportunity to develop ultrafast, all-optically reconfigurable nanophotonic devices.[71–76]

As a result of the aforementioned developments in the field, this review showcases the most recent and important theoretical and experimental advances in ultrafast plasmonics, and it is structured as

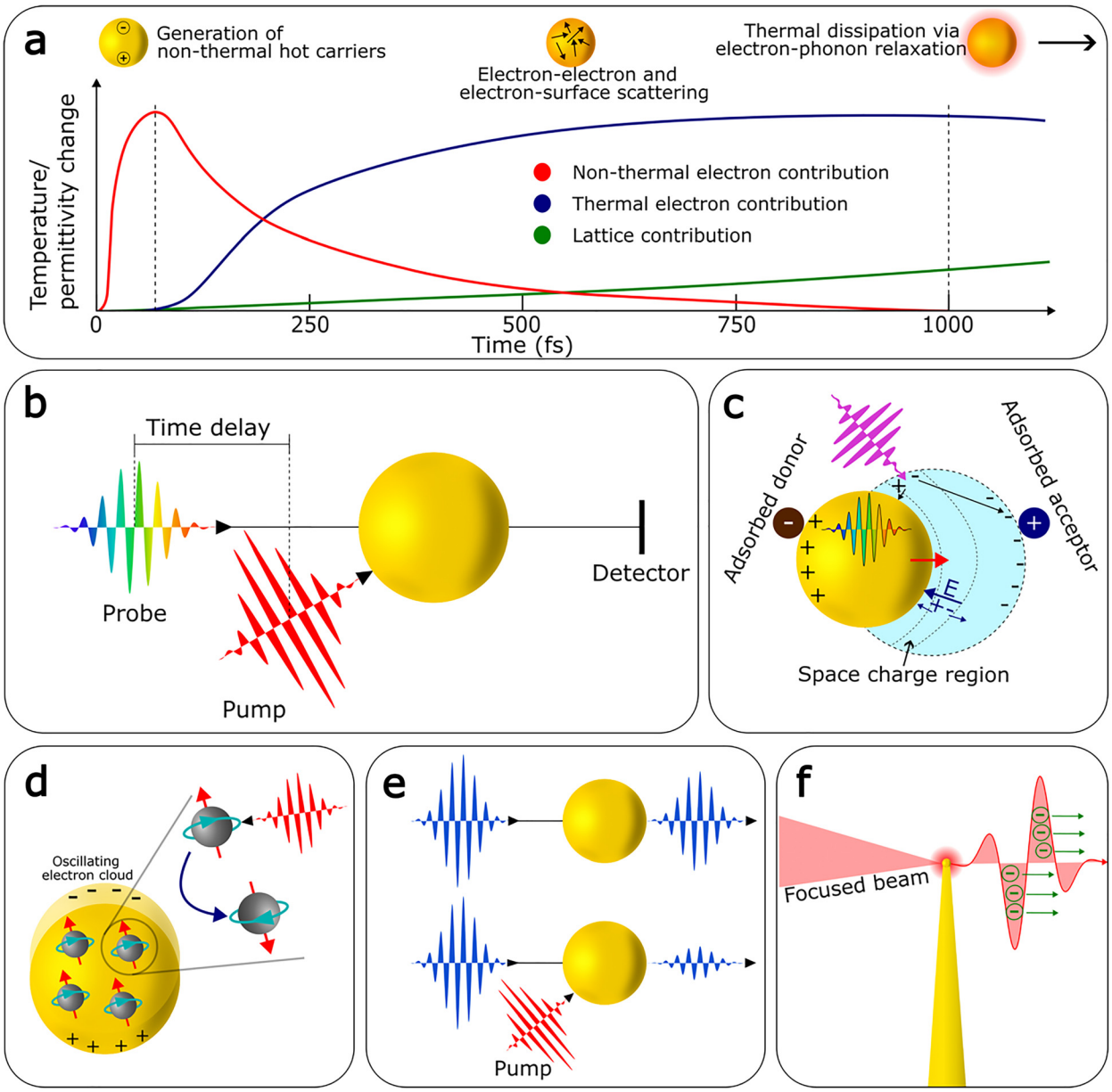

FIG. 1. Conceptual illustrations of the different sections of the review. (a) Illustration of the timescales involving carrier relaxation processes following LSP excitation (the same concept can be applied also to SPPs). First, non-thermal hot carriers are generated (1–100 fs). Afterwards, their energy dissipates into thermal energy via electron–electron, electron–surface, and electron–phonon scattering, causing a rise in electron and lattice temperatures. The change in electronic temperature reflects in a change of the permittivity of the structure. (b) In Sec. II, we give an overview of the most recent developments in modeling and experimental characterization of ultrafast plasmon dynamics, for instance by performing optical pump–probe experiments. (c) Section III is dedicated to plasmon-driven chemistry. One of the main applications discussed is plasmon-enhanced photocatalysis. (d) In Sec. IV, we introduce the reader to active ultrafast plasmonics, where materials possessing different properties (for instance, both plasmonic and magnetic, the so-called magnetoplasmonic materials) are used to control spin dynamics at the nanoscale. (e) Section V is dedicated to the most common applications of ultrafast plasmonics, in particular plasmon-driven switching of optical signals. (f) Section VI focuses on the rising field of relativistic plasmonics, where high intensity ultrashort light pulses can excite strong plasma oscillations in metallic nano-tips resulting in matter ionization, and a consequent coherent light-driven acceleration of electrons.

follows. Section I gives a general introduction to the topic, followed by Sec. II, where we provide a broad and updated overview of modeling and experimental characterization techniques used in the field of ultrafast plasmonics. These techniques can be applied to a vast range of out-of-equilibrium timescales, from the attosecond to the microsecond timescale. We then continue with Sec. III, which focuses on the challenges and opportunities of ultrafast plasmon-driven chemistry with particular focus on plasmon-enhanced photocatalysis on timescales

spanning from the ps to the μs timescale. Section IV highlights the most recent advances in ultrafast multi-functional plasmonics, providing insights on how to leverage on charge, spin, and lattice degrees of freedom for active and ultrafast control of optical and electronic properties at the nanoscale, by utilizing either plasmon or phonon polaritons, on timescales of the order of 0.1–100 ps. Section V provides insights into new materials and the most common applications of ultrafast plasmonics, in particular on all-optical switching (AOS) on the sub-ps timescale. Finally, Sec. VI gives a brief overview of the raising field of relativistic plasmonics, where laser intensity reaches 10^{11}–10^{13} W/cm^2. For sake of clarity, a schematic overview of the review main contents is shown in Figs. 1(b)–1(f). We conclude by giving our personal vision on the prospects of the several research areas in ultrafast plasmonics covered in this review. Despite our best attempt to report accurately the most important advances in the field and do justice to all its novel developments and its diversity, the research area is expanding so fast that there remains great latitude in deciding what to include in this review, which in turn means that some areas might not be adequately represented here. However, we feel that the sections that form this review, each written by experts in the field and addressing a specific subject, provide an accurate snapshot of where this research field stands today. Correspondingly, it should act as a valuable reference point and guideline for emerging research directions in ultrafast plasmonics, as well as illustrate the directions this research field might take in the foreseeable future.

II. EXPERIMENTAL CHARACTERIZATION AND MODELING OF ULTRAFAST PLASMON DYNAMICS

Metallic nanostructures featuring both SPPs and LSPs are highly promising because of their ultrafast dynamics and potential to confine the electromagnetic (EM) field in sub-nanometric spatial regions.[77–80] Understanding and controlling plasmons are crucial for advancements in a wide range of applications, including sensing, spectroscopy, photocatalysis, nanoscale metrology, ultrafast computation, and renewable energy.[81–87] However, different lengths and time scales involved make the study of these effects rather complex. To fully understand the physics underlying ultrafast plasmonic processes, multiple experimental and modeling approaches have been developed over the last decade, each one providing key insights into the general picture. In this section, we provide a concise yet comprehensive overview of these experimental and theoretical methodologies.

A. Experimental techniques

The ability to image plasmon near-fields, that is EM fields between 1 and 10 nm from the plasmonic structures surface oscillating with the period of few light cycles, is crucial to guide future directions in ultrafast plasmonics research. Such techniques require both sub-cycle time and sub-wavelength spatial resolution, spanning the so-called nano–femto scale. One widely used approach is time-resolved photoemission electron microscopy (TR-PEEM), which has been successfully applied to image both SPPs and LSPs.[88–90] In such experiments, a short light pulse (called pump) excites plasmons in a nanostructured material. A time-delayed phase-stable duplicate of the first pulse then interferes with the plasmons and promotes photoelectrons to the vacuum through a multi-photon photo-emission process. Electrons are subsequently collected using electron objective/projective and an electron sensitive camera in a low-energy electron microscope, providing the necessary nm spatial resolution. In the past, this technique has been applied to image the dynamics of both LSPs and SPPs in metallic nanostructures,[91–97] providing also a way to understand more deeply the most important factors in plasmon damping.[98] Furthermore, TR-PEEM has been used to study nanofocusing of SPPs,[99] with many potential applications including heat-assisted magnetic recording,[100] or plasmon-induced electron emission.[101,102] Recently, TR-PEEM was advanced by Davis *et al.* to include full vectorial mapping of the plasmonic near-field,[103] as shown in Fig. 2(a).

In their experiments, a light pulse excites SPPs from grooves in the sample that lead to non-trivial plasmonic fields. The plasmons then interfere with the probe pulse that arrives on the sample with an adjustable time delay and frees photoelectrons into vacuum. In contrast to previous approaches, they perform a set of two independent measurements with orthogonal polarization of the probe pulses. This allows to retrieve the full vectorial composition of the plasmonic field, making possible the demonstration of plasmonic spin-momentum locking, as well as excitation of plasmonic skyrmions. The proposed vector microscopy promises the exploration of exciting phenomena associated with spin-photon coupling and orbital angular momentum (OAM) physics. Noteworthy, PEEM can be used not only for imaging plasmon dynamics, but also to study charge carrier dynamics on semiconductor surfaces.[106–109] Hence, we foresee that TR-PEEM will be instrumental to unravel plasmon-generated hot-carrier dynamics on surfaces of novel plasmonic media (e.g., heavily doped semiconductors) beyond the traditional noble metals.

Another efficient approach for plasmon imaging is the ultrafast transmission electron microscopy (U-TEM).[110–113] In this case, the sample is excited by a light pulse from a fs-laser source, and probed by a time-delayed electron pulse generated by photo-emission inside an electron microscope using the same laser source. While using TEM nm spatial resolution is readily available, however, creating short electron pulses and keeping them from spreading in time before reaching the sample is very challenging due to their intrinsic dispersion in vacuum.[114] For this reason, traditionally radio frequency cavities are employed for the compression of electron pulses, but the need for active synchronization leads to unavoidable timing-jitter of the compressed pulses.[115–118] A way to circumvent active synchronization is to use the cycles of laser-generated THz-fields for electron compression in an all-optical scheme.[119–122] Such THz pulses can be generated from the same laser source that is employed for photo-emission, giving possibility to suppress timing jitter to sub-fs timescale.[123] U-TEM has been successfully used to study acousto-optic dynamics in plasmonic nanoparticles,[124] and polaritonic strain waves in MoS_2 nanoflakes propagating at approximately the speed of sound (7 nm/ps).[125] Nevertheless, to date electron pulses inside a U-TEM are still around two orders of magnitude too long to measure plasmon charge oscillations directly. However, when interacting with the sample, the electrons inside an electron pulse can absorb a photoexcited plasmon or excite a second plasmon through stimulated electron energy loss in a quantum-coherent fashion, i.e., considering the wave nature of the electron. Hence, via post selection of only the transmitted electrons that have gained/lost energy, the plasmonic near-field can be imaged using the photon-induced near-field electron microscopy (PINEM) technique. Following the pioneering work of Barwick *et al.*,[53] PINEM has been used for near-field imaging of many different nanostructures, including metallic nanoparticles[126,127] and nanoantennas.[128–130]

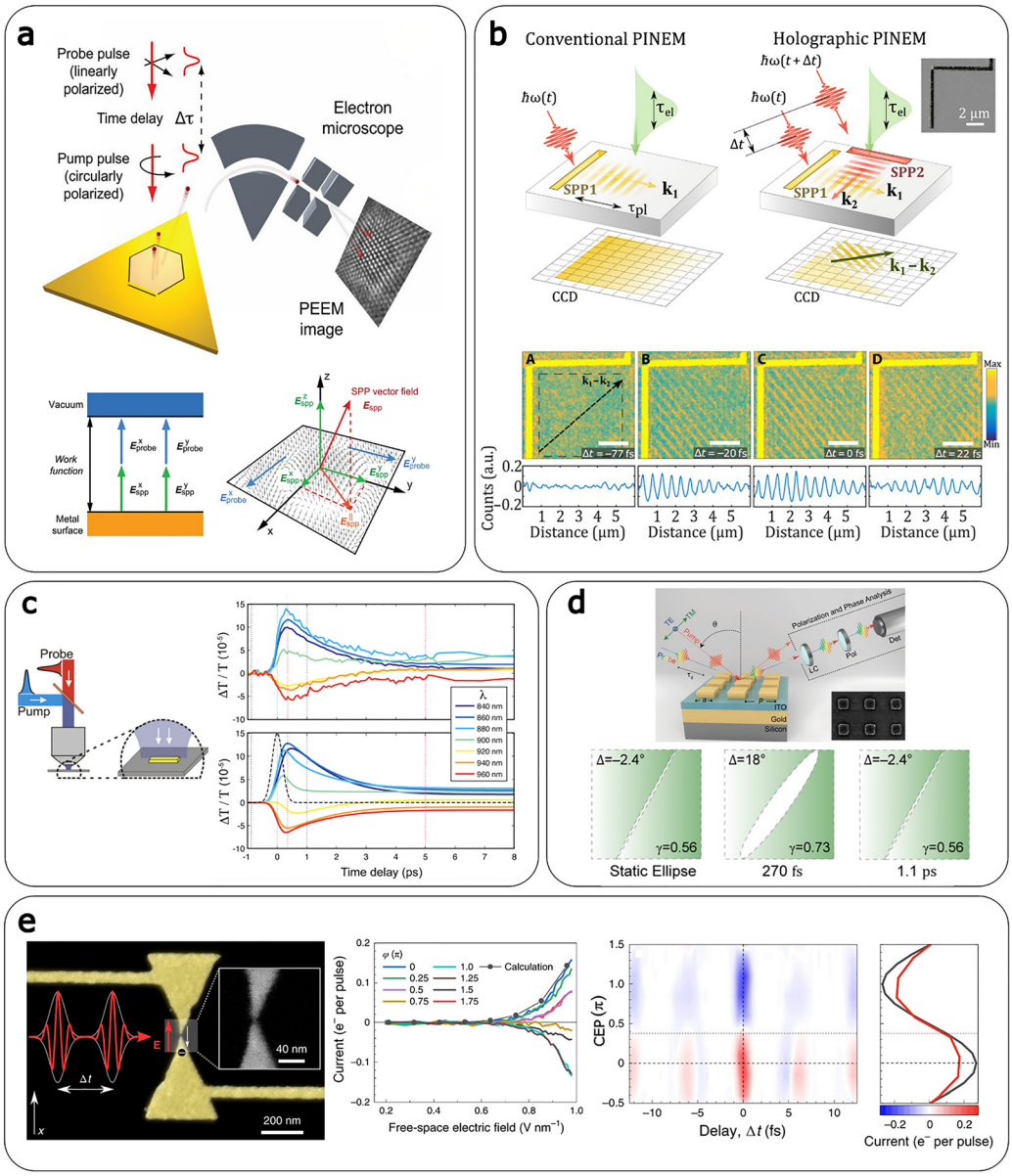

FIG. 2. Different experimental methodologies to study and control ultrafast optical and electronic dynamics in plasmonic architectures. (a) Ultrafast time-resolved vector microscopy of plasmonic fields using photo-emission electron microscopy (PEEM). Two-photon-PEEM process is used to obtain vector and time information from surface plasmons. Vectorial components are obtained via the two orthogonal probe fields during two separate measurements, which allows imaging of plasmonic skyrmions in three dimensions. Reproduced with permission from Davis *et al.*, Science **368**, 386 (2020). Copyright 2020 AAAS.[103] (b) Holographic photon-induced near-field electron microscopy (PINEM). In contrast to conventional PINEM that images the time-averaged propagating SP envelope, two propagating SPs form a standing wave that can be imaged as a periodic modulation of PINEM intensity. Holographic images obtained at different delays between the excited SPs are used to determine their phase and group velocities.[57] Reproduced with permission from Madan *et al.*, Sci. Adv. **5**, eaav8358 (2019); Copyright 2019 Author(s), licensed under a Creative Commons Attribution (CC BY) license. (c) Pump–probe spectroscopy employed to study the dynamics of single gold nanoantennas. Experimental differential transmission (upper) of the plasmonic dynamics when pumped by a 780 nm wavelength laser is approximated using numerical simulations based on the three-temperature model (3TM) (lower). The colors represent different probe wavelengths.[104] Reproduced with permission from Zavelani-Rossi *et al.*, ACS Photonics **2**, 521 (2015). Copyright 2015 American Chemical Society. (d) Ultrafast control of phase and polarization. Schematic of a plasmonic crystal consisting of gold nanoparticles on a layer of indium tin oxide (ITO), placed on a gold film. The pump–probe spectroscopy setup is used to estimate the phase and polarization of the crystal, estimated from the reflected light using a liquid crystal phase retarder (LC) and a polarizer (POL), respectively. The polarization dynamics (lower) are measured at different time delays when the crystal is excited by an on-resonance pump.[105] Reproduced with permission from Taghinejad *et al.*, Nano Lett. **18**, 5544 (2018). Copyright 2018 American Chemical Society. (e) Ultrafast currents in a nanocircuit controlled by single-cycle light pulses. The carrier-envelope phase (CEP) of the biasing pulses can be tuned to control the transfer of individual electrons in the nanocircuit. Interferometric current autocorrelations via two driving pulses allow to study electron transport at sub-fs timescales.[48] Reproduced with permission from Ludwig *et al.*, Nat. Phys. **16**, 341 (2019). Copyright 2019 Springer Nature.

Furthermore, the coherent interaction with the light field in PINEM was used to study and prepare tailored quantum states of free-electrons.[60,131–139] Although sub-optical-cycle resolution is not readily available in current PINEM setups, which prevents at the moment the measurement of plasmonic fields directly in space and time, plasmon interference in PINEM can be used to reveal properties of plasmon propagation and decay.[140] Recently, this direction was followed by Madan *et al.*, who used holographic plasmon imaging to quantitatively measure phase and group velocity of SPPs with as and nm resolution [see Fig. 2(b)].[57] In contrast to conventional PINEM, where only one optical pump pulse is used, they employed two pump pulses, of which each launches a SPP [see upper panel in Fig. 2(b)]. By varying the time delay between the pump pulses, they could control the plasmon interference pattern, allowing to measure the corresponding SPP propagation parameters [see lower panel in Fig. 2(b)]. Finally, phase-resolved sampling of plasmonic fields using PINEM with as electron pulse trains has just been demonstrated, allowing for even higher temporal resolution and superior sensitivity, making such an approach promising for future studies of photonic nanostructures at ultimate dimensions in space and time.[141–144]

Beyond the possibility to generate coherent charge oscillations, plasmon-generated hot charge carriers represent a rich source of localized energy that can be harvested, for instance, either in photovoltaic devices or supplied to adsorbed molecules to drive chemical reactions. This change of electronic band-population induced by plasmon decay leads to transient changes in the optical properties of a material that can be tracked using short light pulses. To this end, optical pump–probe spectroscopy is ideally suited to study the redistribution of electronic energy on sub-ps time scales. In such experiments, a light pulse excites a sample (pump), and a second, time-delayed pulse is used to measure changes in the optical response of the system (probe). Due to stroboscopic sampling, the time-resolution in pump–probe experiment is not limited by the response time of the detector, but rather determined by the duration of the optical pulses that are used.[145] The need to resonantly excite plasmons at different frequencies and detect broad spectral signatures of transient states calls not only for the shortest durations but also for broad tunability of pump and probe pulses. In this context, the development and commercial availability of novel laser sources and, in particular, next-generation optical parametric amplifiers (OPAs) has greatly accelerated research in the field in the last few decades, as they can provide ultra-tunable pulses with few-fs time durations.[146,147] Spectroscopy systems based on Ti:Sapphire technology are well established nowadays in many labs, as short pulses below 10 fs can be directly obtained from the laser oscillator.[148] Furthermore, Ti:Sapphire-driven OPA systems have been demonstrated with carrier frequencies ranging from ultraviolet to mid- and far-infrared.[149–151] More recent efforts also focused on developing alternative systems based on ytterbium laser sources, as they can provide excellent stability and tunable repetition rate up to several hundreds of kHz.[152]

In a pioneering study by Sun *et al.*, pump–probe experiments were performed to study the dynamics of hot electrons in thin gold films.[153] Since then, many works followed focusing on the nonlinear optical response of metals[154] and, in particular, plasmonic nanostructures.[130–137] Zavelani-Rossi *et al.* have used pump–probe spectroscopy to investigate plasmon detuning and other physical mechanisms dominating the nonlinear plasmon dynamics in individual plasmonic antennas [Fig. 2(c)],[104] and more recently, they have introduced novel concepts for ultrafast active control of the optical response of plasmonic metasurfaces[49,76] and metagratings.[74] In this context, it is worth mentioning the pioneering work by Taghinejad *et al.*, who demonstrated the active ultrafast modulation of the phase, polarization, and amplitude of light through the nonlinear modification of the optical response of a plasmonic crystal that supports subradiant, high Q, and polarization-selective resonance modes [Fig. 2(d)].[105] Noteworthy, the time-resolution of the pump–probe experiments can be pushed even into the sub-fs timescale by employing high harmonic generation (HHG).[155–158] Combining extreme ultraviolet attosecond pulses with near infrared pumping, Niedermayr *et al.* recently studied nonequilibrium optical properties of aluminum, revealing few-fs dynamics of hot charge carriers relevant for ultrafast plasmonics applications in the UV.[159] By leveraging on nm-gap size in bow-tie plasmonic nanocircuits, Ludwig *et al.* have shown sub-fs resolution by tuning the interference of carrier-envelope-phase-stable single-cycle infrared pulses [see Fig. 2(e)].[48,160] Interferometric correlation measurements showed control of the transfer of individual electrons between two metallic nanocontacts, which can be further controlled by applying an external dc bias over the gap.[161] It is worth to highlight here that all these studies open new avenues of investigating plasmonic integrated surfaces for optical logics operating at PHz speed frequencies.

B. Theoretical models and methods

In parallel with the development of advanced technologies to implement complex time-resolved experiments to access the ultrafast dynamics in plasmonic systems, theory has been instrumental in corroborating experimental findings and suggesting novel plasmon-related phenomena that were subsequently probed experimentally. Most of the models presented so far can be mainly grouped into three broad categories: (i) those studies that employ a classical continuum-based description of the nanoparticle (NP), whose optical response is dictated by its shape and dielectric function; (ii) those that describe the NP using jellium model, where the electronic wavefunction explicitly include only valence electrons, while the nuclei and the core electrons are considered as a homogeneous frozen background; and (iii) those that include explicitly the nuclear and electronic structure using *ab initio* techniques. Classical electrodynamics-based methods, such as FDTD[162] and Time-Domain Boundary-Element-Method (TD-BEM)[49,163–165] have been used to investigate the real-time dynamics of plasmonic materials [see Figs. 3(a) and 3(b)], even their interaction with nearby molecules.[166,167] Building on such descriptions, classical models based on modified bulk dielectric functions in combination with kinetics rate equations[168–170] have been extensively employed to interpret pump-induced ultrafast nonlinear responses in plasmonic systems.[104,171]

In particular, the three-temperature model (3TM) was used.[104,154,172] This rate equation model describes the energetic relaxation process of the nanostructure in terms of three degrees of freedom, i.e., the density of excess energy stored in the hot carriers population created by plasmon decay, the thermalized electron gas temperature and the lattice temperature.[173,174] This approach has been successfully applied to simulate the ultrafast transient absorption spectra of gold-nanoparticles,[165] making it possible to rationalize the findings of state-of-the-art experimental data. Moreover, following the preliminary

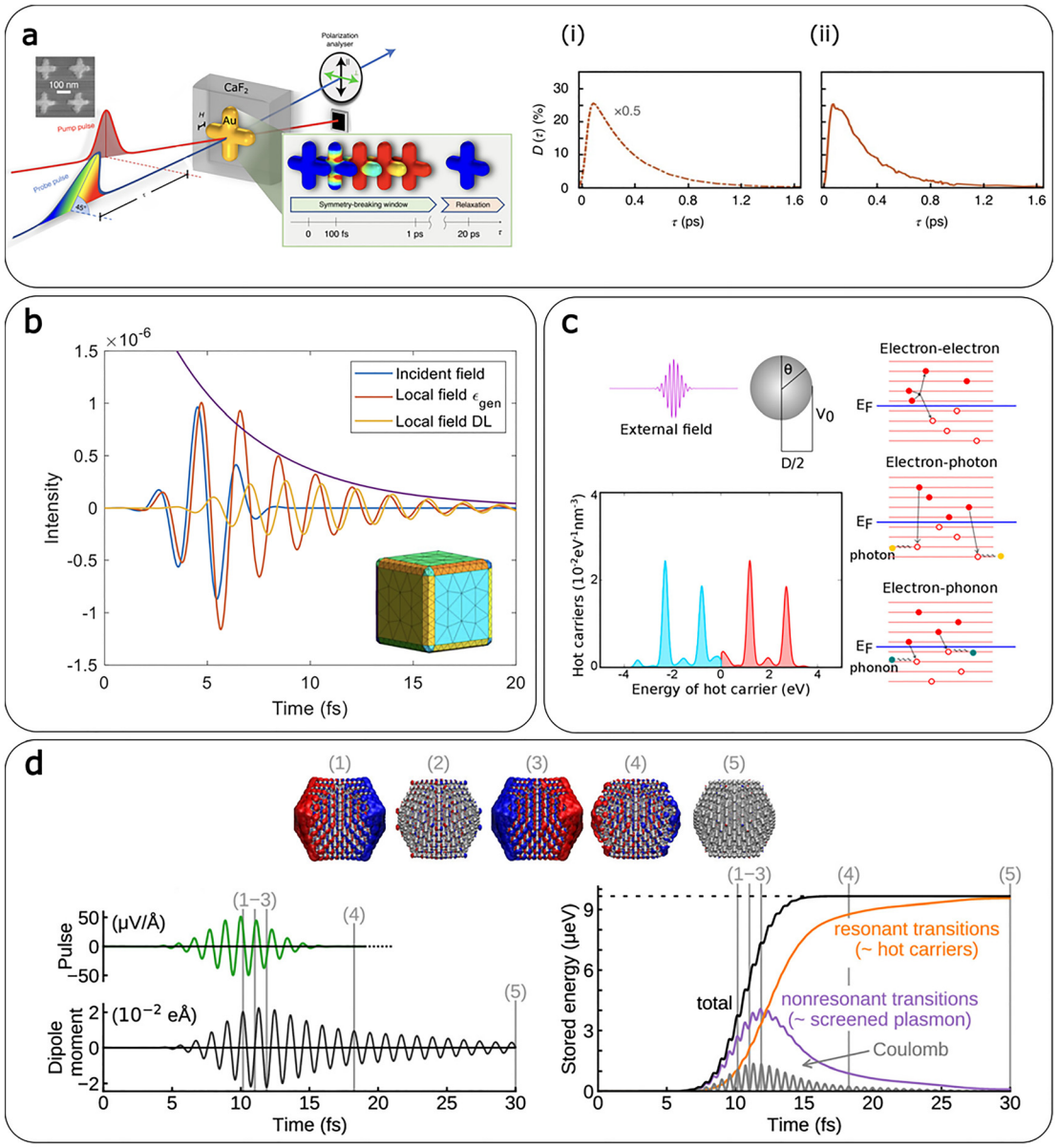

FIG. 3. Theoretical approaches aimed at investigating plasmon dynamics and plasmon-induced effects. (a) Sub-ps broadband dichroism recovery achieved utilizing spatial inhomogeneities of photogenerated hot carriers in a symmetric gold nanostructure. Schematic of the pump–probe spectroscopy used to measure the broadband dichroism dynamics of the structure. The inset is an illustration of the inhomogeneous change in imaginary permittivity at different time delays. The dichroic ratio is (i) estimated using a numerical model based on the FEM and a spatially dependent 3TM and (ii) determined from experimental dynamic measurements of polarization of the structure.[49] Reproduced with permission from Schirato *et al.*, Nat. Photonics **14**, 723 (2020). Copyright 2020 Springer Nature. (b) Time evolution of the incident and local fields nearby a gold nanocube featuring a side length of 10 nm whose time-resolved response is obtained by TD-BEM. The plasmon-induced local field is computed assuming two different dielectric function models, namely, Drude-Lorentz-like (yellow curve) and the generic dielectric function approach (orange curve). The excitation pulse has a frequency of 2.07 eV and it is represented by a sinusoidal wave modulated by a Gaussian envelope.[164] Reproduced with permission from Dall'Osto *et al.*, J. Chem. Phys. **153**, 184114 (2020). Copyright 2020 AIP Publishing. (c) Plasmon-induced hot carriers generation in a silver jellium NP having a diameter of 6 nm under resonant excitation at 3.5 eV. The lower-left panel displays the hot electrons (red) and hot-holes (blue) distribution per unit volume as a function of energy relative to the Fermi level. The relaxation channels for the hot carriers that were considered are shown on the right: electron–electron, electron–photon (radiative recombination), and electron–phonon scattering.[175] Reproduced with permission from Liu *et al.*, ACS Photonics **5**, 2584 (2017). Copyright 2017 American Chemical Society. (d) Real-time dynamics of the plasmonic response of a silver Ag561 NP by means of rt-TDDFT. The incoming pulse profile is shown on the left (green curve) along with the NP dipolar time-dependent response (black curve). Electron density oscillations are shown on top at different time intervals (1–5) where the red and blue colors stand for density increase and decrease, respectively. The lower right plot shows the time evolution of the total energy stored in the excited system and its decomposition in terms of non-resonant transitions ("screened plasmon contribution," purple curve), resonant transitions ("hot carriers contribution," orange curve) and Coulomb energy (gray).[176] Rossi *et al.*, ACS Nano **14**, 9963 (2020). Copyright 2020 Author(s), licensed under a Creative Commons Attribution (CC BY) license.

approaches based on Lorentz oscillator model[44] and time-domain resonant-mode-expansion theory,[45] Lin *et al.* have developed various active control approaches including coherent control techniques,[46,51] polarization manipulation,[58] and adaptive laser pulse shaping methods[50] to control the ultrafast dynamics in complex plasmonic nanostructure geometries.

A seminal work based on a jellium model by Manjavacas *et al.*, aiming at describing the plasmon-induced hot-carriers generation rate dates back to 2014.[177] Since then, other methodologies based on a jellium-like description of the NP tried to develop a time-resolved picture of the electronic dynamics upon plasmon excitation, including, e.g., e–e and e–ph scattering effects [see Fig. 3(c)].[175,178–184] Despite the undoubted usefulness of jellium models, they cannot account for the real material atomistic structure (and the resulting band structure), that has been shown to be relevant for the quantitative estimation of transport properties, lifetimes, as well as energy and momentum distributions of hot carriers.[173,185–187] For this reason, there has been growing interest in applying *ab initio* methods to nanometallic systems, despite their higher computational cost. Most of these studies rely on approaches such as DFT and others like the embedded correlated wavefunction (ECW) method.[188,189] In this case the systems is split into two regions, where the most interesting one is treated through high level quantum mechanical theories in the presence of an embedding potential obtained by a DFT calculation, mimicking the presence of the surroundings. Different studies have described the time-resolved electron dynamics by employing real-time Time Dependent Density Functional Theory (rt-TDDFT), where the response of the system is simulated by integrating in time the time-dependent Kohn–Sham equations in the presence of an external pulse [see Fig. 3(d)].[176,190–196] Many Body Perturbation Theory (MBPT) approaches used to calculate the self-energy of a many-body system of electrons, such as the GW approximation, have also been used to describe the e–e scattering contribution to the carrier lifetimes,[197] also in combination with non-linear Boltzmann equations to model the time-resolved dynamics.[198] Along these lines, more recently, first-principle real-time non equilibrium Green's function formulations fully including e–e and e–ph scattering have been developed,[199] laying the foundation for upcoming promising works in the field.

III. ULTRAFAST PLASMON-DRIVEN CHEMISTRY

Recently, our society is striving to do, in a few decades, what nature has achieved in millions of years in order to address some of humanity's greatest challenges, for instance, decreasing the greenhouse gas emissions and, at the same time, generating "green" energy. To this end, designing photocatalysts based on plasmonic structures is a promising method to achieve efficient light-to-chemical energy conversion in the visible range of the electromagnetic spectrum.[86,200,201] As discussed in Sec. I, once the plasmon resonances have been excited, the energy of the oscillating electron plasma decays either radiatively, by re-emitting light (with a rate proportional to the nanoparticle's volume) or non-radiatively, by generating energetic electron–hole pairs (hot carriers).[3] Then, the temporal evolution of the hot carriers' distribution follows the well-known timeline, described by the three-temperature model (see Sec. II),[104,153] which sets a time limit after which we can no longer extract the energy of the hot carriers, e.g., driving a chemical reaction, since that energy is lost as heat.

Despite the merits of metal plasmonic nanostructures (e.g., Ag, Au, Cu), such as high tunability of their plasmonic resonances throughout the visible range of the EM spectrum and their high absorption cross sections, they also present unassailable deficiencies for photocatalysis. Due to the free carriers in metal nanostructures, almost half the time the energy of plasmon resonances is stored as kinetic energy, which is lost at the rate of electron scattering in the metal[202] (see Sec. II). This means that, although metal plasmonic nanostructures absorb much visible light, a large proportion is lost and cannot be used for photocatalysis. Furthermore, the metals that are best for plasmonics (Ag, Au, Cu) are not as catalytically active as conventional metal catalysts, such as Pt, Pd, or Rh, leading to low photocatalytic efficiencies. Consequently, hybrid plasmonic structures have been proposed to circumvent this issue.[203,204] The combinations for developing hybrid plasmonic photocatalysts are endless. In all of them, a plasmonic nanostructure, which acts as an antenna capturing light, can be paired with a catalytically active metal (Pt, Pd, etc.),[205,206] a semiconductor, perovskites, or metal-organic frameworks, to name just a few.[207–210] The idea is that, instead of using directly the plasmonic nanoparticle to drive a chemical reaction, it could be used to harness the visible light, generating hot carriers, which can be transferred to nearby semiconductor (such as TiO_2), that would otherwise not absorb light in the visible range. To export hot electrons to a nearby semiconductor for any practical application, the charge transfer process needs to be completed at a rate faster than the electron–phonon scattering process. To facilitate hot electron injection, three fundamental aspects need to be fulfilled: (i) sufficient initial hot electrons energy to overcome the interfacial Schottky barrier, (ii) direct contact between metal and the semiconductor, and (iii) minimal lattice defects and impurities at the interface. The semiconductor then would drive the chemical reaction. There are two mechanisms for charge transfer from the metal nanoparticle to acceptor states (either belonging to a molecule or to a semiconductor): a direct charge transfer upon excitation by light (which is also at the basis of the so-called chemical interface damping of the plasmon) and a sequential mechanism where plasmons first decay into hot carriers through surface-assisted Landau damping, and then tunnel to the acceptor states.[211,212] Because of the Schottky barrier formed at the metal nanoparticle/semiconductor interface, the hot carriers are not likely to be transferred back to the metal.[213,214] In this context, ultrafast optical spectroscopy allows us to monitor directly the dynamics of hot carriers at the metal–semiconductor interface,[214] and to design more efficient plasmonic photocatalysts.[215] A seminal work in the field of hybrid plasmonic nanostructures is the study of Wu *et al.*,[216] who designed hybrid Au-cadmium selenide (CdSe) nanostructures with a quantum yield of 24% for light energy over 1 eV. They highlighted the presence of a direct charge transfer pathway from Au to the conduction band of CdSe, by which the plasmon resonance in gold decays directly into electron–hole pairs, with the electron localized in the conduction band of CdSe. By performing ultrafast measurements, they were able to monitor the dynamics of plasmon-induced hot carriers in the hybrid Au-CdSe nanostructures. The charge transfer to the CdSe takes place in 20 fs, consistent with the direct charge transfer mechanism, while the back charge transfer, from CdSe to Au, took place in about 1.45 ps. This seminal work showed that a high charge transfer quantum yield

can be achieved through a direct charge transfer pathway, avoiding the usual losses associated with plasmonic chemistry.[216,217] Theoretical modeling is also pivotal in characterizing the charge transfer mechanism in some cases. Zhang *et al.* studied Au nanorods close to MoS_2, by combining rt-TDDFT with fewest-switching surface hopping for non-adiabatic nuclear effects.[218] They were able to show the presence of an indirect charge transfer process in which a fast plasmon decay (< 30 fs) first led to hot carriers formation in the NP, followed by their injection into MoS_2 within 100 fs (see Fig. 4).

Direct and indirect mechanisms can also coexist as shown by Long *et al.* for Au nanoclusters close to a TiO_2 slab who also suggested that the degree of coupling between the NP and the semiconductor could strongly influence the type of mechanism observed.[219]

As opposed to the very fast dynamics of charge carriers in plasmonic (hybrid) catalysts, that take place in the fs timescale, the motion of nuclei in molecules happens on the ps timescale while the kinetics of chemical reactions takes place on the microsecond to second timescale (9 to 15 orders of magnitude slower than hot carriers thermalization).[215] The difference between the characteristic timescales of hot carriers and chemical reaction dynamics is perhaps the most important bottleneck in plasmonic chemistry.[86,215] This rough timescale analysis illustrates why ultrafast optics is mostly used to probe the dynamics of charge carriers in (hybrid) catalysts, and not in molecules: chemical reactions simply do not proceed on such short timescales. Of course, this does not mean that there are no processes taking place on the fs timescale (or even faster) in molecules.[220] Starting with the well-known work of Zewail in fs chemistry,[221] this field has been a prospering one, investigating fundamental ultrafast processes in molecules. Indeed, over the last few years there has been growing interest in affecting chemical reactions at short time scales,[222] for instance by means of strong light–matter coupling, where the formation of hybrid light–matter polaritonic states leads to a sub-ps rearrangement of the molecular electronic energy levels that can in turn affect the subsequent photochemistry and reaction dynamics.[223–229] To give an example, optical cavities have been used to suppress or enhance chemical reactions both in ground and excited states, resulting in interesting chemical applications such as singlet fission[230] and selective isomerization.[231–233] Despite the fact that strong light–matter coupling can also be achieved using plasmonic systems,[232] the field is still in its infancy, in particular on the experimental side, especially if compared to the use of polaritonic optical cavities, for which ultrafast investigations already appeared.[234] For these reasons, in what follows we omit a detailed discussion of ultrafast investigation of chemical reactions modified by plasmon–molecule strong interactions and we will focus on plasmonic chemistry related to chemical reactions that are usually much slower than the electronic processes taking place in heterogeneous catalysts (such as molecular dissociation, desorption, diffusion).[215] Thus, in the following, we focus on the applications of ultrafast optical processes in plasmonic (hybrid) catalysts, highlighting how ultrafast optics can direct the design and understanding of the fundamental processes taking place in these materials.[200,213]

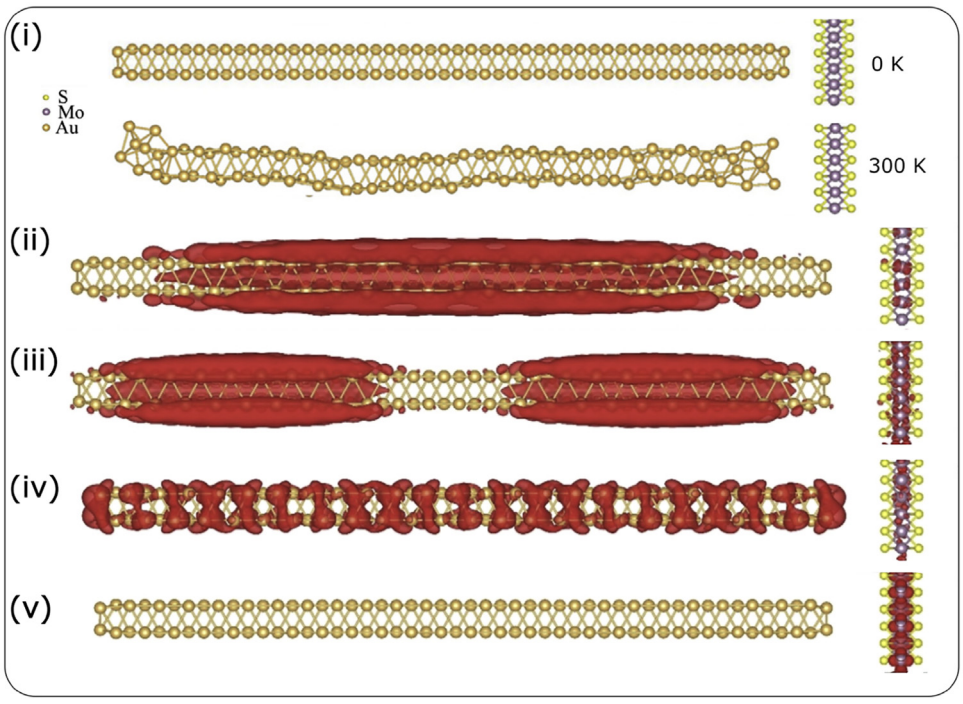

FIG. 4. Computational investigation of hot-electron injection from Au nanorods into MoS_2 combining rt-TDDFT and nonadiabatic molecular dynamics. (i) Optimized structure of the Au_{100}-$(MoS_2)_{12}$ system under study at 0 K, and one representative geometry obtained from the molecular dynamics simulation run at 300 K. Thermal fluctuations leads on average to an increase in the metal–semiconductor distance, thus reducing the strength of their interaction. (ii) and (iii) Charge density plots of plasmon-like states of the Au_{100} nanorod corresponding to two close absorption peaks around 2 eV, which upon excitation quickly (< 30 fs) lead to the population of Au bulk-states (iv) from which electron transfer to the acceptor state of MoS_2 (v) can then take place.[218] Reproduced with permission from Zhang *et al.*, Chem **4**, 1112 (2018). Copyright 2018 Elsevier Inc.

In one exemplary study on Au/Pt core–shell NPs, Engelbrekt *et al.* tracked the transfer of energy from the Au core to the Pt shell, where chemical reactions can take place.[206] By carefully monitoring the Pt shell thickness through photoelectron spectroscopy, the authors were able to finely control the content of Pt, from sub-monolayer to multiple layers. The most important finding of this study is that the energy of the plasmon generated hot carriers can be transferred on the sub-ps scale to the Pt shell, where it can drive chemical reactions. Although the addition of the Pt shell leads to a faster dephasing of the plasmon resonance due to the collision of the electrons participating in the plasmon resonance with the Pt electrons and faster charge transfer, the electron density in the Au core and the localized surface plasmon resonance (LSPR) oscillator strength remain fairly constant. This is important since it confirms that indeed the plasmon resonance is only due to the electrons in the Au core, without contributions from the Pt electrons. Moreover, the broadening of the AuNPs LSPR due to the addition of Pt should not negatively influence the photo-catalytic efficiency of Au/Pt NPs with broad-band excitation (such as solar light). Engelbrekt *et al.* used both spectral and time domain data to get information on the ultrafast response of the Au and Au/Pt core–shell NPs. In the spectral domain, the authors were able to extract information about the earliest time-dynamics, the plasmon dephasing time [see Fig. 5(a)].[206] As expected, with increasing Pt content, the plasmon dephasing rate increased due to interfacial damping. After the plasmon dephasing on the fs scale, the dynamics of hot carriers could be tracked directly in the time domain. The hot carriers' dynamics is characterized by a faster decay time, due to electron–phonon coupling (thermalization), and a slower decay time of the phonon–phonon coupling, leading to the cooling of Au and Au/Pt NPs.

Another study highlighting the use of ultrafast optics to design more efficient plasmonic photocatalysts was reported by Kumar *et al.*[235] The authors showed that gold nanoparticles (AuNPs) covered with reduced graphene oxide (r-GO) are more effective than platinum (Pt)-covered AuNPs at converting CO_2 to formic acid (HCOOH). With a selectivity toward HCOOH > 90%, the quantum yield of HCOOH using r-GO–AuNPs is 1.52%, superior to that of Pt-coated AuNPs (quantum yield: 1.14%), when excited close to the surface plasmon resonance of the AuNPs, at 520 nm. The reason for the higher quantum yield of the r-GO–AuNPs is the higher mobility of electrons in the graphene monolayer, which favors a higher rate of electron transfer to adsorbed CO_2. By using TiO_2 as an electron acceptor, they found an electron transfer time of less than 220 fs for the r-GO–AuNPs, leading to a charge transfer rate eight times higher than for AuNPs, and 4 times higher than GO–AuNPs [see Fig. 5(b)]. Therefore, by optimizing the ultrafast response of hybrid Au–GO plasmonic nanostructures, the design of cheaper and more efficient photocatalysts could be achieved. Interestingly, Hoggard *et al.* also analyzed the ultrafast charge transfer from AuNPs to graphene monolayers. By monitoring the plasmon resonance linewidth of single AuNPs deposited on graphene, they were able to extract a time of 160 fs for the direct metal–graphene charge transfer, and estimate that such a transfer has an efficiency of 10%.[236] In a similar study, Sim *et al.*[237] studied the ultrafast dynamics of plasmon generated hot carriers in AuNPs combined with more traditional catalytic materials, such as Pt and Ni. An important feature that was taken into consideration is the capping agent or ligands on the metal nanoparticles. It was found that the adsorbed molecules can influence the ultrafast dynamics of the plasmon generated hot carriers through, for example, direct metal–molecule charge transfer.[238,239] In particular, in this study by Sim *et al.*, the authors synthesized the bi-metallic Au/Pt and Au/Ni nanoparticles by annealing a 5 nm thick Au thin film fabricated by e-beam evaporation, after which either Pt or Ni thin films, were deposited. By looking at the different pump–probe measurements of the differential transmission spectra, it was found that both Au/Pt and Au/Ni NPs have significantly faster decay dynamics than bare AuNPs. The differential transmission spectra for the three different samples were fitted with a two-temperature model (i.e., two decay components).

The faster decay component was assigned to the electron–phonon coupling, which varied from a few hundred fs to ps, depending on the adsorbed energy density by the NPs, and a slower decay component, assigned to ph–ph coupling.[8,241] It was shown that the more power is adsorbed by the NPs, the more energetic are the plasmon generated hot carriers, and consequently, the longer it takes for them to lose their energy by e–ph coupling. By extrapolating the e–ph coupling time to zero adsorbed power, the characteristic e–ph coupling times were extracted, independent of the adsorbed power. This quantity depends only on the material properties (electron–phonon coupling constant and the electronic heat capacity) thus it can be used to determine the influence of the composition material on the ultrafast dynamics of hot carriers. For AuNPs, an e–ph coupling time of 0.9 ps was found, whereas for both Au/Pt and Au/Ni NPs, a time of 0.4 ps was determined. The slower, ph–ph coupling time was found to be 629 ps for AuNPs and 782 and 349 ps for Au/Pt and Au/Ni nanoparticles, respectively. This longer relaxation time reflects the cooling of nanoparticles through heat diffusion at the surface of the NPs and to the substrate, thus it is intimately linked to the interfacial thermal resistance of each NP.

An important advantage of plasmonic photocatalysts is the dynamical tunability of their optical response not only based on the shape of individual NPs, but also in 2D or 3D collections of plasmonic NPs (i.e., metamaterials).[242] Generally, the plasmonic properties of individual metallic NPs considerably depend on their morphology, shape, and size. For instance, it is well known that an increase in aspect ratio and asymmetry leads to a redshift of dipolar resonances, whereas more symmetrical structures typically display blueshifted and more intense dipolar transitions.[243–245] Moreover, as the NP size gets bigger and bigger, multipolar resonances appear and retardation effects start to play a role. The latter typically induce an additional redshift of plasmonic peak energies and a broadening of the transitions because of radiative damping.[246] Combining these single-NP features with 2D or 3D collections of structures opens up multiple ways of tuning the overall optical response of plasmonic photocatalysts.

In a remarkable study, Harutyunyan *et al.* showed the influence of hot spots (tight spaces in between adjacent nanostructures with enhanced EM fields) in the spectral and time domain response of plasmon resonance and hot carriers dynamics.[240] As opposed to modifying the plasmonic photocatalyst and form hybrid structures for example, the authors changed the geometry of the plasmonic photocatalysts. They used Au disks deposited on an Au surface, with alumina or TiO_2 spacers of varying thickness in between the two metal surfaces. Based on the separation between the gold surfaces (i.e., the gap of the hot-spot), and on the spacer composition, the authors observed anomalously strong changes to the ultrafast temporal and spectral responses of the plasmon generated hot carriers [see Fig. 5(c)]. The authors

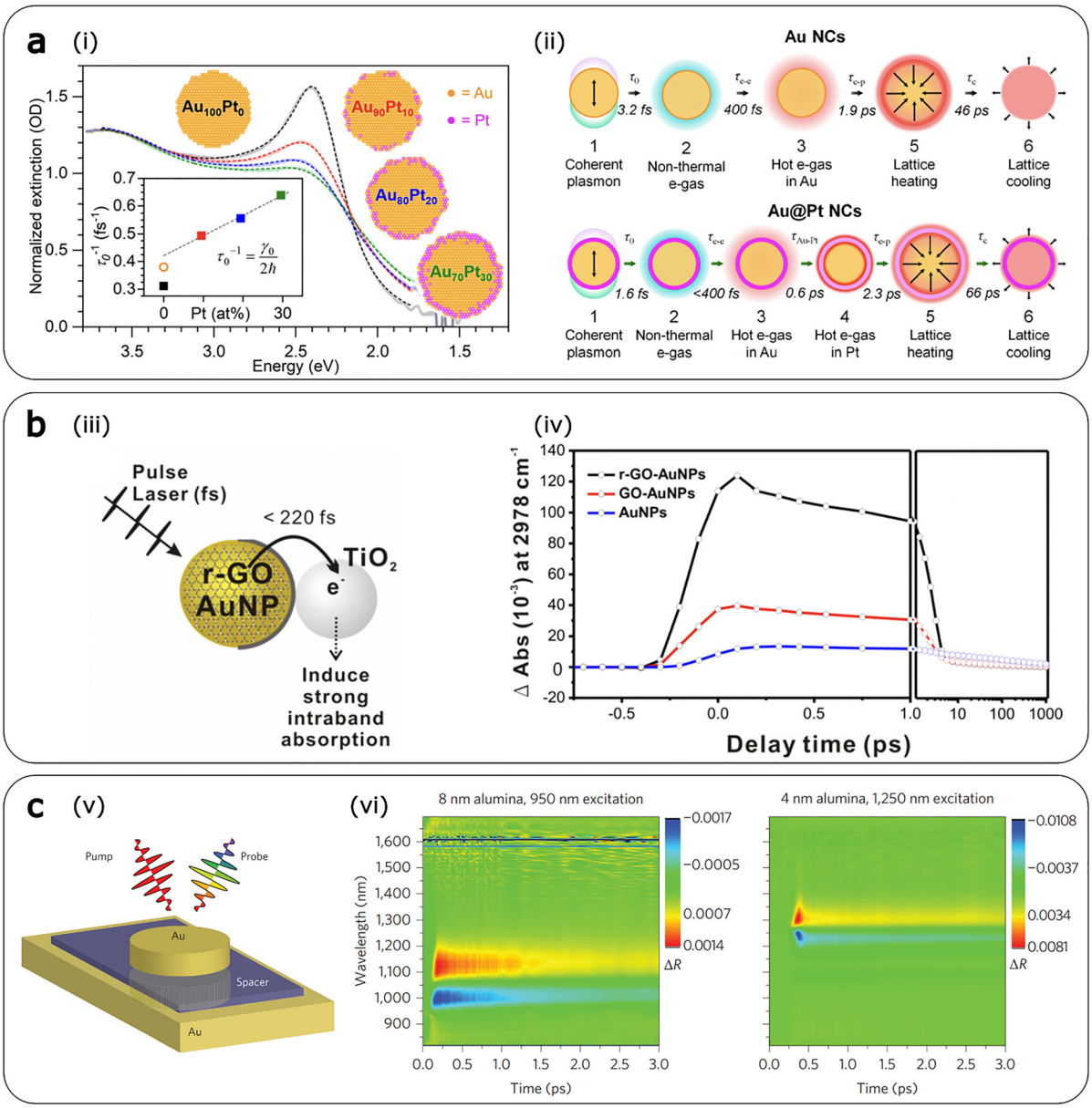

FIG. 5. Ultrafast plasmon generated hot carriers' dynamics and their interaction with adsorbed materials. (a-i) The broadening of the LSPR of gold nanoparticles (AuNPs) following the deposition of Pt layers. The inset shows the plasmon dephasing rate, extracted from the spectral domain optical response, in AuNPs (orange circle) and of Au@Pt core–shell NPs. (a-ii) Time dynamics of surface plasmon resonance excitation and dephasing, in Au NPs and Au@Pt core–shell NPs, respectively.[206] Reproduced with permission from ACS Nano **14**, 5061 (2020). Copyright 2020 American Chemical Society. (b-iii) The ultrafast charge transfer from reduced graphene oxide AuNP (r-GO–AuNP) to adsorbed TiO_2. (b-iv) The change of the charge transfer efficiency from Au NPs to TiO_2 due to the deposition of GO and r-GO, respectively, on AuNPs. The GO monolayer improves the mobility of hot carriers.[235] Reproduced with permission from Nano Lett. **16**, 1760 (2016). Copyright 2016 American Chemical Society. (c-v) Experimental setup for monitoring the influence of hot spots on the ultrafast response of plasmon generated hot carriers. (c-vi) By decreasing the alumina spacer thickness from 8 to 4 nm, an anomalous ultrafast response of the plasmon generated hot carriers appears due to the hot spot.[240] Reproduced with permission from Harutyunyan *et al.*, Nat. Nanotechnol. **10**, 770 (2015). Copyright 2015 Springer Nature.

showed a large ultrafast (pulse width-limited) contribution to the hot carriers' decay signal in nanostructures containing hot spots, which correlates with the efficiency of the generation of highly excited surface electrons. This effect was attributed to the generation of hot carriers from hot spots, with a much higher generation rate than outside those hot points, thus suggesting that plasmonic nanostructures featuring hot spots that are accessible to molecules, should be cleverly designed for an efficient photocatalytic activity.

Alongside the observed evidence through experimental studies, the clarification of the mechanisms of reactions catalyzed by hot carriers is a rather complex task. It has been shown that local thermal effects, hot carriers injection and electromagnetic coupling in confined space can all actively contribute to the modification of reaction yields and rates on the different timescales considered here.[86,87,247–249] Theoretical modeling has the potential to provide original insights. To give some examples, by employing coupled Boltzmann-heat equations and Arrhenius law-based models it was recently suggested that plasmon-induced local heating of the environment may significantly affect chemical reaction rates.[250–253] As remarkable example, Huang *et al.* and Yan *et al.* investigated the water splitting reaction close to Au plasmonic nanoclusters by employing a nuclear-electron quantum dynamics approach based on rt-TDDFT coupled to Ehrenfest dynamics, showing that both the plasmon-induced local field enhancement (FE) and a direct electron transfer to an antibonding orbital of a water molecule, due to de-localized excitations, significantly affect the photoreaction dynamics (see Fig. 6).[254,255]

Noteworthy, modeling has also highlighted situations where hot carriers are not directly involved in plasmon-enhanced reaction. Spata and Carter, by means of high-level quantum mechanical calculations using the ECW embedding scheme, showed that the H_2 desorption from a Pd catalytic reactive center can be favored by coupling the nano system with a plasmonic Al NP thanks to a purely electromagnetic enhancement effect.[256]

On similar grounds, ammonia NH_3 decomposition on ruthenium-doped copper NPs[257] and carbon–fluorine bond activation of CH_3F in the presence of Al–Pd plasmonic nanostructures[258] were both shown to be enhanced under illumination. In both cases, the analysis of the excited state minimum energy path (MEP) computed through ECW revealed lower activation barriers compared to the ground state pathways, thus justifying the speed-up of the reaction rates under light irradiation. In those cases, the plasmon can enhance the population of excited state species,[256,257] possibly induce a decrease in the energy barriers because of hot carriers related effects,[258] or even a simultaneous combination of both.

In addition to these relevant cases, the capability of plasmonic platforms to photo-catalyze many other chemical reactions have been efficaciously showcased over recent years. To give some examples, Au nanoparticles up to ≈50 nm in diameter have been successfully used for bond cleavage reactions, such as H–H,[259] O–O,[260] and C–C[261] scissoring, water splitting[262] and N-demethylation.[247] Au–Pd and Au–Pt bimetallic nanoplates have proved to effectively catalyze photoreduction and photo-oxidation processes,[263,264] whereas Au nanorods

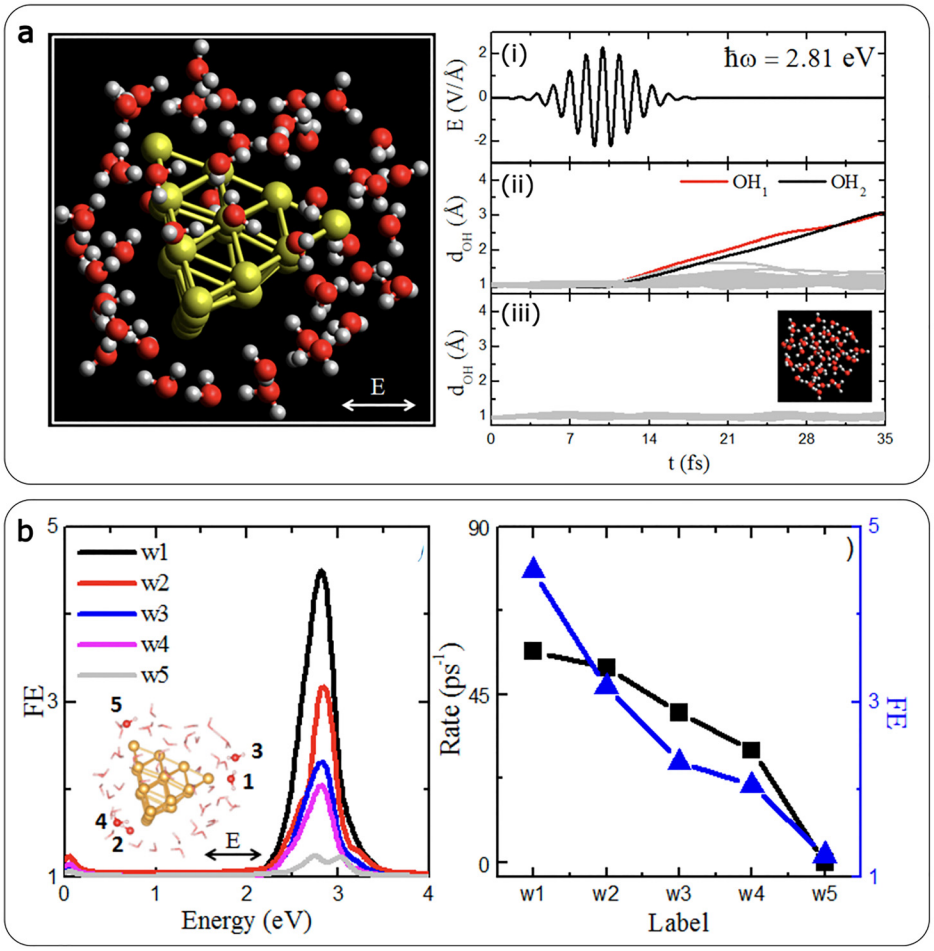

FIG. 6. Theoretical simulations of water splitting reaction close to a plasmonic Au_{20} cluster employing rt-TDDFT coupled to Eherenfest dynamics. (a) Snapshot of the Au_{20} cluster surrounded by water molecules (left panel). The white arrow displays the polarization of the incoming electric field whose frequency and time evolution are displayed on the right (i). Interestingly, upon excitation and in the presence of the Au cluster, some OH bonds break down, as shown by the time evolution of the OH bond lengths of all the water molecules surrounding the cluster (ii), thus triggering the water splitting reaction. Conversely, without the Au cluster (iii), all the OH bonds oscillate over time, remaining intact. (b) Local field enhancement (FE) as a function of excitation energy in different spatial positions (corresponding to different water molecules) surrounding the Au cluster (left panel). The corresponding rate of water splitting evaluated at the same spatial points (w1-5) is shown on the right. Notably, the rate of water splitting does not follow exactly the field enhancement trend, indeed even direct charge transfer excitations turned out to affect the reaction rate for some water molecules depending on their distance to the Au surface.[255] Reproduced with permission from Yan *et al.*, J. Phys. Chem. Lett. **9**, 63–69 (2017). Copyright 2017 American Chemical Society.

covered with Pd nanoparticles displayed the ability of speeding-up Suzuki cross coupling reactions.[265,266] In addition, more complicated Au–Pd superstructures featuring gold nanorods as core have also proved to facilitate molecular oxygen activation and other carbon–carbon coupling processes.[267]

Additionally, despite Au being one of the mostly employed noble metal for plasmonic photocatalysts to date, other plasmonic metals have also been used. For example, Ag nanocubes have been employed for catalyzing ethylene epoxidation[268] and O_2 dissociation,[269] while Ru-doped Cu NPs significantly boosted up NH_3 dissociation[270] and methane dry reforming.[271] To cite another well-known process, CO_2 photoreduction has also being extensively investigated, even in the presence of less conventional plasmonic metals, like Rh(Rhodium)-based nanocubes[200] and nanospheres,[272] thus not only resorting to Au- or Ag-based materials.[273] Clearly, the list of available examples is already so vast that properly accounting for all of them would require a standalone review on its own, going beyond the scope of this work.

Concluding this section, combining experimental and theoretical approaches to study ultrafast phenomena in (hybrid) plasmonic photocatalytic materials is an invaluable and desirable tool to catch a glimpse of the complex fundamental processes involved. As a last example, ultrafast pump–probe optical measurements have unraveled the energy flow in hybrid plasmon photocatalysts. Although it was traditionally assumed that plasmon-generated hot carriers are formed homogeneously throughout the volume of the plasmonic material, recent ultrafast studies have shown that in hybrid plasmonic materials (such as Ag/TiO_2, Au/Pt) the energetic charge carriers are formed predominantly at the interface of the two materials, due to the interfacial energy states.[274–276] This allows efficient charge transfer to adsorbed molecules, driving chemical reactions. This paradigm-shift in plasmonic photocatalysts, enabled partly by ultrafast optics, opens the road to limit increasingly more the losses associated with plasmonic chemistry, and the design of novel plasmon-driven photocatalysts.[277–279]

IV. ULTRAFAST MULTI-FUNCTIONAL PLASMONICS

During the last decade, a new subfield of plasmonics, the so-called *active* plasmonics,[280–282] has emerged, with the goal of tuning plasmons using an external stimulus such as an electric or magnetic field, or even a mechanical stress/acoustic excitation. As noticeable example, instead of the conventional noble metals, the use of magnetic or strongly correlated materials allows for an additional degree of freedom in controlling EM field properties.[283,284] In fact, these materials enable light to interact with the spin of electrons. Thus, light can be used to actively manipulate the magnetic properties of such materials.[285,286] Plasmonic and magnetic properties can be combined in these material at the nanoscale through various magneto-optical effects.[69,283,284,287] Furthermore, plasmonic modulation via lattice vibrations is an additional method for active control of SPs.[288] As a result, multifunctional plasmonic materials that allow for dynamic manipulation of light properties (e.g., amplitude and polarization) at the nanoscale are critical features for future all-optical nanotechnologies based on active photonics. This section provides an overview of recent studies of ultrafast dynamics in micro- and nanostructures with magnetic, acoustic, and plasmonic functionalities, as well as how these functions can be combined to obtain novel ultrafast phenomena at the nanoscale.

A. Ultrafast control of magnetism with plasmonics

Strategies for ultrafast all-optical control of magnetism have been the subject of intensive research for several decades due to the potential impact on technologies such as magnetic memories[289] and spintronics,[290] as well as the opportunities for nonlinear optical control and modulation[291] in applications such as optical isolation and nonreciprocity.[292] One of the most intriguing challenges in this field concerns the maximum modulation speed of nanophotonic devices and the time limit for magnetization reversal (switching) in magnetoplasmonic and, more in general, in magneto-optical devices. In the case of plasmonic structures, this modulation speed depends on the e–ph relaxation time, which in metals is a few ps, resulting in GHz range bandwidth. Several strategies have been proposed to overcome this limitation, for instance by exploiting nonlinear optical effects. In such processes, no direct transfer of carriers into excited states occurs, that is there is no time limitation for the excitation or relaxation processes, and therefore, the phenomenon can take place in a virtually instantaneous manner and it depends only on the duration of the light pulse exciting the structure.[293] This possibility will be discussed in more detail in Sec. V. Here, we focus on discussing the opportunity to achieve ultrafast switching of magnetic degrees of freedom and related applications in the framework of magnetic materials, such as Ni, which can be combined with plasmonic structures[294–296] or be used directly as plasmonic building blocks.[297–301]

As highlighted in Sec. I, plasmonics enables confinement and enhancement of EM radiation well below the diffraction limit. This is a crucial feature for opto-magnetic applications in spintronics, where deterministic control of nanometer-sized magnetic bits is a major objective. Incorporating plasmonic nanostructures into magneto-optical active materials dramatically improves pump-induced control of the magnetization state at the ultrafast timescales. The fastest and least dissipative way of switching the spin of electrons is to trigger an all-coherent precession. Schlauderer *et al.* showed that THz EM pulses allow coherent steering of spins by coupling the antiferromagnetic material $TmFeO_3$ (thulium orthoferrite) with the locally enhanced electric field of custom-tailored antennas [see Fig. 7(a)].[302] Similarly, but using visible (PHz) radiation, Mishra *et al.* employed resonant EM energy funneling through plasmon nanoantennas to influence the demagnetization dynamics of a ferrimagnetic TbCo thin films [see Fig. 7(b)]. They demonstrated how Ag nanoring-shaped antennas under resonant optical fs pumping reduce the overall demagnetization in the underlying films up to three times compared to non-resonant illumination, and attributed such a substantial reduction to the nanoscale confinement of the demagnetization process.[68] Very recently, they have also devised a new architecture simultaneously enabling light-driven bit downscaling, reduction of the required energy for magnetic memory writing, and a subtle control over the degree of demagnetization. To achieve these features, they employed in a magnetophotonic surface crystal featuring a regular array of truncated-nanocone-shaped Au-TbCo antennas showing both localized plasmon and surface lattice resonance modes.[303]

Another interesting approach to achieve ultrafast control of magnetism at the nanoscale is represented by the all-optical switching (AOS) mechanism, where the optical laser pulses are used to deterministically reverse the spin moment.[304–306] This discovery could have important technological implications, since, for example, switching the spin magnetization by an ultrashort pulse could lead to much faster

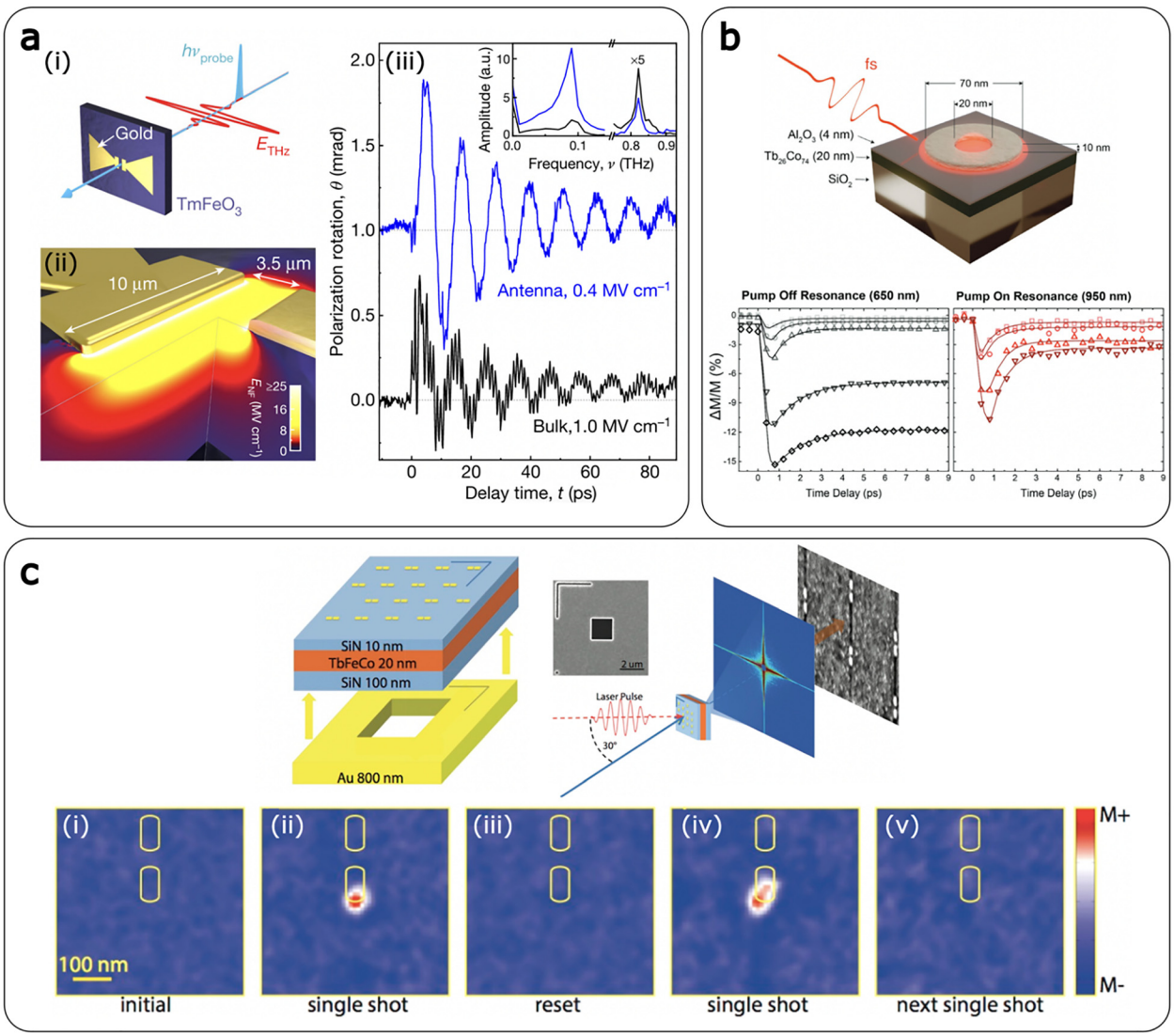

FIG. 7. All-optical plasmon-driven magnetization dynamics. (a) (i) Schematic of the gold bowtie antenna on $TmFeO_3$. The structure is excited from the back side by an intense THz electric field E_{THz} (red waveform) while a co-propagating near-infrared pulse (light blue) probes the induced magnetization dynamics in the feed gap between the two lobes of the antenna. (ii) Peak near-field amplitude in the antenna feed gap calculated by FDTD simulations for an incident THz waveform with a peak field amplitude of 1 MV cm^{-1}. (iii) Experimentally detected polarization rotation signal obtained for a peak electric THz field of 1 MV cm^{-1} on the unstructured substrate (black curve), and when probing the feed gap of the bowtie antenna structure resonantly using a THz waveform with a peak electric field amplitude of 0.4 MV cm^{-1} (blue curve). Inset: corresponding amplitude spectra featuring two modes (at 0.09 and 0.82 THz).[302] Reproduced with permission from Schlauderer *et al.*, Nature **569**, 383 (2019). Copyright 2019 Springer Nature. (b) Schematic of Ag nanoring on $Tb_{26}Co_{74}$. Pump–probe measurements was performed to determine the magnetization dynamics. The differential magnetization using an off resonance (on-resonance) pump is displayed at the bottom left (right), showing a great enhancement of the demagnetization by the on-resonance pump.[68] Reproduced with permission from Mishra *et al.*, Nanoscale **13**, 19367 (2021). Copyright 2021 Author(s), licensed under a Creative Commons Attribution (CC BY) license. (c) The schematic show TbFeCo film with gold two-wire antennas excited by a laser pulse. AOS was achieved with a size of 53 nm using the nanoantennae to confine fields spatially. X-ray holography is used to image the magnetic switching. The switching is shown to be both reproducible (i)–(iv) and reversible (v).[312] Reproduced with permission from Liu *et al.*, Nano Lett. **15**, 6862 (2015). Copyright 2015 American Chemical Society.

writing of magnetic bits in magnetic recording media. The origin of the AOS was initially thought to be linked to the helicity (right or left circular polarization state of the light pulse), i.e., the injected "photonic spin moment" (the so-called spin angular momentum, SAM, of light), but subsequent investigations showed that solely fast laser heating was sufficient to trigger the magnetization reversal.[307] By using a microscope objective[308] or nanopatterning of magnetic materials,[309–311] bit size can be reduced to a few hundred nanometers.

In a seminal work, Liu *et al.* exploited LSPs in gold dimer-nanobar nanoantennas on a TbFeCo alloy thin film to achieve a 50 nm

AOS-switched spot size[312] [see Fig. 7(c)]. Thus, plasmonics can enable AOS to become technologically relevant, since plasmons can allow to reach bit sizes which can be used in heat-assisted magnetic recording[100] and allow deterministic ultrafast all-optical magnetization switching at the nanoscale. Moreover, strong localization of the pump pulse by SP excitation reduces the laser fluence required for the ultrafast demagnetization.[313,314]

One of the possible ways for the photon to act on the spin moment could be through an opto-magnetic effect, the inverse Faraday effect (IFE). This non-linear opto-magnetic effect, discovered in the 1960s, describes the generation of an induced magnetic moment by a circularly polarized EM wave.[315] To explain the IFE in bulk materials, several models have been proposed recently. The deeper understanding of the origin of the IFE is still the subject of ongoing investigations, and here we report the most relevant works in relation to the topic of this review. Hertel developed a plasma model,[316] which was recently used by Nadarajah and Sheldon to estimate the magnetic moment that could be induced in a plasmonic Au nanoparticle.[317] Popova *et al.* employed a four-level hydrogen model with impulsive Raman scattering to show that such a process could lead to a net induced magnetization.[318] Using relativistic electrodynamics, Mondal *et al.* showed that there exists an EM wave–electron spin interaction that provides a linear coupling of the photon SAM to the electron spin, which then acts as an optomagnetic field that generates the induced magnetization.[319] By using a second-order density matrix perturbation theory a quantum theory for the IFE was derived, by taking into account also the optical absorption.[320,321] Carrying out *ab initio* calculations for bulk Au, Berritta *et al.* computed a moment of $7.5 \times 10^{-3}\ \mu_B$, where μ_B is the Bohr magneton, per Au atom by pumping with circular EM radiation with a $10\,GW/cm^2$ intensity at 800 nm.[321] Detailed measurements of the light-induced magnetization in Au, however, are still very few. In an early pioneering investigation, Zheludev *et al.* could measure an induced polarization rotation of $\sim 12 \times 10^{-6}$ rad in an Au film upon pumping with a laser intensity of $1\,GW/cm^2$ and 1260 nm wavelength, a value that is within an order of magnitude consistent with the *ab initio* calculated induced moment.[322] Recently, Cheng *et al.* reported the experimental optically induced magnetization in plasmonic gold nanoparticles, with magnetization and demagnetization kinetics that are instantaneous within the sub-ps time resolution [see Fig. 8(a)].[323] Under typical ultrafast pulse excitation ($>10\,GW/cm^2$ peak intensity), the induced magnetic moment $2.9 \times 10^7\ \mu_B$ or $0.95\ \mu_B$ per Au atom, i.e., two orders of magnitude higher than that predicted by theory for bulk Au.[320]

All the above considerations were built upon exploiting the SAM of the EM field. An optical beam can also carry a well-defined orbital angular momentum (OAM).[324,325] Combining OAM with plasmonics, it has been demonstrated that sub-fs dynamics of OAM can be realized in nanoplasmonic vortices.[91,326–328] Hence, plasmonic vortices carrying OAM can be confined to deep subwavelength spatial dimension and could offer an excellent time resolution. The OAM can, therefore, be expected to enter soon the developing area of magnetophotonics, where the OAM could offer a new functionality to control the nanoscale magnetism.[327] Although there is an emerging understanding of the IFE coupling of the SAM of a beam to the electron spin, a similar understanding of the interaction of OAM with spin or orbital magnetism has still to be established. Recently, observations of interaction of magnetism and an OAM vortex beams were reported.[329,330] Karakhanyan *et al.* quantified numerically the relative contributions of SAM and OAM of light to the IFE in a thin gold film illuminated by different focused beams carrying SAM and/or OAM, by using a hydrodynamic model of the conduction electron gas.[331] The OAM of light provides a new degree of freedom in the control of the IFE and the resulting opto-magnetic field, which has the potential to influence numerous research fields, such as all-optical magnetization switching and spin-wave excitation. A recent work by Prinz *et al.* seems to point in this direction, since they show that is possible to act on demagnetization processes by using OAM.[332] These findings support a mechanism of coherent transfer of angular momentum from the optical field to the electron gas, and they pave the way for optical subwavelength strategies for optical isolation that do not require externally applied magnetic fields. It can already be perceived that taking both spin and orbital degrees of freedom of photonic beams into account will become paramount for the future development of ultrafast magnetophotonics.

Plasmon-enhanced magneto-optical effects can allow to improve by orders of magnitude the detection sensitivity of ultrafast magnetic processes. Novikov *et al.*[66] investigated experimentally the ultrafast modulation of the SP-resonant transverse magneto-optical Kerr effect (TMOKE) induced by a non-resonant 50 fs pump laser pulse in the one-dimensional magnetoplasmonic crystal [see Fig. 8(b)]. They observed the suppression of TMOKE in the SP-resonant probe from 1.15% to 0.4% by the demagnetization of the nickel MPC under a non-resonant pump. The absolute TMOKE difference was around 20-fold enhanced in the MPC compared to the plane nickel film, thus proving the higher sensitivity of plasmonic systems to magnetization dynamics. Furthermore, they demonstrated that the carrier dynamics induced by the ultrashort light pulse affected the SP excitation process itself: the laser heating induces the modification of the SP wavevector through the modulation of the metal optical constants. As a result, a differential reflectivity value as high as 5.5% is achieved in MPC in comparison with 1.1% value in the plane nickel. Finally, it was shown that electron thermalization and relaxation dynamics are slower in MPC relative to the plane nickel, since e–ph relaxation times extracted from the differential reflectance were 800 and 260 fs for the MPC and plane nickel film, respectively.

Similarly, Kazlou *et al.* recently demonstrated SP-assisted control of spin precession phase in hybrid noble metal–dielectric magneto-plasmonic crystals [see Fig. 8(c)].[333,334] These results can be applied to the development of new magnetoplasmonic devices, providing more sensitivity to the magnetic order on the sub-ps timescale, where non-thermal effects occur. In this framework, particularly interesting would be the study of plasmon dephasing (happening on the timescale of few tens of fs) on the spin dynamics in opto-magnetic-active nanomaterials.[69] By exploring non-thermal pathways, where the intrinsic losses due to heating can be overcome by exploiting the dynamics of the electrons on sub-100 fs timescales, can open excellent perspectives in both the fundamental and applied aspect of ultrafast magnetoplasmonics.

B. Ultrafast acousto-magneto-plasmonics

As mentioned at the beginning of this section, plasmonic modulation by means of ultrafast lattice vibrations represents an interesting approach for the active control of SPs, as lattice contraction can redshift the SP resonance frequency.[335] In 1988 van Exter and Lagendijk showed that SP excitation in silver in the Kretschmann geometry can

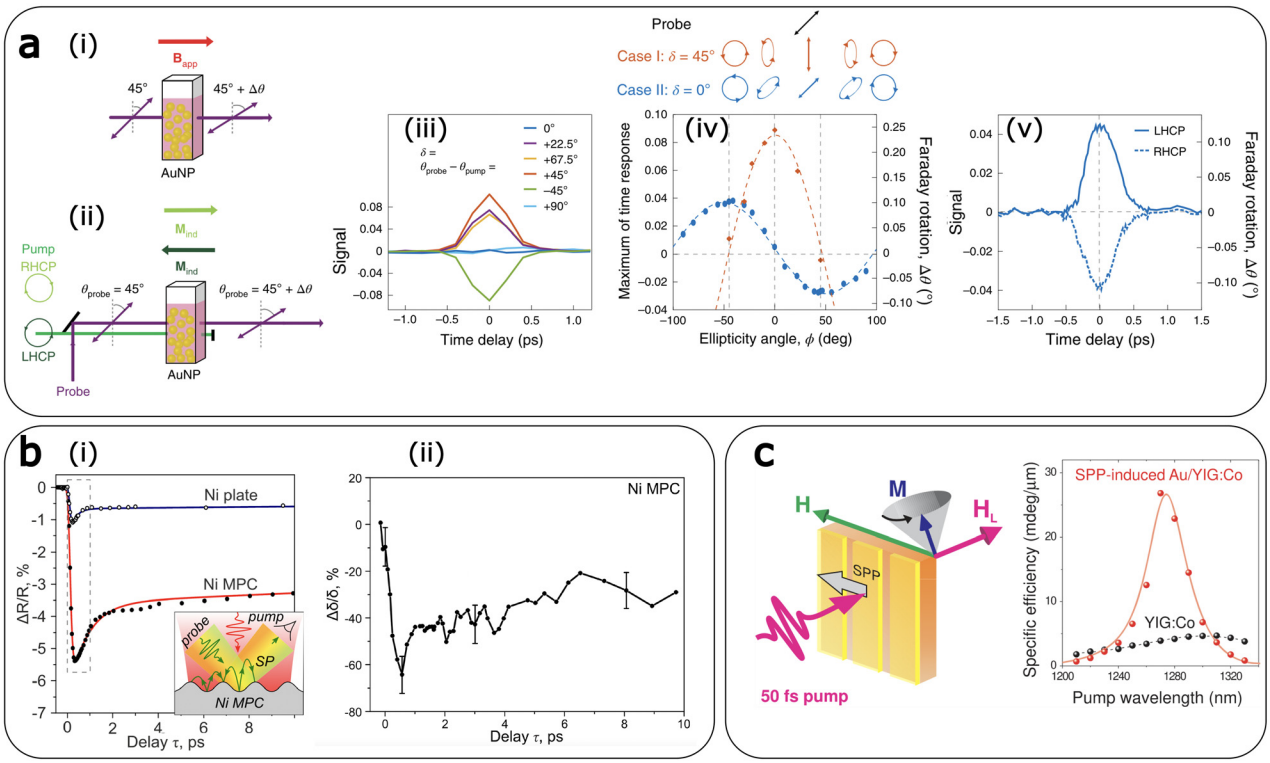

FIG. 8. Ultrafast magneto-plasmonics. (a-i) The Faraday effect is the rotation of the polarization plane of light transmitted through a magnetized medium. (a-ii) The IFE is the induced magnetization of a medium, M_{ind}, during circularly polarized excitation (green line). The direction of induced magnetization depends on the helicity of the light. The optical rotation of a probe beam (purple line) indicates M_{ind}, and B_{app} is the external applied magnetic field; $\Delta\theta$, Faraday rotation angle; R(L)HCP, right-(left-)handed circularly polarized light. (iii) Light-induced rotation due to only the optical Kerr effect ($\phi = 0°$), as a function of δ. (iv) Light-induced rotation as a function of ϕ. Red dots represent data from experiments with the geometry of case I, where $\delta = 45°$. Blue dots represent data for the case II geometry, where $\delta = 0°$. Dashed lines are fits to the data. (v) Light-induced rotation due to pure IFE when the pump is circularly polarized with left-handed helicity ($\phi = -45°$, solid line) or right-handed helicity ($\phi = +45°$, dashed line), corresponding to the positive and negative maxima for case II in (iv).[323] Reproduced with permission from Cheng *et al.*, Nat. Photonics **14**, 365 (2020). Copyright 2020 Springer Nature. (b-i) Inset: Model visualization of ultrafast all-optical modulation of SP-assisted transverse magneto-optical Kerr effect (TMOKE) in a one-dimensional (1D) nickel magnetoplasmonic crystal (MPC). The differential reflectance is displayed for plain nickel and for the nickel MPC. (ii) Laser induced modulation of the SP-enhanced TMOKE in 1D nickel MPC as a function of the pump–probe delay.[66] Reproduced with permission from Novikov *et al.*, Nano Lett. **20**, 8615 (2020). Copyright 2015 American Chemical Society. (c) SP induced amplification of photomagnetic spin precession. A YIG:Co film with Au gratings, placed in an external in-plane magnetic field, that was excited by a 50 fs pump (left) displayed an increase in its specific efficiency of the spin precession (right), as opposed to such a film without the Au. Dots represent experimental data and the full line is results from a numerical simulation.[333] Reproduced with permission from Kazlou *et al.*, ACS Photonics **8**, 2197 (2021). Copyright 2021 Author(s), licensed under a Creative Commons Attribution (CC BY) license.

significantly amplify pump–probe signals compared to standard reflectivity measurements.[336] An acoustic variation of the order of 4% in the lattice density altered the wavevector of the time-delayed SP probe pulses, causing a significant shift in probe reflectivity in the Kretschmann configuration. They concluded that the intrinsic lifespan of longitudinal phonons in silver at 42 GHz surpassed 100 ps based on the decay duration of these thermo-acoustic oscillations, which was mostly governed by the finite (52%) acoustic reflection at the silver–glass interface. Measurements of the mean free path (or lifetime) of high-frequency phonons in solids, caused by the interaction between ballistic and diffusive heat transport, are crucial for understanding the nanoscale thermal characteristics of materials.[337]

Similar time-resolved experiments in thin gold and copper films[338,339] have revealed the contribution of short-lived nonequilibrium electrons to the buildup of mechanical stress driving the initial stage of thermo-acoustic expansion, which is consistent with similar measurements in plasmonic nanoparticles.[340] For example, Deacon *et al.* demonstrated that a highly localized acoustic resonance exists in the nanoparticle-on-mirror structure, near the nanoparticle's narrow base.[341] This bouncing mode has an extremely variable period pertaining to the nanoscale morphology attainable through matched plasmonic coupling by means of a coupled mode whose optical field is likewise tightly contained within the nanoscale void beneath the facet. Due to this restriction on both, the plasmonic and acoustic modes are coupled to the gap by the significantly improved acousto-optic coupling as is observed in comparison to conventional acousto-optic crystals, impacting the SP resonance. Ruello *et al.* measured coherent GHz acoustic phonons in plasmonic gold nanoparticle superlattices (NPSs), with a typical in-depth spatial extension of approximately 45 nm, which is approximately four times the optical skin depth in gold [see Fig. 9(a)].[342]

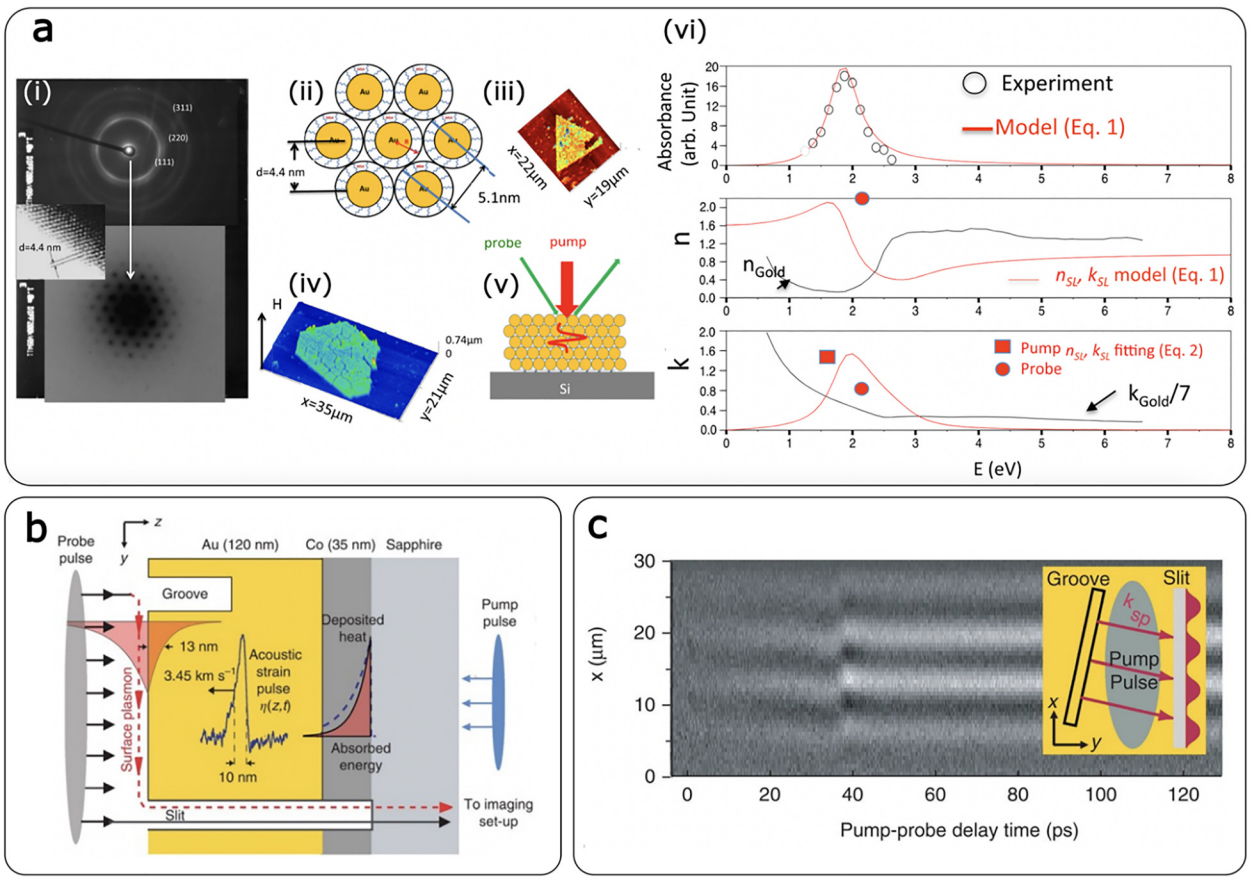

FIG. 9. Ultrafast acousto-plasmonics. (a-i) Transmission electron diffraction (TED) pattern showing the Debye Scherrer rings (top figure) coming from the crystallized cubic gold nanoparticles. In the middle figure, the transmission electron microscopy image (TEM) shows the mesoscopic hexagonal arrangement (hcp) with the two-neighbor plane distance of 4.4 nm. The hcp arrangement is also well evidenced with small angle electron diffraction revealing the sixfold axis (bottom figure). (ii) Sketch of the gold nanoparticles superlattices connected via mercaptosuccinic acid molecules. (iii) Optical microscopy view of a superlattice deposited onto a silicon substrate. (iv) AFM profile of the hexagonal shape superlattice (height H = 180 nm). (v) Sketch of the pump and probe experiments performed on these nanoparticles superlattice where coherent acoustic phonons are generated and detected in the front–front configuration. (vi) Top panel: plasmon resonance of the gold superlattice (experimental data, dots, and calculated, red line). Middle and bottom panels: refractive index (real n and imaginary parts k) of the gold superlattice compared to those of bulk gold. The red symbols (square and circles) are the refractive index values estimated with the photoacoustic response.[342] Reproduced with permission from Ruello *et al.*, Phys. Rev. B **92**, 174304 (2015). Copyright 2015 American Physical Society. (b) Schematic drawing of the acousto-plasmonic pump–probe experiment: surface plasmons propagating at the gold–air interface probe the reflection of acoustic pulses generated in the laser-heated cobalt transducer. (c) Measured acousto-plasmonic pump–probe interferogram showing a pronounced shift of the interference fringes upon reflection of an ultrashort acoustic pulse. The inset illustrates the geometry of the plasmonic slit-groove interferometer.[343] Reprinted with permission from Temnov *et al.*, Opt. Express **17**, 8423 (2009). Copyright 2009 Optica Publishing Group.

The modeling of transient optical reflectivity suggested that phonons are generated by ultrafast heating of the NPs aided by light activation of the volume plasmon polariton. Based on these findings, it has been shown that it is possible to map the photon–electron–phonon interaction in subwavelength nanostructures,[344–346] which provides interesting insights into the fundamental features of these architectures.

Finally, it is worth mentioning that an interesting approach to further boost research in ultrafast active plasmonics is represented by the combination of acoustic, magnetic and plasmonic properties. In this context hybrid gold–cobalt bilayer structures[280] can be suitable candidates for opto-magneto-acoustic switching experiments [see Figs. 9(b) and 9(c)].[343,347]

V. ALL-OPTICAL SWITCHING APPLICATIONS AND NEW MATERIALS

One of the main challenges in all-optical information processing is the creation of an efficient and compact high-speed all-optical switch, the equivalent of the transistor in conventional electronics. For practical applications in integrated photonics, all-optical modulators should ideally feature sub-ps switching times at fJ control light energies, as well as switching contrasts greater than 10 dB and characteristic sizes below 100 nm. To date, no engineered photonic structure that can operate in the THz bandwidth range fulfills all these conditions. In this context, plasmonics emerges as a suitable approach for all-optical processes as plasmons can rapidly alter the complex refractive index of a medium with an enhanced response.[104,348–354] While in Sec. IV, we

discussed all-optical switching of magnetic degrees of freedom in the context of multi-functional (mainly magnetoplasmonic) nanostructures, here we focus on the ultrafast switching of the optical response (e.g., light intensity and polarization states) in plasmonic structures. These are two distinct phenomena, as in one case we act on the spin degree of freedom in materials, while in the second case, treated in this section, we act on light properties by modulating the permittivity of the material. Upon illumination of a metal by a light pulse (pump), non-thermalized electrons are excited, which subsequently decay through several processes, spanning different timescales, from the fs up to ns range, leading to dynamic changes of the material permittivity. In the context of all-optical switching, a control light pulse is used to vary transmission or reflection between high and low states, to modulate the intensity of a signal pulse which carries the information. Given that plasmonic resonators can spectrally tailor light dispersion, wavelength regions showing negligible levels of "slow" temporal components connected to e–ph and ph–ph scattering processes can be attained, where only sub-ps responses dominate. By engineering nanostructured gold, this approach has demonstrated differential transmission modulations up to >20% with temporal widths <300 fs at ~1 mJ/cm^2 pump fluence, as shown in Fig. 10(a).[354] Both positive and negative transmission changes can be observed, depending on the probe wavelength, as enabled by the pump-induced shift of the resonance spectrum. Considering the high electron densities present in noble metals, their electron distributions cannot be substantially modified optically, preventing larger permittivity modulations.[291] In this scenario, indium tin oxide (ITO) arises as a promising material that exhibits significantly smaller—but sufficiently high—excited electron concentrations in the near infrared.[355,356]

Moreover, ITO also possesses an epsilon-near-zero (ENZ) region, characterized by a permittivity spectrum with a zero crossing of the real component, where optically induced variations of the refractive index produce the strongest effects on resonant features.[291,357,362–365] Coupling a thin ITO layer at its ENZ region to an array of gold nanoantennas [see Fig. 10(b)] to modulate the plasmonic resonance has revealed absolute transmission changes around 20% at a pump fluence of only <1 mJ/cm^2 (equivalent to ~0.3 pJ per nanoantenna's geometric cross-sectional area).[357] The fastest reported plasmonic switch has been achieved by exploiting gold's high third order nonlinearity through two-photon absorption (TPA).[358] TPA influences the imaginary part of the refractive index of a medium in a nearly instantaneous manner. In a pump–probe configuration, the transmission of the probe beam changes abruptly whenever a pair of pump and probe photons are absorbed simultaneously, recovering its nominal value as soon as the pulses no longer temporally overlap. The fundamental time limit for this process is practically either the pulse duration or the resonance bandwidth. The differential transmission temporal trace of a Fano-resonant gold metasurface shown in Fig. 10(c), displays a temporal width of only 40 fs, with a modulation depth of ~10% at 0.07 mJ/cm^2 pump fluence (~0.1 pJ per unit cell), which reaches 40% at 0.3 mJ/cm^2 (~0.5 pJ per unit cell).[358] Similar performances have also been measured in nonlinear dielectric nanostructures at Mie resonances [see Fig. 10(d)].[293,359,366] Outstanding differential (absolute) transmission modulations greater than 100% (20%) at ~4 mJ/cm^2 pump fluence, were also reported in ITO nanowires [see Fig. 10(e)].[356,360]

Another avenue to control the strength of light–matter coupling to exceed losses could combine optical/plasmonic field properties of a resonator with the electronic excitations of an active material.[367,368] Layered materials with a 2D character such as graphene and TMDCs have also been considered for all-optical processing devices,[361,369,370] as they support strong light–matter interactions and display optical nonlinearities enabling both atomic-scale and a sub-fs modulation of light properties.[371–373] In the past years, research efforts have been spent to study ultrafast nonlinear optical processes in layered materials, in particular TMDCs.[109,374–381] The most efficient nanoscale all-optical switch has been obtained by using graphene as the nonlinear element.[361] Graphene is a nonlinear saturable absorber, meaning that its transparency increases under intense light excitation due to photogenerated carriers causing Pauli-blocking, with relaxation times in the sub-ps range. To further enhance light–matter interactions, Ono *et al.*[361] placed a graphene bilayer on top of a plasmonic waveguide with a 30 nm slot width [see Fig. 10(f)], significantly reducing the required power for saturable absorption. They demonstrated a differential transmission increase greater than 100% at just 35 fJ switching energy, with a 260-fs temporal response. To reach sub-fJ switching energies, Nozaki *et al.* used a combination of a photonic-crystal nanocavity and strong carrier-induced nonlinearity in InGaAsP to demonstrate low-energy switching within a few tens of ps. Switching energies with a contrast of 3 and 10 dB of 0.42 and 0.66 fJ, respectively, have been obtained.[382] A combination of the last two approaches might pave the way to reach sub-fs and sub-fJ functionality at the same time. Furthermore, low-dimensional material systems such as quantum dots (QDs), graphene, and 2D semiconductors provide an unprecedented avenue to revolutionize information and communications technologies via recently discovered optical nonlinear properties.[383–385]

Nonlinear optics can be used for generating ultrashort pulses, laser spectrum conversion, ultrafast optical switching, and all-optical signal processing. By combining nonlinear optical processes in plasmonic systems with the dynamics of exciton–polaritons, it might be possible to achieve all-optical transistor functionalities with both PHz bandwidth and sub-fJ switching energy. To date, reaching these two goals at the same time has not yet been demonstrated, although switching mechanisms have been exploited in photonic systems made of inorganic semiconductor and displaying exciton–polaritons enabling transistor functionalities at cryogenic temperatures [see Figs. 11(a) and 11(b)].[367] Interestingly, by replacing inorganic semiconductors with an organic semiconductor in an optical microcavity, Zasedatelev *et al.* recently demonstrated that is possible to realize room-temperature operation of a polariton transistor through vibron-mediated stimulated polariton relaxation, with a sub-ps switching time, cascaded amplification and all-optical logic operation, however using micrometer-sized cavities [see Figs. 11(c)–11(f)].[368] They also recently utilized stable excitons dressed with high-energy molecular vibrations to allow single-photon nonlinear operations at ambient conditions.[386] This pivotal result might open new horizons for practical implementations like sub-fs switching, amplification and all-optical logic at the fundamental quantum limit.

The linear Pockels electro-optic effect is another phenomenon that has been exploited for the modulation of electromagnetic waves. Burla *et al.*[387] built a Mach–Zehnder interferometer configuration using two plasmonic slot waveguides filled with a nonlinear material, whose refractive index could be controllably modified by applying an external voltage between the metallic electrodes defining the

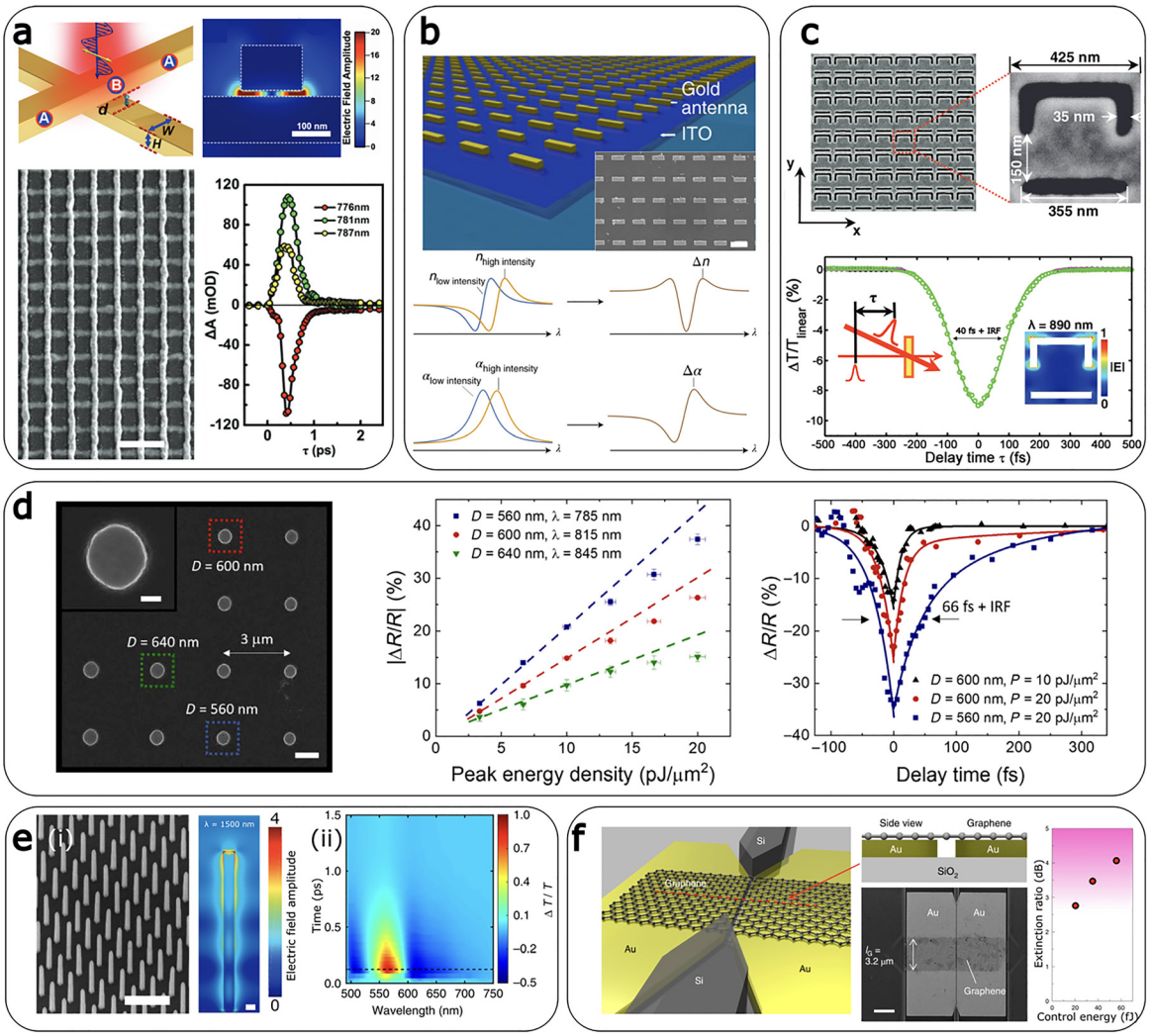

FIG. 10. Ultrafast all-optical switching. (a) Cross-stacked gold nanowire network supporting a Fano resonance. Design, SEM (scanning electron microscopy) image (scale bar, 1 μm), electric field enhancement distribution and ultrafast performance as measured through pump–probe spectroscopy ($\pm$110 mOD corresponds to $\pm$22% transmission modulation).[354] Reproduced with permission from Lin *et al.*, Nanoscale **8**, 1421 (2016). Copyright 2016 Royal Society of Chemistry. (b) Array of gold nanoantennas coupled to an ITO layer (SEM image in the inset; scale bar, 500 nm). A small variation in ITO's refractive index causes a significant spectral shift of the resonance wavelength of the nanoantennas, causing a dramatic change in the effective refractive index (Δn) and absorption ($\Delta\alpha$) experienced by the incoming light.[357] Reproduced with permission from Alam *et al.*, Nat. Photonics 12, 79 (2018). Copyright 2018 Springer Nature. (c) Fano-resonant gold metasurface for sub-100 fs all-optical switching using TPA. IRF stands for instrument response function.[358] Reproduced with permission from Ren *et al.*, Adv. Mater. **23**, 5540 (2011). Copyright 2011 Wiley-VCH. (d) Ultrafast switching in dielectric GaP nanostructures designed as seen in the SEM image (left). The scale bar is 1 μm. Dynamics of the system were evaluated using pump–probe spectroscopy with sub-10 fs laser pulses, peak energy dependence of the differential reflectivity magnitude (middle) and the temporal dependence of the differential reflectivity (right).[359] Reproduced with permission from Grinblat *et al.*, Sci. Adv. **6**, eabb3123 (2020). Copyright 2020 Author(s), licensed under a Creative Commons Attribution (CC BY) license. (e) ITO nanowires pumped at its trans-LSPR in the near infrared (1500 nm wavelength) and probed in the visible range. SEM image (scale bar, 2 μm), electric field distribution (scale bar, 200 nm), normalized with regard to the incoming wave, and differential transmission spectrum at varying pump–probe delay time.[356,360] (i) Reproduced with permission from Guo *et al.*, Nat. Photonics **10**, 267 (2016). Copyright 2016 Springer Nature. (ii) Reproduced with permission from Guo *et al.*, Nat. Commun. **7**, 12892 (2016). Copyright 2016 Author(s), licensed under a Creative Commons Attribution (CC BY) license. (f) Graphene layer coupled to a gold waveguide for enhanced saturable absorption. Schematic, SEM image (scale bar, 2 μm), and all-optical switching extinction ratio as a function of pump pulse energy.[361] Reproduced with permission from Schirato *et al.*, Nat. Photonics **14**, 37 (2020). Copyright 2020 Springer Nature.

waveguides, following the Pockels effect. The system achieved efficient modulation of a CW optical carrier signal injected into the waveguides up to a frequency of the applied electrical signal beyond 500 GHz, showing great potential for THz wireless applications. The device presented high power handling and high linearity, which are necessary qualities for a reliable performance. A similar concept has been later applied by Salamin *et al.*,[388] who used a plasmonic Mach–Zehnder interferometer for the detection of THz waves. In this case, the THz

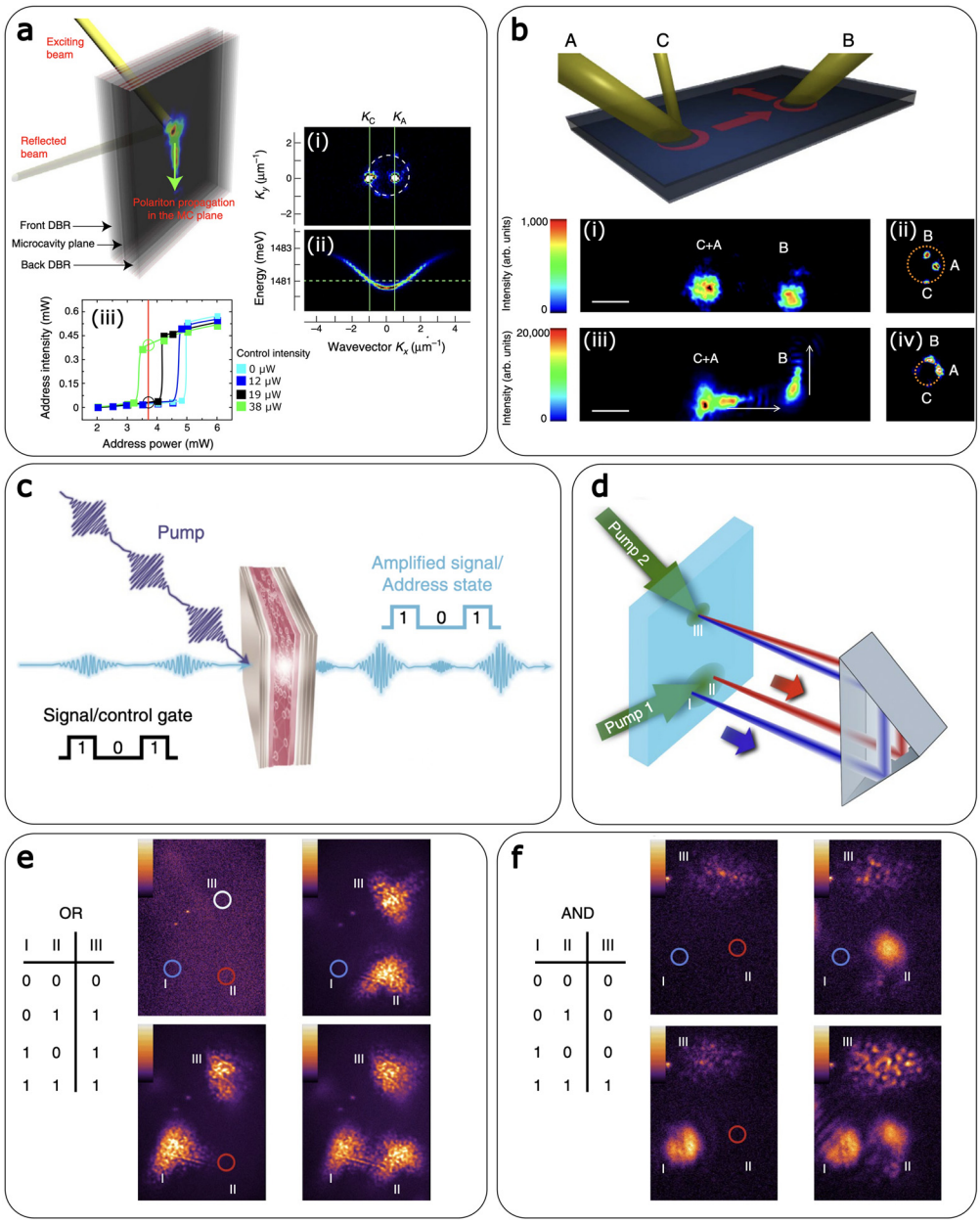

FIG. 11. All-optical transistor. (a) Sketch of the experimental configuration in the work by Ballarini *et al.*[367] The exciting laser beam is directed with an angle on the microcavity sample and partially reflected from the front distributed Bragg reflector (DBR). Polaritons are created within the microcavity plane and propagate with a finite velocity. The one-to-one coupling with the external photons allows the observation of the polariton propagation through the emitted intensity from the back side of the sample. (i) Two-dimensional momentum space image of the emission under high excitation power shows the polariton states created by two laser beams impinging at different angles (K_C and K_A) and same energy. (ii) Polariton dispersion along the direction corresponding to $K_y = 0$ of the upper panel. (iii) The transistor operation is briefly summarized. Address intensity plotted as a function of the Address power for different intensities of the Control: green line ($I_C = 38\ \mu$W), black line ($I_C = 19\ \mu$W), blue line ($I_C = 12\ \mu$W) and without control (light blue line). The red line indicates the power of the Address for which a small change in the Control density brings the Address state from off (black circle) to on (green circle). (b) Illustration of the transistor setup, with two address beams A and B and a control C active at the same location as A. The polariton propagation is indicated with arrows. (i) Emission intensity colormap with both addresses as well as the control below the power thresholds required for resonance. (ii) Far field emission intensity image in momentum space. (iii) Similar image as (i) with C slightly increased. The emission intensity here is about 20 times larger than in (i). (iv) Momentum space image, showing A and B with enhanced emission intensities whilst C is negligible.[367] Reproduced with permission from Ballarini *et al.*, Nat. Commun. **4**, 1778 (2013). Copyright 2013 Springer Nature. (c) Schematic of an all-optical organic polariton transistor. (d) Illustration of AND OR gate operations, with two control pulses regulating addresses I and II. The pump at III is tweaked such that one (two) amplified addresses is necessary to excite the structure at III. (e) Real-space photoluminescence of the transistor with the OR setup and (f) with the AND setup. Working operations are demonstrated in both cases.[368] Reproduced with permission from Zasedatelev *et al.*, Nat. Photonics **13**, 378 (2019). Copyright 2019 Springer Nature.

wave played the role of the externally applied AC electric field in the modulator. The detector performed THz time-domain electro-optic sampling and could directly measure the electric field amplitude and phase of the THz signal. More recently, Koepfli *et al.*[389] showed a >500 GHz bandwidth capability in a plasmonic-metamaterial-enhanced graphene photodetector, which did not need of photonic integrated circuits to operate, outperforming previous implementations including 2D materials[390–394] and easing integration possibilities. Furthermore, by combining the photodetector with plasmonic Mach–Zehnder modulators, they built a plasmonic-to-plasmonic link showing record-breaking 132 Gbps PAM-2 and 128 Gbps PAM-4 data transmission for graphene.

A key aspect of high-speed optical device application is the capability of ultrafast modulation and large modulation depth of HHG.[395] Many of these materials possess ultrafast photoexcitation dynamics and recovery time[396] to facilitate ultrafast control of nonlinear optical phenomena. However, their ultrathin nature makes it challenging to get reasonable efficiency in devices or to allow effective control of light at the nanoscale. This inability to compress light in the nanometric volume and a large momentum mismatch between the far-field photon and the excited optical mode, together with the ultra-thin material thicknesses motivate research efforts to combine these materials with plasmonic resonators and cavities to increase their light–matter interactions.[397,398] The use of plasmonic cavities and resonators together with low-dimensional materials leads to the generation of highly confined and strong EM fields, which can produce nonlinear optical responses such as harmonic generation (second and third harmonic generations, SHG and THG) at relatively low excitation powers (< 3 mW).[399–404] For example, Ren *et al.* reported a SHG enhancement factor of almost 10-fold from $AgInS_2$ QDs embedded in a Ag nanoparticles array under resonance excitation condition (when the LSPR of the Ag nanoparticles' array matches the excitation laser).[404] However, the sensitivity of HHG may become even more prominent under harmonic resonance condition, when the LSPR of the plasmonic system overlaps well with the SHG wavelength of the nanomaterial due to the dipole (SHG)—quadrupole (plasmon) interaction.

As demonstrated by Han *et al.*, overlapping of the LSPR of Ag nanocubes with the propagating SP on Ag film/Al_2O_3 system (nanoparticles on mirror system) with the SHG wavelength at 410 nm from WS_2 monolayer resulted in up to 300-fold enhancement of SHG signal at an excitation power below 100 μW [see Fig. 12(a)].[403] Moreover, a 7000-fold enhancement in the SHG response has been observed when using a plasmonic platform coupled to a WS_2 monolayer.[405] At resonant coupling strength (when the LSPR couples resonantly with the exciton, i.e., in the strong coupling regime), photons confined in the nanometric volume coherently exchange energy with excitons at a rate higher than that of the dephasing processes (i.e., the rate at which photons escape from the cavity or exciton de-phases) creating a nonlinear hybrid quantum state, called polaritons. Such polaritonic states thus, open new avenues like Bose–Einstein condensation,[406] polaritonic lasing,[407] optical parametric amplification,[379] Rydberg excitonic phenomena,[408] etc., in TMDCs to be investigated at near room temperatures owing to the large exciton binding energies in them. Investigation of ultrafast dynamics of these excitonic and polaritonic processes in 2D semiconductor/plasmonic heterostructures is a growing research area with an opportunity to provide a deeper or new understanding of plasmon–exciton energy exchange effects and nonlinear optical modulation on the ultrafast timescale under deep-subwavelength optical confinement.[369,409–417] For example, Tang *et al.*[417] studied the ultrafast dynamics of the nonlinear response from WS_2 monolayer coupled to silver nanodisks in the strong coupling regime. They observed that with increasing fluences, plasmon–exciton polaritons (plexcitons) become weaker. In Fig. 12(b), it is shown a series of reflection spectra demonstrating coherent plexcitons formation at 100 fs under various pump incident fluences. The upper and lower branch modes of the plexcitons systematically shift toward the exciton resonance with increasing fluence resulting in reduction of spectral splitting, and exhibit considerable linewidth broadening, bringing about an apparent rise of the splitting window (increasing valley). Their pump–probe measurement unveiled a giant plasmon induced nonlinearity with non-equilibrium exciton–plasmon processes over distinct time scales governed by (1) repulsive Coulomb interaction between excitons and (2) Pauli blocking resulting in excitonic saturation and reducing exciton–photon coupling strength.[398]

Plasmon induced strong exciton–polariton interaction at the ultrafast timescale in 2D semiconductors is a promising candidate for nano-light sources. For example, ultrafast exciton–polariton modulation is an essential capability for an ideal on-chip nanophotonic device (such as nanolasers). Conventional bulk nonlinear materials can achieve modulation depth on the order of 1–10 dB μm^{-1} with a response time around picoseconds but require a high pulse energy in the tens pJ range.[416,418,419] The current state-of-art graphene based plasmonic modulators have achieved a modulation depth of 0.2 dB μm^{-1} with a switching energy of 155 fJ and have achieved a speed of 2.2 ps.[361,420] Importantly, 2D semiconductors such as black phosphorus and transition-metal dichalcogenides are also known for their strong light–matter interactions and large third-order nonlinear optical susceptibilities near excitonic resonances.[418–420] Furthermore, the excitons in these 2D semiconductors have been experimentally demonstrated to interact with SPPs on a femtosecond timescale.[369] Recently, Klein *et al.*[411] reported a modulation depth per unit length of 0.04 dB μm^{-1} with a switching speed of 290 fs in WSe_2 based plasmonic modulator with an excitation pulse energy of 650 fJ. The modulation bandwidth approaching ~1 THz achieved by Klein *et al.* is very promising for future ultrafast plasmonic amplifiers and switching applications.

In addition to their outstanding capability of light-trapping and concentrating/amplifying an EM field in nanometric volumes, plasmonic nanostructures can also convert light into electrical energy by generating hot electrons.

As mentioned in Sec. III, upon optical absorption and plasmon excitation in the nanostructures, the decaying plasmon field transfers accumulated energy (via Landau damping) to the conduction band electrons. The efficiency of hot electron generation depends on multiple factors.[43] Among them, the most important one is the LSPR effect. At the LSPR resonance frequency the photon excitation produces the maximum number of highly energetic electrons ready to escape the metal surfaces. Thus, hot electrons can transfer into the unoccupied states of nearby semiconductors, when put in contact with the metal nanostructures that are being resonantly excited at the LSPR frequency[43,423] (see also Sec. III). For example, Shan *et al.*[421] demonstrated direct evidence of plasmonic hot electron transfer from a gold

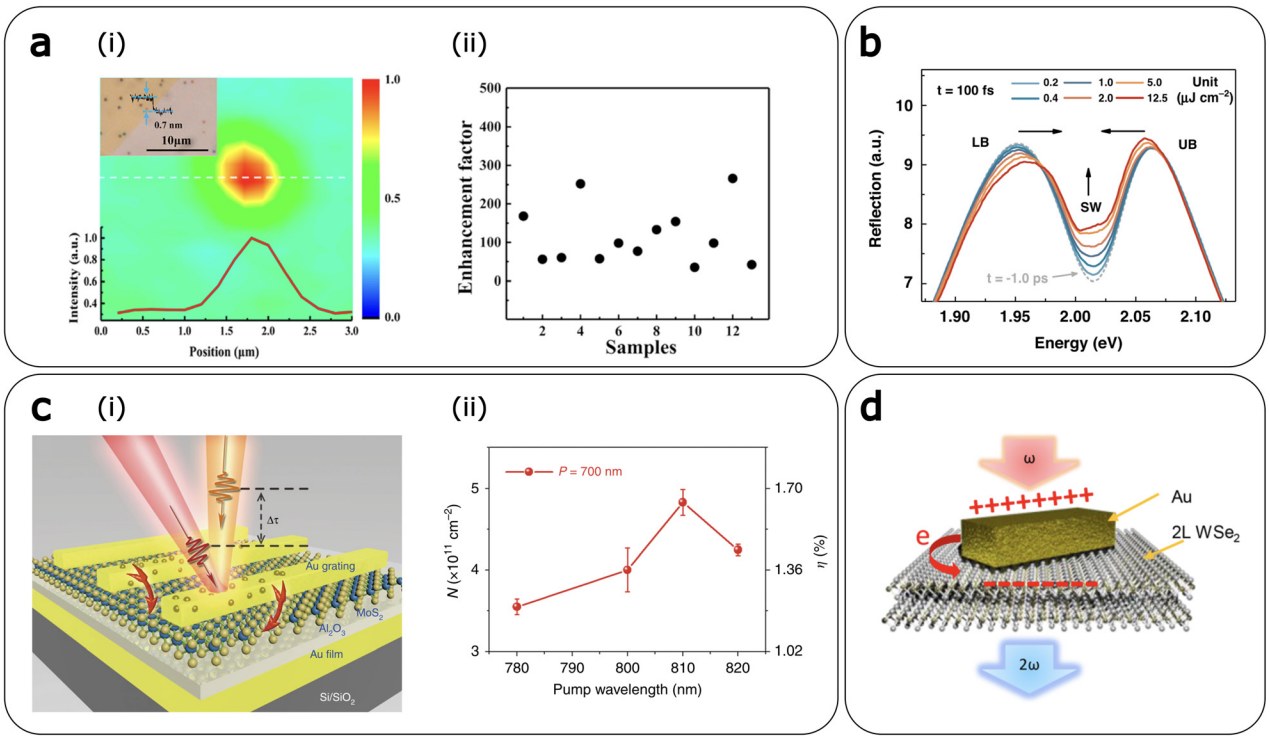

FIG. 12. Application of ultrafast plasmonics in low-dimensional semiconductors. (a-i) Normalized SHG intensity map of a monolayer WS_2 integrated in a plasmonic nanocavity with a scanning step of 200 nm. The curve is the SHG intensity line profile along the white dashed line. Inset shows an optical micrograph of the hybrid system where the black dots are the Ag nanocubes. (ii) SHG enhancement factor with different Ag nanocubes under fixed excitation laser with wavelength of 820 nm.[403] Reproduced with permission from Han *et al.*, ACS Photonics **7**, 562 (2020). Copyright 2020 American Chemical Society. (b) Transient reflection spectra of the WS_2/Au-nanodiscs plexciton system measured at 100 fs at different fluence rate. The gray dashed line is the unaffected probe spectrum by probe pulse at −1 ps.[417] Reproduced with permission from Tang *et al.*, Light: Sci. Appl. **11**, 94 (2022). Copyright 2022 Author(s), licensed under a Creative Commons Attribution (CC BY) license. (c-i) Schematic of pump–probe measurements on Au grating/MoS_2/Al_2O_3/Au sandwiched heterostructure to demonstrate plasmonic hot electron transfer from a gold grating to the MoS_2 monolayer. (ii) Pump wavelength dependent injected hot electron densities using the previous setup from (d) and corresponding efficiency for the heterostructure with 700 nm grating period.[421] Reproduced with permission from Shan *et al.*, Light: Sci. Appl. **8**, 9 (2019). Copyright 2016 Author(s), licensed under a Creative Commons Attribution (CC BY) license. (d) A diagrammatic model to describe the hot electron induced symmetry breaking and probing SHG in a Au/2L WSe_2 hybrid system.[422] Reproduced with permission from Wen *et al.*, Nano Lett. **18**, 1686 (2018). Copyright 2018 American Chemical Society.

grating to a MoS_2 monolayer, that occurs at ∼40 fs with a maximum efficiency of 1.65%. The coupling between LSP of Au grating on top and SPP of Au film underneath [see Fig. 12(c)] facilitated coherent energy exchange and created a strong out-of-plane electric field, which decreases the radiative damping rate of LSPR and accelerates exportation of hot electrons into MoS_2. The net energy produced in the coupling process (the SP energy otherwise produces heat) is recycled to generate hot electrons via LSPR of the gratings. As a result, pumping of hot electrons and the consequent injection into the MoS_2 monolayer was amplified as shown in Fig. 12(c).

Harvesting plasmonic hot electrons into a semiconductor has multi-faceted applications. They can be used for light harvesting and optoelectronics,[213,259] probing mobility via Fröhlich interaction,[424] and photocatalysis as well as H_2 evolution.[425,426] Due to strong spatial confinement of 2D semiconductors, injection of hot electrons may introduce additional effects, which are unseen in bulk systems. For example, a giant bandgap renormalization in WS_2 (550 meV) at room temperature,[427] and semiconducting to metallic phase transition in monolayer MoS_2[428,429] have been reported in the literature. Plasmonic hot electrons can also be used to break the inversion symmetry in 2D semiconductors leading to the observation of SHG signal. Controlling SHG is fundamental to nonlinear optical applications, which requires a non-zero second order susceptibility tensor only observed in a non-centrosymmetric system. Therefore, generating SHG signal in a centrosymmetric bilayer TMDCs systems was endeavored via breaking the inversion symmetry by an external electric field.[430] However, this method of controlling SHG cannot occur at ultrafast timescale, since required voltage is typically high and at high operating frequencies current becomes unsustainable. Wen *et al.*[422] reported the symmetry breaking in bilayer WSe_2 using plasmonic hot electron injection, which works on a similar principle but at an ultrafast timescale [principle of SHG from bilayer WSe_2 is schematically presented in Fig. 12(d)]. The injected electrons create an asymmetric electric field inside the bilayer, causing a symmetry breaking and induce SHG signal, which is also aided by the presence of LSPR induced strong local field at the proximity. The recorded rise and fall time of hot electrons were 119 fs and 1.84 ps, respectively, indicating great promise for ultrafast nonlinear applications.

VI. ULTRAFAST PLASMONICS AT HIGH INTENSITIES, FROM THE STRONG FIELD TO THE RELATIVISTIC REGIME

In the former sections, light pulses with low intensity were utilized to trigger reproducible plasmon-driven physical and chemical processes in various types of nanostructures. When laser intensity reaches 10^{11}–10^{13} W/cm^2, irradiation of nano-objects in vacuum leads to the emission of low energy (1–100 eV) electrons.[431–433] Under certain conditions, these electrons can interact with a resonant state of the nanostructures themselves, i.e., either LSPs[434] or SPPs,[435] which can further accelerate them up to 1 keV. In addition to providing insight into the fundamental processes that take place in this regime,[8,436] these electrons are well suited for various applications, such as U-TEM, as already discussed in Sec. II.[437]

By increasing the laser intensity further, the material starts to be significantly ionized and optically damaged. This way sub-optical cycle metallization of SiO_2 nanospheres has been demonstrated by measuring an increased cutoff energy of the emitted electrons in few-cycle laser pulses around 2×10^{14} W/cm^2 intensity.[438] Already at these low ionization levels, the temporal change of electron density plays an important role as it strongly limits the resonance in time (when the plasma frequency is equal to the laser frequency) and sets the field enhancement factor to about 3 when the critical electron density is surpassed. If the laser intensity is further increased beyond the optical damage threshold, the plasma, that optimally is still nm sized, dominates the interaction with the laser pulse. This is a hot, overdense ($n_e \gg n_{crit}$, where n_{crit} is the critical density) and spatially strongly inhomogeneous plasma, which quickly expands in space and reaches μm extension within a few ps after its generation. A fundamental laser property in the ultrahigh laser intensity regime determining the generation time of the plasma is the high-dynamic-range temporal intensity contrast.[439] It describes the laser intensity at a certain time instant normalized to the peak temporal intensity of the pulse. In practice, depending on the details, 10^6–10^{10} times lower intensity than the peak value can ionize the target and generate plasma. For typical lasers, these levels are reached not only ps, but even ns before the fs laser pulse and thus the limited contrast of modern high-intensity lasers strongly limits their application for nanophotonics and, therefore, also the number of published papers. Various methods such as the generation of the second harmonic and the utilization of the so-called plasma mirror can improve the contrast of lasers at the cost of lower pulse energy. Another alternative is light sources based on Optical Parametric Chirped-Pulse Amplifiers (OPCPA), which typically have excellent contrast.[440]

Atomic clusters, an intermediate form of matter between molecules and solids, with typical diameters of a few nm, have been used as target to investigate laser–cluster interactions. Clusters are generated by a gas jet plume, originating from a cryogenically cooled gas nozzle, expanding into vacuum and cooling during expansion. The interaction of moderately high intensity laser pulses (10^{16}–10^{17} W/cm^2) with gas-phase cluster targets have been investigated under different conditions. Coulomb explosion of hydrogen clusters has yielded protons with 8 keV kinetic energy in good agreement with expectations.[441] However, xenon cluster explosions have produced xenon ions with kinetic energies up to 1 MeV, much beyond ion energies from molecular or small cluster targets.[442] This is explained by the fact that the expansion of the clusters reduces the electron density to a point where the plasma frequency is resonant with the laser frequency. By applying deuterium clusters Ditmire *et al.* have observed D–D fusion from Coulomb exploding clusters and created large number of fusion neutrons (10^5 neutrons/J laser energy) with a table top laser.[443]

At an intensity of about 10^{18} W/cm^2 (at $\sim$1 μm wavelength), a free electron starts to oscillate in the laser field with relativistic velocity, therefore this value is the *relativistic intensity* limit. Due to the demanding temporal contrast requirements, only a few works have been performed at such a high intensity with nanoobjects. One of the existing lines of investigation studied the interaction between the high fields of the laser and propagating surface plasmons [Fig. 13(a)]. To this end, optical gratings were utilized as targets representing nm extension in one dimension and nm modulation in another one, as schematically shown in Fig. 13(b). Certain high-order harmonics are predicted to be generated at the wavelength of the grating period and its harmonics by attosecond electron bunches parallel to the target surface in the case of perpendicular laser incidence.[444] It has been confirmed experimentally by Cerchez *et al.*,[445] by showing that high-order harmonics with parameter-dependent spectral composition from grating targets can be emitted under grazing emission angles separated from the laser fundamental radiation. Grating targets irradiated by 5×10^{19} W/cm^2 laser intensity under resonant conditions resulted in the generation of 100 pC electron bunches with 5–15 MeV energy along the target surface by propagating relativistic surface plasma waves.[446] Flat targets under the same conditions produced much less, lower energy electrons as shown in Fig. 13(c). Resonant excitation of surface waves on thin grating targets also increases the laser absorption and proton energies by a factor of 2.5 from the target normal sheet acceleration as demonstrated by Ceccotti *et al.*[447]

Another line of experiments focused in the generation of volumetric plasmas that are simultaneously dense and hot. In general, a relativistic laser pulse interacting with solid matter creates a layer of plasma at the surface of the material, which stays overdense for the typical time duration of the pulse (5–100 fs). Once established early in the interaction, this overdense plasma prevents the remaining of the incoming laser pulse to penetrate and heat it up deeper than typically a few 100 nm. Effectively, this limits the volume of matter that is efficiently heated and challenges the creation of extreme laser-generated plasmas. However, it has been shown that this constraint can be cleverly avoided when an array of vertically aligned nanowires, shown in Fig. 13(d), is used as laser target.[448] The incident laser pulse propagates along the space between the nanowires, which are about 10 μm long, producing higher electron density ($100n_{crit}$), higher temperatures (multi-keV), higher laser absorption, and increased x-ray radiation than when utilizing flat targets under the same conditions. This technique has been utilized to accelerate ions and realize deuterium–deuterium fusion with increased neutron yield.[449,450]

The last type of investigations is based on single 2D and 3D nanotargets. Numerical simulations have predicted attosecond electron bunches with relativistic energy from the interaction of (overdense) plasma nanodroplets with relativistic intensity laser pulses.[451,452] The interaction is described by a two-step model as illustrated in Figs. 13(e) and 13(f).[453,454] The first step is the nanophotonic emission of relativistic electrons from the target by the localized surface plasmon and the enhanced local fields. This step is mainly governed by the Mie theory and the emission directions correspond to the angles of maximum field enhancement. The second step is

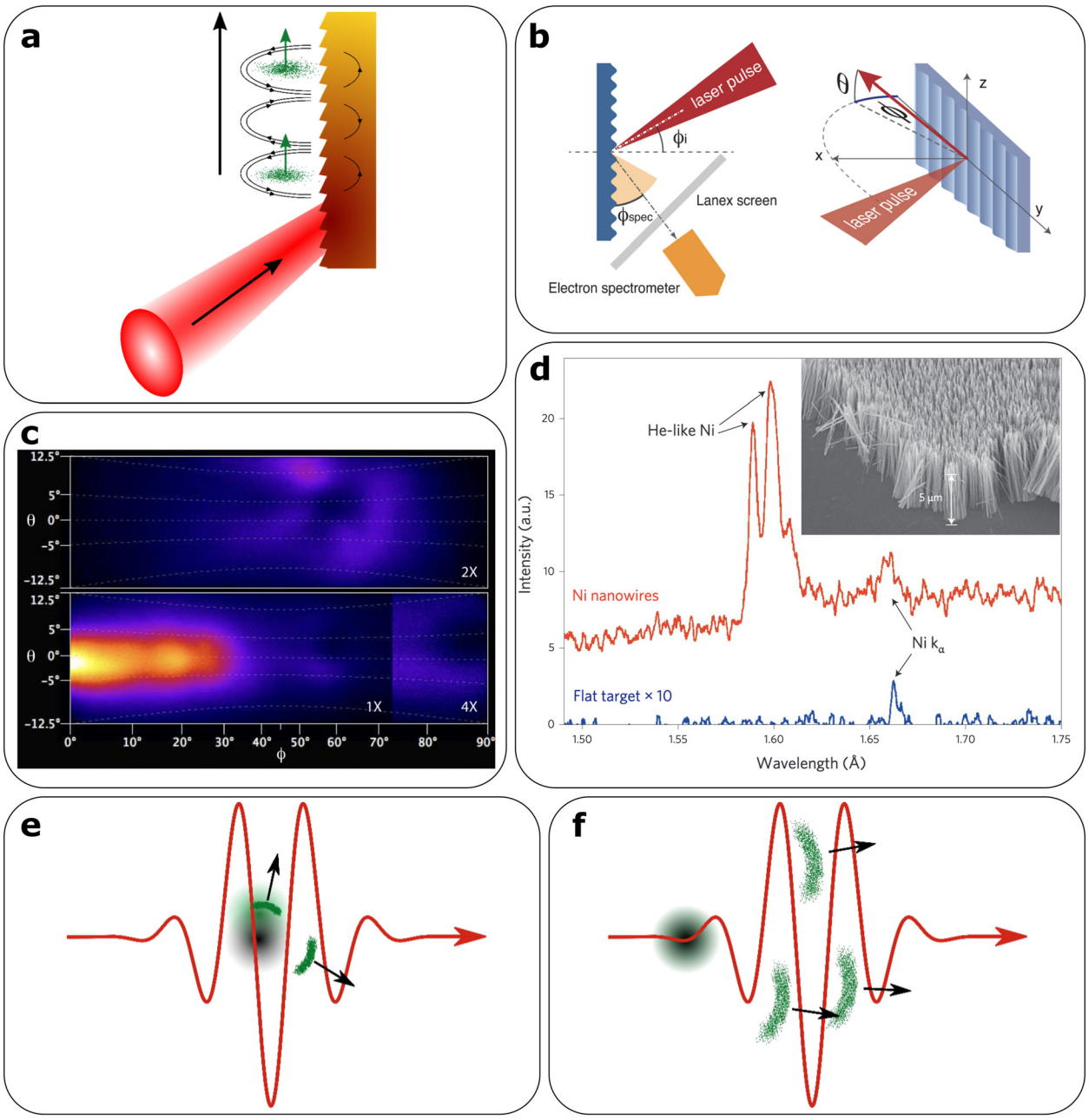

FIG. 13. Different types of relativistic surface plasma experiments. (a) Illustrates the principle of SPP-based electron acceleration. The laser pulse produces plasma on the grating surface (dark red–yellow) and under optimal angle of incidence generates a SPP (represented by black electric field lines) that accelerates electrons (green dots) along the surface. (b) Setup for generating propagating surface plasmons along a grating. (c) Angularly resolved electron emission measured when using a flat surface (top) and a grating (bottom) as targets. A filter placed in front of the detector cut off electrons with energies below 1.3 MeV. The upper and the right bottom panels have been amplified 2× and 4× compared with the bottom left to highlight features in the signals.[446] Reproduced with permission from Fedeli *et al.*, Phys. Rev. Lett. **116**, 015001 (2016). Copyright 2016 American Physical Society. (d) Measured single-shot x-ray emission when utilizing an array of nanowires (red), shown in the inset, and a flat surface (blue) for comparison. Notice that besides the increase in signal corresponding to the K_α line, the array of nanowires shows a strong He-like Ni signature, highlighting the high degree of ionization and plasma density.[448] Reproduced with permission from Purvis *et al.*, Nat. Photonics **7**, 796 (2013). Copyright 2013 Springer Nature. (e) and (f) show the first and second step of relativistic electron acceleration from nanodroplets. First, (e) an electron bunch is extracted and accelerated by LSP away from nanodroplet in a direction determined by Mie scattering for every half cycle of the driving laser. Then, (f) the bunches are further accelerated in the laser propagation direction by vacuum–laser acceleration.

vacuum–laser acceleration (VLA) of these electrons that co-propagate with the laser pulse. Electrons propagate in two main directions on the two sides near the laser direction. This final angular distribution of the electrons is mainly determined by VLA, although the first step has also some influence. Utilizing few-cycle laser pulses, a relativistic isolated attosecond electron bunch is generated on one side, though the process is carrier-envelope phase (CEP) dependent.[455] These nanodroplets, after the electrons are removed by the laser, have been suggested for Coulomb-explosion-dominated ion acceleration to (laser intensity-dependent) few MeV–few 10 MeV ion energy using two-cycle laser pulses.[456]

In an experiment [Fig. 14(a)], nanotips with 100 nm tip diameter have been irradiated with 6×10^{19} W/cm^2 intensity sub-two-cycle pulses and measured intensity-dependent electron propagation angle, corresponding to the relativistic ponderomotive scattering angle.[454] This supports the VLA process, though, slight direction change was also detected when the target size was changed. The electron energy spectrum was broad, peaked at 3–5 MeV and extended up to 9 MeV [Fig. 14(b)], indicating relativistic electron bunches with charges up to 100 pC ($\sim 10^9$ electrons) injected and accelerated within a half optical cycle [in fair agreement with the simulations shown in Fig. 14(c)]. CEP dependence of the propagation angle as well as angular distribution have been demonstrated as shown in Fig. 14(d). Strong indication of >TV/m fields accelerating the electrons has been presented that significantly surpasses former values.

VII. CONCLUSIONS AND FUTURE PERSPECTIVES

In this review, we have explored the current state and future prospects of the field of ultrafast plasmonics, ranging from fundamental science to technological aspects. We have focused the reader attention to the state-of-the-art of modeling methods and experimental techniques that have been developed over the last decade to unveil the interaction of ultrafast pulses with nanostructured optical materials made of noble metals, highly doped semiconductors, and hybrid plasmonic–dielectric/low-dimensional semiconductors and/or molecular systems. To this end, we have showcased most recent works to uncover the light–matter interaction with the highest possible spatial and temporal resolutions. The ability to measure and understand the ultrafast response of materials on the nanoscale is crucial for future development of functioning devices. Therein, pushing the time-resolution of experiments by employment of ever shorter probe pulses, even below one femtosecond, will allow to directly study fundamental material responses on the level of the cycles of light. Further, it is now possible for experimentalists to correlate such fundamental processes, like absorption or emission of light, at the single-particle level, promising many exciting discoveries in ultrafast plasmonics related to the quantum nature underlying the excitation of the material.[457]

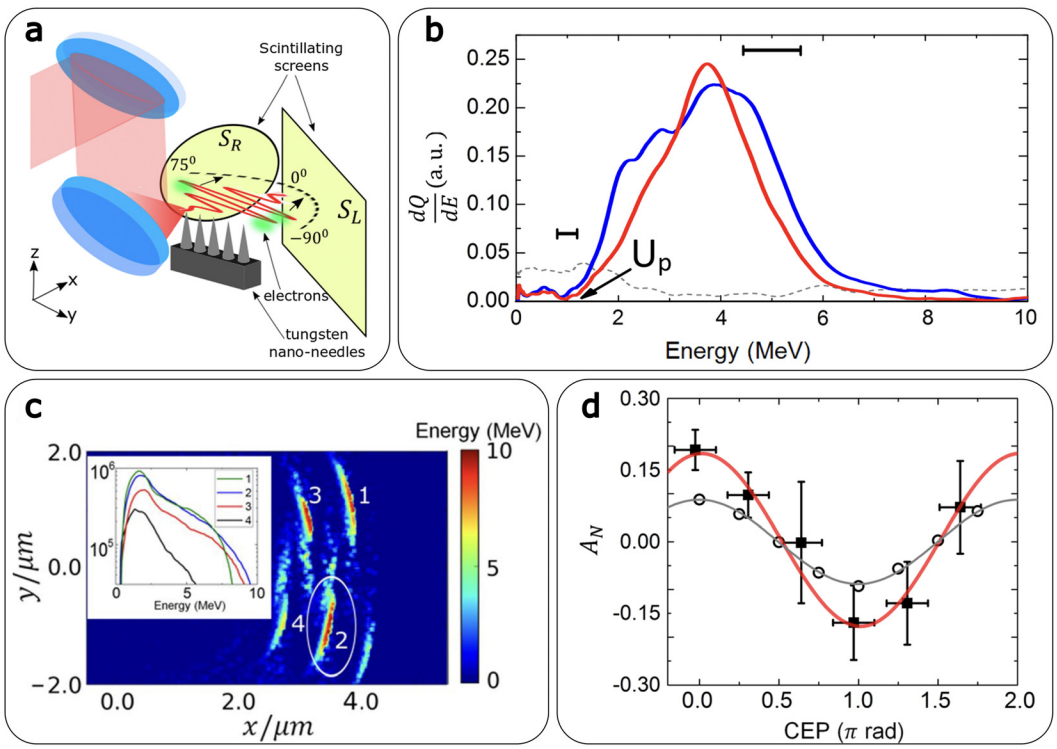

FIG. 14. Acceleration of electrons from isolated nanotips in the relativistic nanophotonics regime. (a) Setup for relativistic electron acceleration using nanotips. The incident pulse is focused on tungsten nano-needles. Scintillating screens are used to detect the generated electron beams. (b) Experimental energy spectrum of the accelerated electrons, with the red and blue curves representing the results of two typical single-shots. (c) Particle in a cell simulation of the emitted electron bunches, with the predicted energy spectra of every bunch as an inset. (d) Correlation between asymmetry in the measured (full squares) and simulated (open circles) electron emission direction and CEP of the driving laser.[454] Reproduced with permission from Cardenas *et al.*, Sci. Rep. **9**, 7321 (2019). Copyright 2019 Author(s), licensed under a Creative Commons Attribution (CC BY) license.

In addition, because of the different length and time scales involved in the plasmon relaxation dynamics, we have pointed out that only a proper synergistic cooperation between state-of-the-art experimental and theoretical methods can be effective for achieving an understanding of such complicated dynamical processes. From a theoretical standpoint, the current scientific interest is directed toward extending real-time *ab initio* methods in combination with multiscale approaches, so to make it computationally feasible the analysis of phenomena that span different length and time scales, such as hot carriers transport properties of plasmonic materials, thus not only focusing on plasmonic absorption and subsequent generation of hot carriers.[174,189] This aspect, which cannot be adequately treated without an appropriate inclusion of the real material atomistic structure,[173] is crucial for a rational design of plasmonic nanomaterials with applications in photocatalysis, energy storage, and so forth. We have also showcased how plasmonic nanostructures have an unprecedented potential to convert light into chemical energy, addressing thus fundamental issues of our modern society, such as decreasing the atmospheric greenhouse gasses and developing new technologies for sustainable energy production. To this end, understanding the ultrafast dynamics of non-thermal (or hot) charge carriers as well as the electron–phonon and phonon–phonon interactions is crucial for developing new efficient plasmonic catalysts. Although the hot carrier dynamic in purely plasmonic systems has been unraveled by ultrafast spectroscopy, this is not yet the case for more complex (and relevant) interfaces, such as hybrid plasmonic catalysts (i.e., metal–metal, metal–semiconductor, or metal–perovskite systems).[203] Thus, exploring the phonon dynamics and hot carrier relaxation mechanisms in plasmonic hybrid systems will help decode the roles of temperature and non-thermal charge carriers for driving and enhancing chemical reactions. This new direction of research can lead to completely new plasmonic hybrid materials in the upcoming years with exciting properties for energy conversion.[458] Furthermore, we have shown how the combination of nanophotonics, magnetoplasmonics, and spintronics opens new possibilities for the practical implementation of magnetic field-controllable nanoscale devices for ultrafast data processing and storage. In this context, plasmonics might enable all-optical magnetization switching to reach the atomic scale.[459–464] By exploiting the non-thermal dynamics of the electron gas, we expect that novel plasmon-driven phenomena can be discovered and controlled for the duration of the laser pulse (sub-10 fs), where the microscopic degrees of freedom, such as the spin, can be strongly coupled to the amplitude, frequency, and polarization of the plasmonic field. This direction is still unexplored and can become a rising research line in the upcoming years, as it might unveil novel pathways to control spin dynamics in the non-thermal regime also with metallic nanostructures, thus overcoming the intrinsic limitations placed by Ohmic and other losses, opening excellent opportunities toward plasmon-driven ultrafast magneto-optics. We have also shown that plasmonics can serve as an important tool to push toward low-power all-optical ultrafast processing applications. Pure plasmonic platforms already offer the possibility of sub-100 fs all-optical modulators, however at the cost of relatively high control energies and offering only low switching contrasts. Recent investigations that combine plasmonics with other nonlinear elements, such as graphene, ITO, or ultrathin semiconductor materials with strong excitonic effects, suggest a promising path toward the development of efficient ultrafast all-optical switches. A route that has not yet been addressed for this purpose is the formation of hybrid systems incorporating high-index dielectric nanoscale resonators, which could help bringing down the required control powers due to their low losses, high optical nonlinearities, and field confinement abilities. We have also summarized some representative nonlinear optical applications of low-dimensional semiconductors incorporated with plasmonic materials, which offer great promise for novel ultrafast optical applications.[12,465,466] Although their ultrathin thickness and large momentum mismatch with photon provide a major challenge to tame light into nanometric volume, we predict new breakthrough experiments combining these materials with plasmonic and dielectric nanophotonic systems in coming years, thus driving the field into new directions. In particular, special emphasis should be given to controlling the optical damage threshold, influence of intrinsic (such as doping, crystal structure, and vdW supercell) as well as extrinsic (such as electric field, strain) parameters on nonlinear optical properties in this novel class of materials, and finally, care must also be taken to developing novel device fabrication processes that preserve the materials' properties. Finally, we gave a snapshot of ultrafast plasmonics in the relativistic realm. The latter is a promising field of science with potential applications in fusion research, or as novel particle and light sources providing properties such as attosecond duration that is not available from other sources nowadays.

ACKNOWLEDGMENTS

N.M. acknowledges support from the Swedish Research Council (Grant No. 2021–05784) and Kempestiftelserna (Grant No. JCK-3122). N.M. and S.C. acknowledge support from the European Innovation Council (Grant No. 101046920 "iSenseDNA"). N.M. and D.B. acknowledge support from the Luxembourg National Research Fund (Grant No. C19/MS/13624497 "ULTRON"). N.M., D.B., and S.C. acknowledge support from the European Commission (Grant No. 964363 "ProID"). D.B. acknowledges support from the European Research Council (Grant No. 819871 "UpTempo") and the European Regional Development Fund Program (Grant No. 2017-03-022-19 "Lux-Ultra-Fast"). L.V. acknowledges support from the Swedish Research Council (Grant Nos. 2019-02376 and 2020-05111), Knut och Alice Wallenberg Stiftelse (Grant No. 2019.0140), and Kempestiftelserna (Grant No. SMK21-0017). A.S. and E.C. acknowledge German Research Foundation under e-conversion Germanýs Excellence Strategy (Grant No. EXC 2089/1-390776260), the Bavarian program Solar Energies Go Hybrid (SolTech), the Center for NanoScience (CeNS) and the European Research Council (Grant No. 802989 "CATALIGHT"). G.G. acknowledges funding from Agencia Nacional de Promoción de la Investigación, el Desarrollo Tecnológico y la Innovación (Grant No. PICT 2019-01886), Consejo Nacional de Investigaciones Científicas y Técnicas (Grant No. PIP 112 202001 01465) and Universidad de Buenos Aires (Project No. 20020190200296BA). D.J. acknowledges partial support by the Asian Office of Aerospace Research and Development of the Air Force Office of Scientific Research (Grant Nos. FA2386-20-1-4074 and FA2386-21-1-4063). M.R. acknowledges support from the German Research Foundation for Walter Benjamin Fellowship (Award No. RA 3646/1-1). D.G. acknowledges support from the European Commission (Grant No. 964995 "DNA-FAIRYLIGHTS"). A.N.K. acknowledges support from the Chinese Academy of sciences President's International

Fellowship Initiative (Grant No. 2023VMC0020). A.S. acknowledges the Alexander von Humboldt Foundation for a postdoctoral fellowship.

AUTHOR DECLARATIONS

Conflict of Interest

The authors have no conflicts to disclose.

Author Contributions

Alemayehu Nana Koya, Marco Romanelli, Joel Kuttruff, Nils Henriksson, Andrei Stefancu, Gustavo Grinblat, Aitor De Andres, Fritz Schnur, Mirko Vanzan, Margherita Marsili, and Mahfujur Rahaman contributed equally to this work.

Alemayehu Nana Koya: Conceptualization (equal); Writing – original draft (equal); Writing – review & editing (equal). **Margherita Marsili:** Conceptualization (equal); Writing – original draft (equal); Writing – review & editing (equal). **Mahfujur Rahaman:** Conceptualization (equal); Writing – original draft (equal); Writing – review & editing (equal). **Alba Viejo Rodríguez:** Conceptualization (supporting); Writing – original draft (supporting); Writing – review & editing (supporting). **Tlek Tapani:** Conceptualization (supporting); Writing – original draft (supporting); Writing – review & editing (supporting). **Haifeng Lin:** Writing – review & editing (supporting). **Bereket Dalga Dana:** Writing – review & editing (supporting). **Jingquan Lin:** Writing – review & editing (supporting). **Grégory Barbillon:** Writing – review & editing (supporting). **Remo Proietti Zaccaria:** Writing – review & editing (supporting). **Daniele Brida:** Funding acquisition (supporting); Writing – review & editing (supporting). **Marco Romanelli:** Conceptualization (equal); Writing – original draft (equal); Writing – review & editing (equal). **Deep Jariwala:** Conceptualization (equal); Funding acquisition (equal); Supervision (equal); Writing – original draft (equal); Writing – review & editing (equal). **László Veisz:** Conceptualization (equal); Funding acquisition (equal); Supervision (equal); Writing – original draft (equal); Writing – review & editing (equal). **Emiliano Cortés:** Conceptualization (equal); Funding acquisition (equal); Supervision (equal); Writing – original draft (equal); Writing – review & editing (equal). **Stefano Corni:** Conceptualization (equal); Funding acquisition (equal); Supervision (equal); Writing – original draft (equal); Writing – review & editing (equal). **Denis Garoli:** Conceptualization (equal); Funding acquisition (equal); Supervision (equal); Writing – original draft (equal); Writing – review & editing (equal). **Nicolò Maccaferri:** Conceptualization (lead); Funding acquisition (equal); Supervision (lead); Writing – original draft (equal); Writing – review & editing (equal). **Joel Kuttruff:** Conceptualization (equal); Writing – original draft (equal); Writing – review & editing (equal). **Nils Henriksson:** Conceptualization (equal); Writing – original draft (equal); Writing – review & editing (equal). **Andrei Stefancu:** Conceptualization (equal); Writing – original draft (equal); Writing – review & editing (equal). **Gustavo Grinblat:** Conceptualization (equal); Writing – original draft (equal); Writing – review & editing (equal). **Aitor De Andres:** Conceptualization (equal); Writing – original draft (equal); Writing – review & editing (equal). **Fritz Schnur:** Conceptualization (equal); Writing – original draft (equal); Writing – review & editing (equal). **Mirko Vanzan:** Conceptualization (equal); Writing – original draft (equal); Writing – review & editing (equal).

DATA AVAILABILITY

Data sharing is not applicable to this article as no new data were created or analyzed in this study.

REFERENCES

[1]E. Ozbay, "Plasmonics: Merging photonics and electronics at nanoscale dimensions," Science **311**(5758), 189–193 (2006).
[2]R. Zia, J. A. Schuller, A. Chandran, and M. L. Brongersma, "Plasmonics: The next chip-scale technology," Mater. Today **9**(7–8), 20–27 (2006).
[3]S. A. Maier, *Plasmonics: Fundamentals and Applications* (Springer US, 2007).
[4]A. Polman, "Plasmonics applied," Science **322**(5903), 868–869 (2008).
[5]D. K. Gramotnev and S. I. Bozhevolnyi, "Plasmonics beyond the diffraction limit," Nat. Photonics **4**(2), 83–91 (2010).
[6]J. A. Schuller, E. S. Barnard, W. Cai, Y. C. Jun, J. S. White, and M. L. Brongersma, "Plasmonics for extreme light concentration and manipulation," Nat. Mater. **9**(3), 193–204 (2010).
[7]M. I. Stockman, "Nanoplasmonics: The physics behind the applications," Phys. Today **64**(2), 39–44 (2011).
[8]M. I. Stockman, "Nanoplasmonics: Past, present, and glimpse into future," Opt. Express **19**(22), 22029 (2011).
[9]D. Brinks, M. Castro-Lopez, R. Hildner, and N. F. van Hulst, "Plasmonic antennas as design elements for coherent ultrafast nanophotonics," Proc. Natl. Acad. Sci. U. S. A. **110**(46), 18386–18390 (2013).
[10]A. N. Koya and J. Lin, "Charge transfer plasmons: Recent theoretical and experimental developments," Appl. Phys. Rev. **4**(2), 021104 (2017).
[11]J. J. Baumberg, J. Aizpurua, M. H. Mikkelsen, and D. R. Smith, "Extreme nanophotonics from ultrathin metallic gaps," Nat. Mater. **18**(7), 668–678 (2019).
[12]N. Maccaferri, G. Barbillon, A. N. Koya, G. Lu, G. P. Acuna, and D. Garoli, "Recent advances in plasmonic nanocavities for single-molecule spectroscopy," Nanoscale Adv. **3**(3), 633–642 (2021).
[13]K. F. MacDonald, Z. L. Sámson, M. I. Stockman, and N. I. Zheludev, "Ultrafast active plasmonics," Nat. Photonics **3**(1), 55–58 (2008).
[14]L. Cao and M. L. Brongersma, "Ultrafast developments," Nat. Photonics **3**(1), 12–13 (2009).
[15]D. N. Basov and M. M. Fogler, "The quest for ultrafast plasmonics," Nat. Nanotechnol. **12**(3), 187–188 (2016).
[16]N. Maccaferri, S. Meuret, N. Kornienko, and D. Jariwala, "Speeding up nanoscience and nanotechnology with ultrafast plasmonics," Nano Lett. **20**(8), 5593–5596 (2020).
[17]S. Kim, T.-I. Jeong, J. Park, M. F. Ciappina, and S. Kim, "Recent advances in ultrafast plasmonics: From strong field physics to ultraprecision spectroscopy," Nanophotonics **11**(11), 2393–2431 (2022).
[18]J. Khurgin, A. Y. Bykov, and A. V. Zayats, "Hot-electron dynamics in plasmonic nanostructures," arXiv:2302.10247 (2023).
[19]P. Vasa, C. Ropers, R. Pomraenke, and C. Lienau, "Ultra-fast nano-optics," Laser Photonics Rev. **3**(6), 483–507 (2009).
[20]L. Piatkowski, N. Accanto, and N. F. van Hulst, "Ultrafast meets ultrasmall: Controlling nanoantennas and molecules," ACS Photonics **3**(8), 1401–1414 (2016).
[21]S. V. Makarov, A. S. Zalogina, M. Tajik, D. A. Zuev, M. V. Rybin, A. A. Kuchmizhak, S. Juodkazis, and Y. Kivshar, "Light-induced tuning and reconfiguration of nanophotonic structures," Laser Photonics Rev. **11**(5), 1700108 (2017).
[22]D. Neshev and I. Aharonovich, "Optical metasurfaces: New generation building blocks for multi-functional optics," Light **7**(1), 58 (2018).
[23]D. D. Hickstein, D. R. Carlson, H. Mundoor, J. B. Khurgin, K. Srinivasan, D. Westly, A. Kowligy, I. I. Smalyukh, S. A. Diddams, and S. B. Papp, "Self-organized nonlinear gratings for ultrafast nanophotonics," Nat. Photonics **13**(7), 494–499 (2019).
[24]E. Herkert, N. Slesiona, M. E. Recchia, T. Deckert, M. F. Garcia-Parajo, E. M. Fantuzzi, A. Pruccoli, I. C. Ragupathy, D. Gudavičius, H. Rigneault, J. Majer, A. Zumbusch, E. Munger, S. Brasselet, A. T. Jones, P. Watson, S. A. Boppart, V. Singh, S. Borkar, F. E. Quintela Rodriguez, W. Langbein, V. Petropoulos,

N. F. van Hulst, M. Maiuri, G. Cerullo, D. Brida, F. Troiani, C. A. Rozzi, E. Molinari, M. Vengris, and P. Borri, "Roadmap on bio-nano-photonics," J. Opt. **23**(7), 073001 (2021).
[25]J.-S. Huang and Y. Kivshar, "Special issue 'Nonlinear and ultrafast nano-photonics,'" ACS Photonics **3**(8), 1333–1335 (2016).
[26]A. M. Weiner, *Ultrafast Optics* (John Wiley & Sons, Inc., Hoboken, NJ, 2009).
[27]T. Hanke, J. Cesar, V. Knittel, A. Trügler, U. Hohenester, A. Leitenstorfer, and R. Bratschitsch, "Tailoring spatiotemporal light confinement in single plasmonic nanoantennas," Nano Lett. **12**(2), 992–996 (2012).
[28]P. Biagioni, D. Brida, J.-S. Huang, J. Kern, L. Duò, B. Hecht, M. Finazzi, and G. Cerullo, "Dynamics of four-photon photoluminescence in gold nanoantennas," Nano Lett. **12**(6), 2941–2947 (2012).
[29]F. Zeuner, M. Muldarisnur, A. Hildebrandt, J. Förstner, and T. Zentgraf, "Coupling mediated coherent control of localized surface plasmon polaritons," Nano Lett. **15**(6), 4189–4193 (2015).
[30]V. Knittel, M. P. Fischer, T. de Roo, S. Mecking, A. Leitenstorfer, and D. Brida, "Nonlinear photoluminescence spectrum of single gold nanostructures," ACS Nano **9**(1), 894–900 (2015).
[31]M. P. Fischer, C. Schmidt, E. Sakat, J. Stock, A. Samarelli, J. Frigerio, M. Ortolani, D. J. Paul, G. Isella, A. Leitenstorfer, P. Biagioni, and D. Brida, "Optical activation of germanium plasmonic antennas in the mid-infrared," Phys. Rev. Lett. **117**(4), 047401 (2016).
[32]E. Sakat, I. Bargigia, M. Celebrano, A. Cattoni, S. Collin, D. Brida, M. Finazzi, C. D'Andrea, and P. Biagioni, "Time-resolved photoluminescence in gold nanoantennas," ACS Photonics **3**(8), 1489–1493 (2016).
[33]G. Sartorello, N. Olivier, J. Zhang, W. Yue, D. J. Gosztola, G. P. Wiederrecht, G. Wurtz, and A. V. Zayats, "Ultrafast optical modulation of second- and third-harmonic generation from cut-disk-based metasurfaces," ACS Photonics **3**(8), 1517–1522 (2016).
[34]B. Metzger, M. Hentschel, and H. Giessen, "Ultrafast nonlinear plasmonic spectroscopy: From dipole nanoantennas to complex hybrid plasmonic structures," ACS Photonics **3**(8), 1336–1350 (2016).
[35]M. P. Fischer, A. Riede, K. Gallacher, J. Frigerio, G. Pellegrini, M. Ortolani, D. J. Paul, G. Isella, A. Leitenstorfer, P. Biagioni, and D. Brida, "Plasmonic mid-infrared third harmonic generation in germanium nanoantennas," Light **7**(1), 106 (2018).
[36]M. Hensen, B. Huber, D. Friedrich, E. Krauss, S. Pres, P. Grimm, D. Fersch, J. Lüttig, V. Lisinetskii, B. Hecht, and T. Brixner, "Spatial variations in femtosecond field dynamics within a plasmonic nanoresonator mode," Nano Lett. **19**(7), 4651–4658 (2019).
[37]R. B. Davidson, A. Yanchenko, J. I. Ziegler, S. M. Avanesyan, B. J. Lawrie, and R. F. Haglund, "Ultrafast plasmonic control of second harmonic generation," ACS Photonics **3**(8), 1477–1481 (2016).
[38]M. I. Stockman, M. F. Kling, U. Kleineberg, and F. Krausz, "Attosecond nanoplasmonic-field microscope," Nat. Photonics **1**(9), 539–544 (2007).
[39]G. V. Hartland, "Optical studies of dynamics in noble metal nanostructures," Chem. Rev. **111**(6), 3858–3887 (2011).
[40]C. Boerigter, U. Aslam, and S. Linic, "Mechanism of charge transfer from plasmonic nanostructures to chemically attached materials," ACS Nano **10**(6), 6108–6115 (2016).
[41]M. Ahlawat, D. Mittal, and V. G. Rao, "Plasmon-induced hot-hole generation and extraction at nano-heterointerfaces for photocatalysis," Commun. Mater. **2**(1), 114 (2021).
[42]L. D. Landau, "On the vibrations of the electronic plasma," in *Collected Papers of L. D. Landau,* edited by D. Ter Haar (Pergamon, 1965), pp. 445–460.
[43]M. L. Brongersma, N. J. Halas, and P. Nordlander, "Plasmon-induced hot carrier science and technology," Nat. Nanotechnol. **10**(1), 25–34 (2015).
[44]M. Aeschlimann, T. Brixner, A. Fischer, M. Hensen, B. Huber, D. Kilbane, C. Kramer, W. Pfeiffer, M. Piecuch, and P. Thielen, "Determination of local optical response functions of nanostructures with increasing complexity by using single and coupled Lorentzian oscillator models," Appl. Phys. B **122**(7), 199 (2016).
[45]R. Faggiani, A. Losquin, J. Yang, E. Mårsell, A. Mikkelsen, and P. Lalanne, "Modal analysis of the ultrafast dynamics of optical nanoresonators," ACS Photonics **4**(4), 897–904 (2017).
[46]A. N. Koya, B. Ji, Z. Hao, and J. Lin, "Coherent control of gap plasmons of a complex nanosystem by shaping driving femtosecond pulses," Plasmonics **12**(6), 1693–1699 (2016).
[47]G. Aguirregabiria, D.-C. Marinica, M. Ludwig, D. Brida, A. Leitenstorfer, J. Aizpurua, and A. G. Borisov, "Dynamics of electron-emission currents in plasmonic gaps induced by strong fields," Faraday Discuss. **214**, 147–157 (2019).
[48]M. Ludwig, G. Aguirregabiria, F. Ritzkowsky, T. Rybka, D. C. Marinica, J. Aizpurua, A. G. Borisov, A. Leitenstorfer, and D. Brida, "Sub-femtosecond electron transport in a nanoscale gap," Nat. Phys. **16**(3), 341–345 (2019).
[49]A. Schirato, M. Maiuri, A. Toma, S. Fugattini, R. P. Zaccaria, P. Laporta, P. Nordlander, G. Cerullo, A. Alabastri, and G. D. Valle, "Transient optical symmetry breaking for ultrafast broadband dichroism in plasmonic metasurfaces," Nat. Photonics **14**(12), 723–727 (2020).
[50]H. Song, P. Lang, B. Ji, X. Song, and J. Lin, "Controlling the dynamics of the plasmonic field in the nano-femtosecond scale by chirped femtosecond laser pulse," Opt. Mater. Express **11**(9), 2817 (2021).
[51]B. D. Dana, A. N. Koya, X. Song, and J. Lin, "Ultrafast plasmon dynamics in asymmetric gold nanodimers," Chin. Phys. B **31**(6), 064208 (2022).
[52]A. Schirato, M. Maiuri, G. Cerullo, and G. Della Valle, "Ultrafast hot electron dynamics in plasmonic nanostructures: Experiments, modelling, design," Nanophotonics **12**(1), 1–28 (2023).
[53]B. Barwick, D. J. Flannigan, and A. H. Zewail, "Photon-induced near-field electron microscopy," Nature **462**(7275), 902–906 (2009).
[54]E. Mårsell, A. Losquin, R. Svärd, M. Miranda, C. Guo, A. Harth, E. Lorek, J. Mauritsson, C. L. Arnold, H. Xu, A. L'Huillier, and A. Mikkelsen, "Nanoscale imaging of local few-femtosecond near-field dynamics within a single plasmonic nanoantenna," Nano Lett. **15**(10), 6601–6608 (2015).
[55]E. Mårsell, R. Svärd, M. Miranda, C. Guo, A. Harth, E. Lorek, J. Mauritsson, C. L. Arnold, H. Xu, A. L'Huillier, A. Mikkelsen, and A. Losquin, "Direct subwavelength imaging and control of near-field localization in individual silver nanocubes," Appl. Phys. Lett. **107**(20), 201111 (2015).
[56]J. Qin, P. Lang, B.-Y. Ji, N. K. Alemayehu, H.-Y. Tao, X. Gao, Z.-Q. Hao, and J.-Q. Lin, "Imaging ultrafast plasmon dynamics within a complex dolmen nanostructure using photoemission electron microscopy," Chin. Phys. Lett. **33**(11), 116801 (2016).
[57]I. Madan, G. M. Vanacore, E. Pomarico, G. Berruto, R. J. Lamb, D. McGrouther, T. T. A. Lummen, T. Latychevskaia, F. J. G. de Abajo, and F. Carbone, "Holographic imaging of electromagnetic fields via electron-light quantum interference," Sci. Adv. **5**(5), eaav8358 (2019).
[58]Y. Xu, Y. Qin, B. Ji, X. Song, and J. Lin, "Polarization manipulated femtosecond localized surface plasmon dephasing time in an individual bowtie structure," Opt. Express **28**(7), 9310 (2020).
[59]Q. Sun, S. Zu, and H. Misawa, "Ultrafast photoemission electron microscopy: Capability and potential in probing plasmonic nanostructures from multiple domains," J. Chem. Phys. **153**(12), 120902 (2020).
[60]O. Kfir, H. Lourenço-Martins, G. Storeck, M. Sivis, T. R. Harvey, T. J. Kippenberg, A. Feist, and C. Ropers, "Controlling free electrons with optical whispering-gallery modes," Nature **582**(7810), 46–49 (2020).
[61]B. Ji, J. Qin, H. Tao, Z. Hao, and J. Lin, "Subwavelength imaging and control of ultrafast optical near-field under resonant- and off-resonant excitation of bowtie nanostructures," New J. Phys. **18**(9), 093046 (2016).
[62]B. Ji, J. Qin, P. Lang, A. N. Koya, Z. Hao, X. Song, and J. Lin, Proc. SPIE **10028**, 10028G (2016).
[63]X. Song, B. Ji, P. Lang, and J. Lin, Proc. SPIE **10530**, 1053018 (2018).
[64]X. Liu, A. Merhe, E. Jal, R. Delaunay, R. Jarrier, V. Chardonnet, M. Hennes, S. G. Chiuzbaian, K. Légaré, M. Hennecke, I. Radu, C. V. K. Schmising, S. Grunewald, M. Kuhlmann, J. Lüning, and B. Vodungbo, "Sub-15-fs x-ray pump and x-ray probe experiment for the study of ultrafast magnetization dynamics in ferromagnetic alloys," Opt. Express **29**(20), 32388 (2021).
[65]D. Schick, M. Borchert, J. Braenzel, H. Stiel, J. Tümmler, D. E. Bürgler, A. Firsov, C. von, K. Schmising, B. Pfau, and S. Eisebitt, "Laser-driven resonant magnetic soft-x-ray scattering for probing ultrafast antiferromagnetic and structural dynamics," Optica **8**(9), 1237 (2021).
[66]I. A. Novikov, M. A. Kiryanov, P. K. Nurgalieva, A. Y. Frolov, V. V. Popov, T. V. Dolgova, and A. A. Fedyanin, "Ultrafast magneto-optics in nickel magnetoplasmonic crystals," Nano Lett. **20**(12), 8615–8619 (2020).

[67]D. Ksenzov, A. A. Maznev, V. Unikandanunni, F. Bencivenga, F. Capotondi, A. Caretta, L. Foglia, M. Malvestuto, C. Masciovecchio, R. Mincigrucci, K. A. Nelson, M. Pancaldi, E. Pedersoli, L. Randolph, H. Rahmann, S. Urazhdin, S. Bonetti, and C. Gutt, "Nanoscale transient magnetization gratings created and probed by femtosecond extreme ultraviolet pulses," Nano Lett. **21**(7), 2905–2911 (2021).
[68]K. Mishra, A. Ciuciulkaite, M. Zapata-Herrera, P. Vavassori, V. Kapaklis, T. Rasing, A. Dmitriev, A. Kimel, and A. Kirilyuk, "Ultrafast demagnetization in a ferrimagnet under electromagnetic field funneling," Nanoscale **13**(46), 19367–19375 (2021).
[69]A. Kimel, A. Zvezdin, S. Sharma, S. Shallcross, N. de Sousa, A. García-Martín, G. Salvan, J. Hamrle, O. Stejskal, J. McCord, S. Tacchi, G. Carlotti, P. Gambardella, G. Salis, M. Münzenberg, M. Schultze, V. Temnov, I. V. Bychkov, L. N. Kotov, N. Maccaferri, D. Ignatyeva, V. Belotelov, C. Donnelly, A. H. Rodriguez, I. Matsuda, T. Ruchon, M. Fanciulli, M. Sacchi, C. R. Du, H. Wang, N. P. Armitage, M. Schubert, V. Darakchieva, B. Liu, Z. Huang, B. Ding, A. Berger, and P. Vavassori, "The 2022 magneto-optics roadmap," J. Phys. D **55**(46), 463003 (2022).
[70]M. P. Fischer, N. Maccaferri, K. Gallacher, J. Frigerio, G. Pellegrini, D. J. Paul, G. Isella, A. Leitenstorfer, P. Biagioni, and D. Brida, "Field-resolved detection of the temporal response of a single plasmonic antenna in the mid-infrared," Optica **8**(6), 898 (2021).
[71]A. N. Koya, "Plasmonic nanoarchitectures for single-molecule explorations: An overview," Adv. Photonics Res. **3**(3), 2100325 (2021).
[72]A. N. Koya, J. Cunha, T.-L. Guo, A. Toma, D. Garoli, T. Wang, S. Juodkazis, D. Cojoc, and R. P. Zaccaria, "Novel plasmonic nanocavities for optical trapping-assisted biosensing applications," Adv. Opt. Mater. **8**(7), 1901481 (2020).
[73]A. Schirato and M. Maiuri, "(Invited) Design of symmetric nanoresonators to scale the ultrafast optical modulation in plasmonic metasurfaces," Opt. Mater.: X **12**, 100101 (2021).
[74]A. Schirato, A. Mazzanti, R. Proietti Zaccaria, P. Nordlander, A. Alabastri, and G. Della Valle, "All-optically reconfigurable plasmonic metagrating for ultrafast diffraction management," Nano Lett. **21**(3), 1345–1351 (2021).
[75]A. Schirato, G. Crotti, R. P. Zaccaria, A. Alabastri, and G. D. Valle, "Hot carrier spatio-temporal inhomogeneities in ultrafast nanophotonics," New J. Phys. **24**(4), 045001 (2022).
[76]A. Schirato, A. Toma, R. P. Zaccaria, A. Alabastri, G. Cerullo, G. D. Valle, and M. Maiuri, "All-optical reconfiguration of ultrafast dichroism in gold metasurfaces," Adv. Opt. Mater. **10**(10), 2102549 (2022).
[77]E. Petryayeva and U. J. Krull, "Localized surface plasmon resonance: Nanostructures, bioassays and biosensing—A review," Anal. Chim. Acta **706**(1), 8–24 (2011).
[78]M. Sui, S. Kunwar, P. Pandey, and J. Lee, "Strongly confined localized surface plasmon resonance (LSPR) bands of Pt, AgPt, AgAuPt nanoparticles," Sci. Rep. **9**(1), 16582 (2019).
[79]G. Barbillon, "Plasmonics and its applications," Materials **12**(9), 1502 (2019).
[80]R. A. Alvarez-Puebla, J.-F. Li, and X. Y. Ling, "Introduction to advances in plasmonics and its applications," Nanoscale **13**(12), 5935–5936 (2021).
[81]V. Giannini, A. I. Fernández-Domínguez, S. C. Heck, and S. A. Maier, "Plasmonic nanoantennas: Fundamentals and their use in controlling the radiative properties of nanoemitters," Chem. Rev. **111**(6), 3888–3912 (2011).
[82]A. B. Zrimsek, N. Chiang, M. Mattei, S. Zaleski, M. O. McAnally, C. T. Chapman, A.-I. Henry, G. C. Schatz, and R. P. V. Duyne, "Single-molecule chemistry with surface- and tip-enhanced Raman spectroscopy," Chem. Rev. **117**(11), 7583–7613 (2016).
[83]A. B. Taylor and P. Zijlstra, "Single-molecule plasmon sensing: Current status and future prospects," ACS Sens. **2**(8), 1103–1122 (2017).
[84]J. Lee, K. T. Crampton, N. Tallarida, and V. A. Apkarian, "Visualizing vibrational normal modes of a single molecule with atomically confined light," Nature **568**(7750), 78–82 (2019).
[85]B. Yang, G. Chen, A. Ghafoor, Y. Zhang, Y. Zhang, Y. Zhang, Y. Luo, J. Yang, V. Sandoghdar, J. Aizpurua, Z. Dong, and J. G. Hou, "Sub-nanometre resolution in single-molecule photoluminescence imaging," Nat. Photonics **14**(11), 693–699 (2020).
[86]E. Cortés, L. V. Besteiro, A. Alabastri, A. Baldi, G. Tagliabue, A. Demetriadou, and P. Narang, "Challenges in plasmonic catalysis," ACS Nano **14**(12), 16202–16219 (2020).
[87]M. Sayed, J. Yu, G. Liu, and M. Jaroniec, "Non-noble plasmonic metal-based photocatalysts," Chem. Rev. **122**(11), 10484–10537 (2022).
[88]Y. Qin, B. Ji, X. Song, and J. Lin, "Characterization of ultrafast plasmon dynamics in individual gold bowtie by time-resolved photoemission electron microscopy," Appl. Phys. B **125**(1), 3 (2018).
[89]A. Gliserin, S. H. Chew, S. Choi, K. Kim, D. T. Hallinan, J.-W. Oh, S. Kim, and D. E. Kim, "Interferometric time- and energy-resolved photoemission electron microscopy for few-femtosecond nanoplasmonic dynamics," Rev. Sci. Instrum. **90**(9), 093904 (2019).
[90]M. Dąbrowski, Y. Dai, and H. Petek, "Ultrafast photoemission electron microscopy: Imaging plasmons in space and time," Chem. Rev. **120**(13), 6247–6287 (2020).
[91]G. Spektor, D. Kilbane, A. K. Mahro, B. Frank, S. Ristok, L. Gal, P. Kahl, D. Podbiel, S. Mathias, H. Giessen, F.-J. M. Zu Heringdorf, M. Orenstein, and M. Aeschlimann, "Revealing the subfemtosecond dynamics of orbital angular momentum in nanoplasmonic vortices," Science **355**(6330), 1187–1191 (2017).
[92]A. Kubo, K. Onda, H. Petek, Z. Sun, Y. S. Jung, and H. K. Kim, "Femtosecond imaging of surface plasmon dynamics in a nanostructured silver film," Nano Lett. **5**(6), 1123–1127 (2005).
[93]A. Kubo, N. Pontius, and H. Petek, "Femtosecond microscopy of surface plasmon polariton wave packet evolution at the silver/vacuum interface," Nano Lett. **7**(2), 470–475 (2007).
[94]P. Kahl, S. Wall, C. Witt, C. Schneider, D. Bayer, A. Fischer, P. Melchior, M. H. Hoegen, M. Aeschlimann, and F.-J. M. zu Heringdorf, "Normal-Incidence Photoemission Electron Microscopy (NI-PEEM) for imaging surface plasmon polaritons," Plasmonics **9**(6), 1401–1407 (2014).
[95]P. Kahl, D. Podbiel, C. Schneider, A. Makris, S. Sindermann, C. Witt, D. Kilbane, M. H. Hoegen, M. Aeschlimann, and F. M. zu Heringdorf, "Direct observation of surface plasmon polariton propagation and interference by time-resolved imaging in normal-incidence two photon photoemission microscopy," Plasmonics **13**(1), 239–246 (2017).
[96]Y. Gong, A. G. Joly, D. Hu, P. Z. El-Khoury, and W. P. Hess, "Ultrafast imaging of surface plasmons propagating on a gold surface," Nano Lett. **15**(5), 3472–3478 (2015).
[97]T. J. Davis, B. Frank, D. Podbiel, P. Kahl, F.-J. M. zu Heringdorf, and H. Giessen, "Subfemtosecond and nanometer plasmon dynamics with photoelectron microscopy: Theory and efficient simulations," ACS Photonics **4**(10), 2461–2469 (2017).
[98]P. Johns, G. Beane, K. Yu, and G. V. Hartland, "Dynamics of surface plasmon polaritons in metal nanowires," J. Phys. Chem. C **121**(10), 5445–5459 (2017).
[99]B. Frank, P. Kahl, D. Podbiel, G. Spektor, M. Orenstein, L. Fu, T. Weiss, M. H. Hoegen, T. J. Davis, F.-J. M. Zu Heringdorf, and H. Giessen, "Short-range surface plasmonics: Localized electron emission dynamics from a 60-nm spot on an atomically flat single-crystalline gold surface," Sci. Adv. **3**(7), e1700721 (2017).
[100]W. A. Challener, C. Peng, A. V. Itagi, D. Karns, W. Peng, Y. Peng, X. Yang, X. Zhu, N. J. Gokemeijer, Y.-T. Hsia, G. Ju, R. E. Rottmayer, M. A. Seigler, and E. C. Gage, "Heat-assisted magnetic recording by a near-field transducer with efficient optical energy transfer," Nat. Photonics **3**(4), 220–224 (2009).
[101]J. Vogelsang, J. Robin, B. J. Nagy, P. Dombi, D. Rosenkranz, M. Schiek, P. Groß, and C. Lienau, "Ultrafast electron emission from a sharp metal nanotaper driven by adiabatic nanofocusing of surface plasmons," Nano Lett. **15**(7), 4685–4691 (2015).
[102]B. Schröder, M. Sivis, R. Bormann, S. Schäfer, and C. Ropers, "An ultrafast nanotip electron gun triggered by grating-coupled surface plasmons," Appl. Phys. Lett. **107**(23), 231105 (2015).
[103]T. J. Davis, D. Janoschka, P. Dreher, B. Frank, F.-J. M. zu Heringdorf, and H. Giessen, "Ultrafast vector imaging of plasmonic skyrmion dynamics with deep subwavelength resolution," Science **368**(6489), 386 (2020).
[104]M. Zavelani-Rossi, D. Polli, S. Kochtcheev, A.-L. Baudrion, J. Béal, V. Kumar, E. Molotokaite, M. Marangoni, S. Longhi, G. Cerullo, P.-M. Adam, and G. Della Valle, "Transient optical response of a single gold nanoantenna: The role of plasmon detuning," ACS Photonics **2**(4), 521–529 (2015).
[105]M. Taghinejad, H. Taghinejad, Z. Xu, K.-T. Lee, S. P. Rodrigues, J. Yan, A. Adibi, T. Lian, and W. Cai, "Ultrafast control of phase and polarization of light expedited by hot-electron transfer," Nano Lett. **18**(9), 5544–5551 (2018).

[106]K. Fukumoto, K. Onda, Y. Yamada, T. Matsuki, T. Mukuta, S. Tanaka, and S. Koshihara, "Femtosecond time-resolved photoemission electron microscopy for spatiotemporal imaging of photogenerated carrier dynamics in semiconductors," Rev. Sci. Instrum. **85**(8), 083705 (2014).

[107]K. Fukumoto, Y. Yamada, K. Onda, and S. Koshihara, "Direct imaging of electron recombination and transport on a semiconductor surface by femtosecond time-resolved photoemission electron microscopy," Appl. Phys. Lett. **104**(5), 053117 (2014).

[108]M. K. L. Man, A. Margiolakis, S. Deckoff-Jones, T. Harada, E. L. Wong, M. B. M. Krishna, J. Madéo, A. Winchester, S. Lei, R. Vajtai, P. M. Ajayan, and K. M. Dani, "Imaging the motion of electrons across semiconductor heterojunctions," Nat. Nanotechnol. **12**(1), 36–40 (2016).

[109]L. Wang, C. Xu, M.-Y. Li, L.-J. Li, and Z.-H. Loh, "Unraveling spatially heterogeneous ultrafast carrier dynamics of single-layer WSe_2 by femtosecond time-resolved photoemission electron microscopy," Nano Lett. **18**(8), 5172–5178 (2018).

[110]L. Piazza, D. J. Masiel, T. LaGrange, B. W. Reed, B. Barwick, and F. Carbone, "Design and implementation of a fs-resolved transmission electron microscope based on thermionic gun technology," Chem. Phys. **423**, 79–84 (2013).

[111]A. Feist, K. E. Echternkamp, J. Schauss, S. V. Yalunin, S. Schäfer, and C. Ropers, "Quantum coherent optical phase modulation in an ultrafast transmission electron microscope," Nature **521**(7551), 200–203 (2015).

[112]M. T. McDowell, K. L. Jungjohann, and U. Celano, "Dynamic nanomaterials phenomena investigated with *in situ* transmission electron microscopy: A nano letters virtual issue," Nano Lett. **18**(2), 657–659 (2018).

[113]P. Das, J. D. Blazit, M. Tencé, L. F. Zagonel, Y. Auad, Y. H. Lee, X. Y. Ling, A. Losquin, C. Colliex, O. Stéphan, F. J. G. de Abajo, and M. Kociak, "Stimulated electron energy loss and gain in an electron microscope without a pulsed electron gun," Ultramicroscopy **203**, 44–51 (2019).

[114]P. Baum, "On the physics of ultrashort single-electron pulses for time-resolved microscopy and diffraction," Chem. Phys. **423**, 55–61 (2013).

[115]E. Fill, L. Veisz, A. Apolonski, and F. Krausz, "Sub-fs electron pulses for ultrafast electron diffraction," New J. Phys. **8**(11), 272–272 (2006).

[116]L. Veisz, G. Kurkin, K. Chernov, V. Tarnetsky, A. Apolonski, F. Krausz, and E. Fill, "Hybrid dc–ac electron gun for fs-electron pulse generation," New J. Phys. **9**(12), 451–451 (2007).

[117]T. van Oudheusden, P. L. E. M. Pasmans, S. B. van der Geer, M. J. de Loos, M. J. van der Wiel, and O. J. Luiten, "Compression of subrelativistic space-charge-dominated electron bunches for single-shot femtosecond electron diffraction," Phys. Rev. Lett. **105**(26), 264801 (2010).

[118]A. Gliserin, A. Apolonski, F. Krausz, and P. Baum, "Compression of single-electron pulses with a microwave cavity," New J. Phys. **14**(7), 073055 (2012).

[119]C. Kealhofer, W. Schneider, D. Ehberger, A. Ryabov, F. Krausz, and P. Baum, "All-optical control and metrology of electron pulses," Science **352**(6284), 429–433 (2016).

[120]D. Zhang, A. Fallahi, M. Hemmer, X. Wu, M. Fakhari, Y. Hua, H. Cankaya, A.-L. Calendron, L. E. Zapata, N. H. Matlis, and F. X. Kärtner, "Segmented terahertz electron accelerator and manipulator (STEAM)," Nat. Photonics **12**(6), 336–342 (2018).

[121]E. Snively, M. Othman, M. Kozina, B. Ofori-Okai, S. Weathersby, S. Park, X. Shen, X. Wang, M. Hoffmann, R. Li, and E. Nanni, "Femtosecond compression dynamics and timing jitter suppression in a THz-driven electron bunch compressor," Phys. Rev. Lett. **124**(5), 054801 (2020).

[122]L. Zhao, H. Tang, C. Lu, T. Jiang, P. Zhu, L. Hu, W. Song, H. Wang, J. Qiu, C. Jing, S. Antipov, D. Xiang, and J. Zhang, "Femtosecond relativistic electron beam with reduced timing Jitter from THz driven beam compression," Phys. Rev. Lett. **124**(5), 054802 (2020).

[123]J. Kuttruff, M. V. Tsarev, and P. Baum, "Jitter-free terahertz pulses from $LiNbO_3$," Opt. Lett. **46**(12), 2944 (2021).

[124]D. T. Valley, V. E. Ferry, and D. J. Flannigan, "Imaging intra- and interparticle acousto-plasmonic vibrational dynamics with ultrafast electron microscopy," Nano Lett. **16**(11), 7302–7308 (2016).

[125]A. J. McKenna, J. K. Eliason, and D. J. Flannigan, "Spatiotemporal evolution of coherent elastic strain waves in a single MoS_2 flake," Nano Lett. **17**(6), 3952–3958 (2017).

[126]A. Yurtsever and A. H. Zewail, "Direct visualization of near-fields in nanoplasmonics and nanophotonics," Nano Lett. **12**(6), 3334–3338 (2012).

[127]A. Yurtsever, J. S. Baskin, and A. H. Zewail, "Entangled nanoparticles: Discovery by visualization in 4D electron microscopy," Nano Lett. **12**(9), 5027–5032 (2012).

[128]L. Piazza, T. T. A. Lummen, E. Quiñonez, Y. Murooka, B. W. Reed, B. Barwick, and F. Carbone, "Simultaneous observation of the quantization and the interference pattern of a plasmonic near-field," Nat. Commun. **6**(1), 6407 (2015).

[129]M. Liebtrau, M. Sivis, A. Feist, H. Lourenço-Martins, N. Pazos-Pérez, R. A. Alvarez-Puebla, F. J. G. de Abajo, A. Polman, and C. Ropers, "Spontaneous and stimulated electron–photon interactions in nanoscale plasmonic near fields," Light **10**(1), 82 (2021).

[130]T. R. Harvey, J.-W. Henke, O. Kfir, H. Lourenço-Martins, A. Feist, F. J. G. de Abajo, and C. Ropers, "Probing chirality with inelastic electron-light scattering," Nano Lett. **20**(6), 4377–4383 (2020).

[131]G. M. Vanacore, I. Madan, G. Berruto, K. Wang, E. Pomarico, R. J. Lamb, D. McGrouther, I. Kaminer, B. Barwick, F. J. G. de Abajo, and F. Carbone, "Attosecond coherent control of free-electron wave functions using semi-infinite light fields," Nat. Commun. **9**(1), 2694 (2018).

[132]G. M. Vanacore, G. Berruto, I. Madan, E. Pomarico, P. Biagioni, R. J. Lamb, D. McGrouther, O. Reinhardt, I. Kaminer, B. Barwick, H. Larocque, V. Grillo, E. Karimi, F. J. G. de Abajo, and F. Carbone, "Ultrafast generation and control of an electron vortex beam via chiral plasmonic near fields," Nat. Mater. **18**(6), 573–579 (2019).

[133]A. Feist, S. V. Yalunin, S. Schäfer, and C. Ropers, "High-purity free-electron momentum states prepared by three-dimensional optical phase modulation," Phys. Rev. Res. **2**(4), 043227 (2020).

[134]S. V. Yalunin, A. Feist, and C. Ropers, "Tailored high-contrast attosecond electron pulses for coherent excitation and scattering," Phys. Rev. Res. **3**(3), L032036 (2021).

[135]R. Dahan, A. Gorlach, U. Haeusler, A. Karnieli, O. Eyal, P. Yousefi, M. Segev, A. Arie, G. Eisenstein, P. Hommelhoff, and I. Kaminer, "Imprinting the quantum statistics of photons on free electrons," Science **373**(6561), 1324 (2021).

[136]K. Wang, R. Dahan, M. Shentcis, Y. Kauffmann, A. B. Hayun, O. Reinhardt, S. Tsesses, and I. Kaminer, "Coherent interaction between free electrons and a photonic cavity," Nature **582**(7810), 50–54 (2020).

[137]J.-W. Henke, A. S. Raja, A. Feist, G. Huang, G. Arend, Y. Yang, F. J. Kappert, R. N. Wang, M. Möller, J. Pan, J. Liu, O. Kfir, C. Ropers, and T. J. Kippenberg, "Integrated photonics enables continuous-beam electron phase modulation," Nature **600**(7890), 653–658 (2021).

[138]W. Cai, O. Reinhardt, I. Kaminer, and F. J. G. de Abajo, "Efficient orbital angular momentum transfer between plasmons and free electrons," Phys. Rev. B **98**(4), 045424 (2018).

[139]W. Cai, O. Reinhardt, I. Kaminer, and F. J. G. de Abajo, "Erratum: Efficient orbital angular momentum transfer between plasmons and free electrons [Phys. Rev. B **98**, 045424 (2018)]," Phys. Rev. B **99**(7), 079904 (2019).

[140]T. T. A. Lummen, R. J. Lamb, G. Berruto, T. LaGrange, L. D. Negro, F. J. G. de Abajo, D. McGrouther, B. Barwick, and F. Carbone, "Imaging and controlling plasmonic interference fields at buried interfaces," Nat. Commun. **7**(1), 13156 (2016).

[141]A. Ryabov, J. W. Thurner, D. Nabben, M. V. Tsarev, and P. Baum, "Attosecond metrology in a continuous-beam transmission electron microscope," Sci. Adv. **6**(46), eabb1393 (2020).

[142]Y. Morimoto and P. Baum, "Diffraction and microscopy with attosecond electron pulse trains," Nat. Phys. **14**(3), 252–256 (2017).

[143]K. E. Priebe, C. Rathje, S. V. Yalunin, T. Hohage, A. Feist, S. Schäfer, and C. Ropers, "Attosecond electron pulse trains and quantum state reconstruction in ultrafast transmission electron microscopy," Nat. Photonics **11**(12), 793–797 (2017).

[144]D. Nabben, J. Kuttruff, L. Stolz, A. Ryabov, and P. Baum, "Attosecond electron microscopy of sub-cycle optical dynamics," Nature (2023).

[145]D. Polli, D. Brida, S. Mukamel, G. Lanzani, and G. Cerullo, "Effective temporal resolution in pump-probe spectroscopy with strongly chirped pulses," Phys. Rev. A **82**(5), 053809 (2010).

[146]D. Brida, C. Manzoni, G. Cirmi, M. Marangoni, S. Bonora, P. Villoresi, S. D. Silvestri, and G. Cerullo, "Few-optical-cycle pulses tunable from the visible to the mid-infrared by optical parametric amplifiers," J. Opt. **12**(1), 013001 (2009).

[147]C. Manzoni and G. Cerullo, "Design criteria for ultrafast optical parametric amplifiers," J. Opt. **18**(10), 103501 (2016).
[148]U. Morgner, F. X. Kärtner, S. H. Cho, Y. Chen, H. A. Haus, J. G. Fujimoto, E. P. Ippen, V. Scheuer, G. Angelow, and T. Tschudi, "Sub-two-cycle pulses from a Kerr-lens mode-locked Ti: sapphire laser," Opt. Lett. **24**(6), 411 (1999).
[149]F. Junginger, A. Sell, O. Schubert, B. Mayer, D. Brida, M. Marangoni, G. Cerullo, A. Leitenstorfer, and R. Huber, "Single-cycle multiterahertz transients with peak fields above 10 MV/cm," Opt. Lett. **35**(15), 2645 (2010).
[150]P. Baum, S. Lochbrunner, and E. Riedle, "Tunable sub-10-fs ultraviolet pulses generated by achromatic frequency doubling," Opt. Lett. **29**(14), 1686 (2004).
[151]Y. Yin, A. Chew, X. Ren, J. Li, Y. Wang, Y. Wu, and Z. Chang, "Towards terawatt sub-cycle long-wave infrared pulses via chirped optical parametric amplification and indirect pulse shaping," Sci. Rep. **7**(1), 45794 (2017).
[152]A. Grupp, A. Budweg, M. P. Fischer, J. Allerbeck, G. Soavi, A. Leitenstorfer, and D. Brida, "Broadly tunable ultrafast pump-probe system operating at multi-kHz repetition rate," J. Opt. **20**(1), 014005 (2017).
[153]C.-K. Sun, F. Vallée, L. H. Acioli, E. P. Ippen, and J. G. Fujimoto, "Femtosecond-tunable measurement of electron thermalization in gold," Phys. Rev. B **50**(20), 15337–15348 (1994).
[154]G. Della Valle, M. Conforti, S. Longhi, G. Cerullo, and D. Brida, "Real-time optical mapping of the dynamics of nonthermal electrons in thin gold films," Phys. Rev. B **86**(15), 155139 (2012).
[155]P. B. Corkum, "Plasma perspective on strong field multiphoton ionization," Phys. Rev. Lett. **71**(13), 1994–1997 (1993).
[156]M. Schultze, E. M. Bothschafter, A. Sommer, S. Holzner, W. Schweinberger, M. Fiess, M. Hofstetter, R. Kienberger, V. Apalkov, V. S. Yakovlev, M. I. Stockman, and F. Krausz, "Controlling dielectrics with the electric field of light," Nature **493**(7430), 75–78 (2012).
[157]M. Schultze, K. Ramasesha, C. D. Pemmaraju, S. A. Sato, D. Whitmore, A. Gandman, J. S. Prell, L. J. Borja, D. Prendergast, K. Yabana, D. M. Neumark, and S. R. Leone, "Attosecond band-gap dynamics in silicon," Science **346**(6215), 1348–1352 (2014).
[158]M. Volkov, S. A. Sato, F. Schlaepfer, L. Kasmi, N. Hartmann, M. Lucchini, L. Gallmann, A. Rubio, and U. Keller, "Attosecond screening dynamics mediated by electron localization in transition metals," Nat. Phys. **15**(11), 1145–1149 (2019).
[159]A. Niedermayr, M. Volkov, S. Sato, N. Hartmann, Z. Schumacher, S. Neb, A. Rubio, L. Gallmann, and U. Keller, "Few-femtosecond dynamics of free-free opacity in optically heated metals," Phys. Rev. X **12**(2), 021045 (2022).
[160]T. Rybka, M. Ludwig, M. F. Schmalz, V. Knittel, D. Brida, and A. Leitenstorfer, "Sub-cycle optical phase control of nanotunnelling in the single-electron regime," Nat. Photonics **10**(10), 667–670 (2016).
[161]M. Ludwig, A. K. Kazansky, G. Aguirregabiria, D. C. Marinica, M. Falk, A. Leitenstorfer, D. Brida, J. Aizpurua, and A. G. Borisov, "Active control of ultrafast electron dynamics in plasmonic gaps using an applied bias," Phys. Rev. B **101**(24), 241412 (2020).
[162]A. Taflove, S. C. Hagness, and M. Piket-May, in *The Electrical Engineering Handbook* (Elsevier, 2005), pp. 629–670.
[163]E. Coccia, J. Fregoni, C. A. Guido, M. Marsili, S. Pipolo, and S. Corni, "Hybrid theoretical models for molecular nanoplasmonics," J. Chem. Phys. **153**(20), 200901 (2020).
[164]G. Dall'Osto, G. Gil, S. Pipolo, and S. Corni, "Real-time dynamics of plasmonic resonances in nanoparticles described by a boundary element method with generic dielectric function," J. Chem. Phys. **153**(18), 184114 (2020).
[165]A. Schirato, G. Crotti, M. Gonçalves Silva, D. C. Teles-Ferreira, C. Manzoni, R. Proietti Zaccaria, P. Laporta, A. M. de Paula, G. Cerullo, and G. Della Valle, "Ultrafast plasmonics beyond the perturbative regime: Breaking the electronic-optical dynamics correspondence," Nano Lett. **22**(7), 2748–2754 (2022).
[166]H. Chen, J. M. McMahon, M. A. Ratner, and G. C. Schatz, "Classical electrodynamics coupled to quantum mechanics for calculation of molecular optical properties: A RT-TDDFT/FDTD approach," J. Phys. Chem. C **114**(34), 14384–14392 (2010).
[167]H. T. Smith, T. E. Karam, L. H. Haber, and K. Lopata, "Capturing plasmon--molecule dynamics in dye monolayers on metal nanoparticles using classical electrodynamics with quantum embedding," J. Phys. Chem. C **121**(31), 16932–16942 (2017).
[168]L. V. Besteiro, X.-T. Kong, Z. Wang, G. Hartland, and A. O. Govorov, "Understanding hot-electron generation and plasmon relaxation in metal nanocrystals: Quantum and classical mechanisms," ACS Photonics **4**(11), 2759–2781 (2017).
[169]L. Chang, L. V. Besteiro, J. Sun, E. Y. Santiago, S. K. Gray, Z. Wang, and A. O. Govorov, "Electronic structure of the plasmons in metal nanocrystals: Fundamental limitations for the energy efficiency of hot electron generation," ACS Energy Lett. **4**(10), 2552–2568 (2019).
[170]E. Y. Santiago, L. V. Besteiro, X.-T. Kong, M. A. Correa-Duarte, Z. Wang, and A. O. Govorov, "Efficiency of hot-electron generation in plasmonic nanocrystals with complex shapes: Surface-induced scattering, hot spots, and interband transitions," ACS Photonics **7**(10), 2807–2824 (2020).
[171]M. Ferrera, G. D. Valle, M. Sygletou, M. Magnozzi, D. Catone, P. O'Keeffe, A. Paladini, F. Toschi, L. Mattera, M. Canepa, and F. Bisio, "Thermometric calibration of the ultrafast relaxation dynamics in plasmonic Au nanoparticles," ACS Photonics **7**(4), 959–966 (2020).
[172]P. O'Keeffe, D. Catone, L. D. Mario, F. Toschi, M. Magnozzi, F. Bisio, A. Alabastri, R. P. Zaccaria, A. Toma, G. D. Valle, and A. Paladini, "Disentangling the temporal dynamics of nonthermal electrons in photoexcited gold nanostructures," Laser Photonics Rev. **15**(6), 2100017 (2021).
[173]R. Sundararaman, P. Narang, A. S. Jermyn, W. A. Goddard III, and H. A. Atwater, "Theoretical predictions for hot-carrier generation from surface plasmon decay," Nat. Commun. **5**(1), 5788 (2014).
[174]P. Narang, R. Sundararaman, and H. A. Atwater, "Plasmonic hot carrier dynamics in solid-state and chemical systems for energy conversion," Nanophotonics **5**(1), 96–111 (2016).
[175]J. G. Liu, H. Zhang, S. Link, and P. Nordlander, "Relaxation of plasmon-induced hot carriers," ACS Photonics **5**(7), 2584–2595 (2017).
[176]T. P. Rossi, P. Erhart, and M. Kuisma, "Hot-carrier generation in plasmonic nanoparticles: The importance of atomic structure," ACS Nano **14**(8), 9963–9971 (2020).
[177]A. Manjavacas, J. G. Liu, V. Kulkarni, and P. Nordlander, "Plasmon-induced hot carriers in metallic nanoparticles," ACS Nano **8**(8), 7630–7638 (2014).
[178]Y. Zhang, "Theory of plasmonic hot-carrier generation and relaxation," J. Phys. Chem. A **125**(41), 9201–9208 (2021).
[179]A. Crai, A. Pusch, D. E. Reiter, L. R. Castellanos, T. Kuhn, and O. Hess, "Coulomb effects on the photoexcited quantum dynamics of electrons in a plasmonic nanosphere," Phys. Rev. B **98**(16), 165411 (2018).
[180]S. Tanaka, T. Yoshida, K. Watanabe, Y. Matsumoto, T. Yasuike, D. Novko, M. Petrović, and M. Kralj, "Ultrafast plasmonic response ensured by atomic scale confinement," ACS Photonics **9**(3), 837–845 (2022).
[181]J. R. M. Saavedra, A. Asenjo-Garcia, and F. J. García de Abajo, "Hot-electron dynamics and thermalization in small metallic nanoparticles," ACS Photonics **3**(9), 1637–1646 (2016).
[182]H. Zhang and A. O. Govorov, "Optical generation of hot plasmonic carriers in metal nanocrystals: The effects of shape and field enhancement," J. Phys. Chem. C **118**(14), 7606–7614 (2014).
[183]A. O. Govorov, H. Zhang, and Y. K. Gun'ko, "Theory of photoinjection of hot plasmonic carriers from metal nanostructures into semiconductors and surface molecules," J. Phys. Chem. C **117**(32), 16616–16631 (2013).
[184]X.-T. Kong, Z. Wang, and A. O. Govorov, "Plasmonic nanostars with hot spots for efficient generation of hot electrons under solar illumination," Adv. Opt. Mater. **5**(15), 1600594 (2016).
[185]X. Zubizarreta, E. V. Chulkov, I. P. Chernov, A. S. Vasenko, I. Aldazabal, and V. M. Silkin, "Quantum-size effects in the loss function of Pb(111) thin films: An *ab initio* study," Phys. Rev. B **95**(23), 235405 (2017).
[186]M. Bernardi, J. Mustafa, J. B. Neaton, and S. G. Louie, "Theory and computation of hot carriers generated by surface plasmon polaritons in noble metals," Nat. Commun. **6**(1), 7044 (2015).
[187]O. A. Douglas-Gallardo, M. Berdakin, T. Frauenheim, and C. G. Sánchez, "Plasmon-induced hot-carrier generation differences in gold and silver nanoclusters," Nanoscale **11**(17), 8604–8615 (2019).
[188]F. Libisch, C. Huang, and E. A. Carter, "Embedded correlated wavefunction schemes: Theory and applications," Acc. Chem. Res. **47**(9), 2768–2775 (2014).

[189]J. M. P. Martirez, J. L. Bao, and E. A. Carter, "First-principles insights into plasmon-induced catalysis," Annu. Rev. Phys. Chem. **72**(1), 99–119 (2021).
[190]W. Chu, W. A. Saidi, and O. V. Prezhdo, "Long-lived hot electron in a metallic particle for plasmonics and catalysis: *Ab initio* nonadiabatic molecular dynamics with machine learning," ACS Nano **14**(8), 10608–10615 (2020).
[191]H. Yin, H. Zhang, and X.-L. Cheng, "Plasmon resonances and the plasmon-induced field enhancement in nanoring dimers," J. Appl. Phys. **113**(11), 113107 (2013).
[192]M. Berdakin, G. Soldano, F. P. Bonafé, V. Liubov, B. Aradi, T. Frauenheim, and C. G. Sánchez, "Dynamical evolution of the Schottky barrier as a determinant contribution to electron–hole pair stabilization and photocatalysis of plasmon-induced hot carriers," Nanoscale **14**(7), 2816–2825 (2022).
[193]K. M. Conley, N. Nayyar, T. P. Rossi, M. Kuisma, V. Turkowski, M. J. Puska, and T. S. Rahman, "Plasmon excitations in mixed metallic nanoarrays," ACS Nano **13**(5), 5344–5355 (2019).
[194]G. U. Kuda-Singappulige, D. B. Lingerfelt, X. Li, and C. M. Aikens, "Ultrafast nonlinear plasmon decay processes in silver nanoclusters," J. Phys. Chem. C **124**(37), 20477–20487 (2020).
[195]L. Yan, M. Guan, and S. Meng, "Plasmon-induced nonlinear response of silver atomic chains," Nanoscale **10**(18), 8600–8605 (2018).
[196]G. U. Kuda-Singappulige and C. M. Aikens, "Excited-state absorption in silver nanoclusters," J. Phys. Chem. C **125**(45), 24996–25006 (2021).
[197]A. M. Brown, R. Sundararaman, P. Narang, W. A. Goddard, and H. A. Atwater, "Nonradiative plasmon decay and hot carrier dynamics: Effects of phonons, surfaces, and geometry," ACS Nano **10**(1), 957–966 (2015).
[198]A. M. Brown, R. Sundararaman, P. Narang, A. M. Schwartzberg, W. A. Goddard, and H. A. Atwater, "Experimental and *ab initio* ultrafast carrier dynamics in plasmonic nanoparticles," Phys. Rev. Lett. **118**(8), 087401 (2017).
[199]G. Stefanucci and R. van Leeuwen, *Nonequilibrium Many-Body Theory of Quantum Systems* (Cambridge University Press, 2013).
[200]X. Zhang, X. Li, D. Zhang, N. Q. Su, W. Yang, H. O. Everitt, and J. Liu, "Product selectivity in plasmonic photocatalysis for carbon dioxide hydrogenation," Nat. Commun. **8**(1), 14542 (2017).
[201]L. Mascaretti, A. Schirato, P. Fornasiero, A. Boltasseva, V. M. Shalaev, A. Alabastri, and A. Naldoni, "Challenges and prospects of plasmonic metasurfaces for photothermal catalysis," Nanophotonics **11**(13), 3035–3056 (2022).
[202]J. B. Khurgin, "How to deal with the loss in plasmonics and metamaterials," Nat. Nanotechnol. **10**(1), 2–6 (2015).
[203]S. Ezendam, M. Herran, L. Nan, C. Gruber, Y. Kang, F. Gröbmeyer, R. Lin, J. Gargiulo, A. Sousa-Castillo, and E. Cortés, "Hybrid plasmonic nanomaterials for hydrogen generation and carbon dioxide reduction," ACS Energy Lett. **7**(2), 778–815 (2022).
[204]U. Aslam, S. Chavez, and S. Linic, "Controlling energy flow in multimetallic nanostructures for plasmonic catalysis," Nat. Nanotechnol. **12**(10), 1000–1005 (2017).
[205]S. Chavez, U. Aslam, and S. Linic, "Design principles for directing energy and energetic charge flow in multicomponent plasmonic nanostructures," ACS Energy Lett. **3**(7), 1590–1596 (2018).
[206]C. Engelbrekt, K. T. Crampton, D. A. Fishman, M. Law, and V. A. Apkarian, "Efficient plasmon-mediated energy funneling to the surface of Au@Pt core–-shell nanocrystals," ACS Nano **14**(4), 5061–5074 (2020).
[207]L. Qin, G. Wang, and Y. Tan, "Plasmonic Pt nanoparticles—TiO_2 hierarchical nano-architecture as a visible light photocatalyst for water splitting," Sci. Rep. **8**(1), 16198 (2018).
[208]Y. Negrín-Montecelo, M. Comesaña-Hermo, L. K. Khorashad, A. Sousa-Castillo, Z. Wang, M. Pérez-Lorenzo, T. Liedl, A. O. Govorov, and M. A. Correa-Duarte, "Photophysical effects behind the efficiency of hot electron injection in plasmon-assisted catalysis: The joint role of morphology and composition," ACS Energy Lett. **5**(2), 395–402 (2020).
[209]X. Cai, M. Zhu, O. A. Elbanna, M. Fujitsuka, S. Kim, L. Mao, J. Zhang, and T. Majima, "Au nanorod photosensitized La_2 Ti_2O_7 nanosteps: Successive surface heterojunctions boosting visible to near-infrared photocatalytic H_2 evolution," ACS Catal. **8**(1), 122–131 (2018).
[210]M. Wen, K. Mori, Y. Kuwahara, and H. Yamashita, "Plasmonic Au@Pd nanoparticles supported on a basic metal–organic framework: Synergic boosting of H_2 production from formic acid," ACS Energy Lett. **2**(1), 1–7 (2017).
[211]G. V. Hartland, L. V. Besteiro, P. Johns, and A. O. Govorov, "What's so hot about electrons in metal nanoparticles?," ACS Energy Lett. **2**(7), 1641–1653 (2017).
[212]D. C. Ratchford, "Plasmon-induced charge transfer: Challenges and outlook," ACS Nano **13**(12), 13610–13614 (2019).
[213]F. V. A. Camargo, Y. Ben-Shahar, T. Nagahara, Y. E. Panfil, M. Russo, U. Banin, and G. Cerullo, "Visualizing ultrafast electron transfer processes in semiconductor–metal hybrid nanoparticles: Toward excitonic–plasmonic light harvesting," Nano Lett. **21**(3), 1461–1468 (2021).
[214]K. R. Keller, R. Rojas-Aedo, H. Zhang, P. Schweizer, J. Allerbeck, D. Brida, D. Jariwala, and N. Maccaferri, "Ultrafast thermionic electron injection effects on exciton formation dynamics at a van der Waals semiconductor/metal interface," ACS Photonics **9**(8), 2683–2690 (2022).
[215]E. Cortés, R. Grzeschik, S. A. Maier, and S. Schlücker, "Experimental characterization techniques for plasmon-assisted chemistry," Nat. Rev. Chem. **6**(4), 259–274 (2022).
[216]K. Wu, J. Chen, J. R. McBride, and T. Lian, "Efficient hot-electron transfer by a plasmon-induced interfacial charge-transfer transition," Science **349**(6248), 632–635 (2015).
[217]J. Song, J. Long, Y. Liu, Z. Xu, A. Ge, B. D. Piercy, D. A. Cullen, I. N. Ivanov, J. R. McBride, M. D. Losego, and T. Lian, "Highly efficient plasmon induced hot-electron transfer at Ag/TiO_2 interface," ACS Photonics **8**(5), 1497–1504 (2021).
[218]Z. Zhang, L. Liu, W.-H. Fang, R. Long, M. V. Tokina, and O. V. Prezhdo, "Plasmon-mediated electron injection from Au nanorods into MoS_2: Traditional versus photoexcitation mechanism," Chem **4**(5), 1112–1127 (2018).
[219]R. Long and O. V. Prezhdo, "Instantaneous generation of charge-separated state on TiO_2 surface sensitized with plasmonic nanoparticles," J. Am. Chem. Soc. **136**(11), 4343–4354 (2014).
[220]F. Remacle and R. D. Levine, "An electronic time scale in chemistry," Proc. Natl. Acad. Sci. U. S. A. **103**(18), 6793–6798 (2006).
[221]A. H. Zewail, "Laser femtochemistry," Science **242**(4886), 1645–1653 (1988).
[222]I. C. D. Merritt, D. Jacquemin, and M. Vacher, "Attochemistry: Is controlling electrons the future of photochemistry?," J. Phys. Chem. Lett. **12**(34), 8404–8415 (2021).
[223]J. Feist, J. Galego, and F. J. Garcia-Vidal, "Polaritonic chemistry with organic molecules," ACS Photonics **5**(1), 205–216 (2017).
[224]J. Fregoni, F. J. Garcia-Vidal, and J. Feist, "Theoretical challenges in polaritonic chemistry," ACS Photonics **9**(4), 1096–1107 (2022).
[225]P. Zeng, J. Cadusch, D. Chakraborty, T. A. Smith, A. Roberts, J. E. Sader, T. J. Davis, and D. E. Gómez, "Photoinduced electron transfer in the strong coupling regime: Waveguide–plasmon polaritons," Nano Lett. **16**(4), 2651–2656 (2016).
[226]J. Galego, F. J. Garcia-Vidal, and J. Feist, "Cavity-induced modifications of molecular structure in the strong-coupling regime," Phys. Rev. X **5**(4), 041022 (2015).
[227]M. Kowalewski, K. Bennett, and S. Mukamel, "Cavity femtochemistry: Manipulating nonadiabatic dynamics at avoided crossings," J. Phys. Chem. Lett. **7**(11), 2050–2054 (2016).
[228]B. Munkhbat, M. Wersäll, D. G. Baranov, T. J. Antosiewicz, and T. Shegai, "Suppression of photo-oxidation of organic chromophores by strong coupling to plasmonic nanoantennas," Sci. Adv. **4**(7), eaas9552 (2018).
[229]M. Du, "Theory reveals novel chemistry of photonic molecules," Chem **5**(5), 1009–1011 (2019).
[230]L. A. Martínez-Martínez, M. Du, R. F. Ribeiro, S. Kéna-Cohen, and J. Yuen-Zhou, "Polariton-assisted singlet fission in acene aggregates," J. Phys. Chem. Lett. **9**(8), 1951–1957 (2018).
[231]J. Galego, F. J. Garcia-Vidal, and J. Feist, "Suppressing photochemical reactions with quantized light fields," Nat. Commun. **7**(1), 13841 (2016).
[232]J. Fregoni, G. Granucci, M. Persico, and S. Corni, "Strong coupling with light enhances the photoisomerization quantum yield of azobenzene," Chem **6**(1), 250–265 (2020).
[233]S. Satapathy, M. Khatoniar, D. K. Parappuram, B. Liu, G. John, J. Feist, F. J. Garcia-Vidal, and V. M. Menon, "Selective isomer emission via funneling of exciton polaritons," Sci. Adv. **7**(44), eabj0997 (2021).
[234]J. A. Hutchison, T. Schwartz, C. Genet, E. Devaux, and T. W. Ebbesen, "Modifying chemical landscapes by coupling to vacuum fields," Angew. Chem., Int. Ed. **51**(7), 1592–1596 (2012).

[235]D. Kumar, A. Lee, T. Lee, M. Lim, and D.-K. Lim, "Ultrafast and efficient transport of hot plasmonic electrons by graphene for Pt Free, highly efficient visible-light responsive photocatalyst," Nano Lett. **16**(3), 1760–1767 (2016).
[236]A. Hoggard, L.-Y. Wang, L. Ma, Y. Fang, G. You, J. Olson, Z. Liu, W.-S. Chang, P. M. Ajayan, and S. Link, "Using the plasmon linewidth to calculate the time and efficiency of electron transfer between gold nanorods and graphene," ACS Nano **7**(12), 11209–11217 (2013).
[237]S. Sim, A. Beierle, P. Mantos, S. McCrory, R. P. Prasankumar, and S. Chowdhury, "Ultrafast relaxation dynamics in bimetallic plasmonic catalysts," Nanoscale **12**(18), 10284–10291 (2020).
[238]S. Wu, O. H.-C. Cheng, B. Zhao, N. Hogan, A. Lee, D. H. Son, and M. Sheldon, "The connection between plasmon decay dynamics and the surface enhanced Raman spectroscopy background: Inelastic scattering from non-thermal and hot carriers," J. Appl. Phys. **129**(17), 173103 (2021).
[239]S. A. Lee, B. Ostovar, C. F. Landes, and S. Link, "Spectroscopic signatures of plasmon-induced charge transfer in gold nanorods," J. Chem. Phys. **156**(6), 064702 (2022).
[240]H. Harutyunyan, A. B. F. Martinson, D. Rosenmann, L. K. Khorashad, L. V. Besteiro, A. O. Govorov, and G. P. Wiederrecht, "Anomalous ultrafast dynamics of hot plasmonic electrons in nanostructures with hot spots," Nat. Nanotechnol. **10**(9), 770–774 (2015).
[241]S. Link and M. A. El-Sayed, "Spectral properties and relaxation dynamics of surface plasmon electronic oscillations in gold and silver nanodots and nanorods," J. Phys. Chem. B **103**(40), 8410–8426 (1999).
[242]X. Liu, J. Wang, L. Tang, L. Xie, and Y. Ying, "Flexible plasmonic metasurfaces with user-designed patterns for molecular sensing and cryptography," Adv. Funct. Mater. **26**(30), 5515–5523 (2016).
[243]K. L. Kelly, E. Coronado, L. L. Zhao, and G. C. Schatz, "The optical properties of metal nanoparticles: The influence of size, shape, and dielectric environment," J. Phys. Chem. B **107**(3), 668–677 (2003).
[244]L. Tong, H. Wei, S. Zhang, Z. Li, and H. Xu, "Optical properties of single coupled plasmonic nanoparticles," Phys. Chem. Chem. Phys. **15**(12), 4100–4109 (2013).
[245]X. Lu, M. Rycenga, S. E. Skrabalak, B. Wiley, and Y. Xia, "Chemical synthesis of novel plasmonic nanoparticles," Annu. Rev. Phys. Chem. **60**(1), 167–192 (2009).
[246]R. Yu, L. M. Liz-Marzán, and F. J. García de Abajo, "Universal analytical modeling of plasmonic nanoparticles," Chem. Soc. Rev. **46**(22), 6710–6724 (2017).
[247]Z. Fusco, K. Catchpole, and F. J. Beck, "Investigation of the mechanisms of plasmon-mediated photocatalysis: Synergistic contribution of near-field and charge transfer effects," J. Mater. Chem. C **10**(19), 7511–7524 (2022).
[248]Z. Li and D. Kurouski, "Plasmon-driven chemistry on mono- and bimetallic nanostructures," Acc. Chem. Res. **54**(10), 2477–2487 (2021).
[249]M. Vanzan, G. Gil, D. Castaldo, P. Nordlander, and S. Corni, "Energy transfer to molecular adsorbates by transient hot electron spillover," Nano Lett. **23**(7), 2719–2725 (2023).
[250]Y. Dubi and Y. Sivan, "'Hot' electrons in metallic nanostructures—non-thermal carriers or heating?," Light: Sci. Appl. **8**(1), 89 (2019).
[251]Y. Dubi, I. W. Un, and Y. Sivan, "Thermal effects—An alternative mechanism for plasmon-assisted photocatalysis," Chem. Sci. **11**(19), 5017–5027 (2020).
[252]Y. Sivan, I. W. Un, and Y. Dubi, "Assistance of metal nanoparticles in photocatalysis—Nothing more than a classical heat source," Faraday Discuss. **214**, 215–233 (2019).
[253]Y. Sivan, J. Baraban, I. W. Un, and Y. Dubi, "Comment on 'Quantifying hot carrier and thermal contributions in plasmonic photocatalysis'," Science **364**(6439), aaw9367 (2019).
[254]J. Huang, X. Zhao, X. Huang, and W. Liang, "Understanding the mechanism of plasmon-driven water splitting: Hot electron injection and a near field enhancement effect," Phys. Chem. Chem. Phys. **23**(45), 25629–25636 (2021).
[255]L. Yan, J. Xu, F. Wang, and S. Meng, "Plasmon-Induced Ultrafast Hydrogen Production in Liquid Water," J. Phys. Chem. Lett. **9**(1), 63–69 (2017).
[256]V. A. Spata and E. A. Carter, "Mechanistic insights into photocatalyzed hydrogen desorption from palladium surfaces assisted by localized surface plasmon resonances," ACS Nano **12**(4), 3512–3522 (2018).
[257]J. L. Bao and E. A. Carter, "Rationalizing the hot-carrier-mediated reaction mechanisms and kinetics for ammonia decomposition on ruthenium-doped copper nanoparticles," J. Am. Chem. Soc. **141**(34), 13320–13323 (2019).
[258]H. Robatjazi, J. L. Bao, M. Zhang, L. Zhou, P. Christopher, E. A. Carter, P. Nordlander, and N. J. Halas, "Plasmon-driven carbon–fluorine (C(sp3)–F) bond activation with mechanistic insights into hot-carrier-mediated pathways," Nat. Catal. **3**(7), 564–573 (2020).
[259]S. Mukherjee, F. Libisch, N. Large, O. Neumann, L. V. Brown, J. Cheng, J. B. Lassiter, E. A. Carter, P. Nordlander, and N. J. Halas, "Hot electrons do the impossible: Plasmon-induced dissociation of H_2 on Au," Nano Lett. **13**(1), 240–247 (2013).
[260]C. Fasciani, C. J. B. Alejo, M. Grenier, J. C. Netto-Ferreira, and J. C. Scaiano, "High-temperature organic reactions at room temperature using plasmon excitation: Decomposition of dicumyl peroxide," Org. Lett. **13**(2), 204–207 (2011).
[261]H. Huh, H. D. Trinh, D. Lee, and S. Yoon, "How does a plasmon-induced hot charge carrier break a C–C bond?," ACS Appl. Mater. Interfaces **11**(27), 24715–24724 (2019).
[262]C. W. Moon, M.-J. Choi, J. K. Hyun, and H. W. Jang, "Enhancing photoelectrochemical water splitting with plasmonic Au nanoparticles," Nanoscale Adv. **3**(21), 5981–6006 (2021).
[263]Z. Li, P. Z. El-Khoury, and D. Kurouski, "Tip-enhanced Raman imaging of photocatalytic reactions on thermally-reshaped gold and gold–palladium microplates," Chem. Commun. **57**(7), 891–894 (2021).
[264]Z. Li and D. Kurouski, "Elucidation of photocatalytic properties of gold–platinum bimetallic nanoplates using tip-enhanced Raman spectroscopy," J. Phys. Chem. C **124**(23), 12850–12854 (2020).
[265]Z. Li, R. Wang, and D. Kurouski, "Nanoscale photocatalytic activity of gold and gold–palladium nanostructures revealed by tip-enhanced raman spectroscopy," J. Phys. Chem. Lett. **11**(14), 5531–5537 (2020).
[266]F. Wang, C. Li, H. Chen, R. Jiang, L.-D. Sun, Q. Li, J. Wang, J. C. Yu, and C.-H. Yan, "Plasmonic harvesting of light energy for suzuki coupling reactions," J. Am. Chem. Soc. **135**(15), 5588–5601 (2013).
[267]J. Guo, Y. Zhang, L. Shi, Y. Zhu, M. F. Mideksa, K. Hou, W. Zhao, D. Wang, M. Zhao, X. Zhang, J. Lv, J. Zhang, X. Wang, and Z. Tang, "Boosting hot electrons in hetero-superstructures for plasmon-enhanced catalysis," J. Am. Chem. Soc. **139**(49), 17964–17972 (2017).
[268]P. Christopher, H. Xin, and S. Linic, "Visible-light-enhanced catalytic oxidation reactions on plasmonic silver nanostructures," Nat. Chem. **3**(6), 467–472 (2011).
[269]P. Christopher, H. Xin, A. Marimuthu, and S. Linic, "Singular characteristics and unique chemical bond activation mechanisms of photocatalytic reactions on plasmonic nanostructures," Nat. Mater **11**(12), 1044–1050 (2012).
[270]L. Zhou, D. F. Swearer, C. Zhang, H. Robatjazi, H. Zhao, L. Henderson, L. Dong, P. Christopher, E. A. Carter, P. Nordlander, and N. J. Halas, "Quantifying hot carrier and thermal contributions in plasmonic photocatalysis," Science **362**(6410), 69–72 (2018).
[271]L. Zhou, J. M. P. Martirez, J. Finzel, C. Zhang, D. F. Swearer, S. Tian, H. Robatjazi, M. Lou, L. Dong, L. Henderson, P. Christopher, E. A. Carter, P. Nordlander, and N. J. Halas, "Light-driven methane dry reforming with single atomic site antenna-reactor plasmonic photocatalysts," Nat. Energy **5**(1), 61–70 (2020).
[272]X. Li, H. O. Everitt, and J. Liu, "Confirming nonthermal plasmonic effects enhance CO2 methanation on Rh/TiO_2 catalysts," Nano Res. **12**(8), 1906–1911 (2019).
[273]N. Vu, S. Kaliaguine, and T. Do, "Plasmonic photocatalysts for sunlight-driven reduction of CO_2: Details, developments, and perspectives," ChemSusChem **13**(16), 3967–3991 (2020).
[274]S. Linic, S. Chavez, and R. Elias, "Flow and extraction of energy and charge carriers in hybrid plasmonic nanostructures," Nat. Mater. **20**(7), 916–924 (2021).
[275]B. Foerster, M. Hartelt, S. S. E. Collins, M. Aeschlimann, S. Link, and C. Sönnichsen, "Interfacial states cause equal decay of plasmons and hot electrons at gold–metal oxide interfaces," Nano Lett. **20**(5), 3338–3343 (2020).
[276]S. Tan, A. Argondizzo, J. Ren, L. Liu, J. Zhao, and H. Petek, "Plasmonic coupling at a metal/semiconductor interface," Nat. Photonics **11**(12), 806–812 (2017).
[277]W. Yang, Y. Liu, J. R. McBride, and T. Lian, "Ultrafast and long-lived transient heating of surface adsorbates on plasmonic semiconductor nanocrystals," Nano Lett. **21**(1), 453–461 (2020).

[278]S. S. E. Collins, E. K. Searles, L. J. Tauzin, M. Lou, L. Bursi, Y. Liu, J. Song, C. Flatebo, R. Baiyasi, Y.-Y. Cai, B. Foerster, T. Lian, P. Nordlander, S. Link, and C. F. Landes, "Plasmon energy transfer in hybrid nanoantennas," ACS Nano **15**(6), 9522–9530 (2020).
[279]M. Herran, A. Sousa-Castillo, C. Fan, S. Lee, W. Xie, M. Döblinger, B. Auguié, and E. Cortés, "Tailoring plasmonic bimetallic nanocatalysts toward sunlight-driven H_2 production," Adv. Funct. Mater. **32**(38), 2203418 (2022).
[280]V. V. Temnov, "Ultrafast acousto-magneto-plasmonics," Nat. Photonics **6**(11), 728–736 (2012).
[281]*Active Plasmonics and Tuneable Plasmonic Metamaterials*, edited by A. V. Zayats and S. A. Maier (John Wiley & Sons, Inc., 2013).
[282]N. Jiang, X. Zhuo, and J. Wang, "Active plasmonics: Principles, structures, and applications," Chem. Rev. **118**(6), 3054–3099 (2018).
[283]N. Maccaferri, "Coupling phenomena and collective effects in resonant meta-atoms supporting both plasmonic and (opto-)magnetic functionalities: An overview on properties and applications [Invited]," J. Opt. Soc. Am. B **36**(7), E112 (2019).
[284]N. Maccaferri, I. Zubritskaya, I. Razdolski, I.-A. Chioar, V. Belotelov, V. Kapaklis, P. M. Oppeneer, and A. Dmitriev, "Nanoscale magnetophotonics," J. Appl. Phys. **127**(8), 080903 (2020).
[285]A. Kirilyuk, A. V. Kimel, and T. Rasing, "Ultrafast optical manipulation of magnetic order," Rev. Mod. Phys. **82**(3), 2731–2784 (2010).
[286]A. Kirilyuk, A. V. Kimel, and T. Rasing, "Erratum: Ultrafast optical manipulation of magnetic order [Rev. Mod. Phys. **82**, 2731 (2010)]," Rev. Mod. Phys. **88**(3), 039904 (2016).
[287]N. Maccaferri, A. Gabbani, F. Pineider, T. Kaihara, T. Tapani, and P. Vavassori, "Magnetoplasmonics in confined geometries: Current challenges and future opportunities," Appl. Phys. Lett. **122**, 120502 (2023).
[288]A. Ahmed, M. Pelton, and J. R. Guest, "Understanding how acoustic vibrations modulate the optical response of plasmonic metal nanoparticles," ACS Nano **11**(9), 9360–9369 (2017).
[289]C. D. Stanciu, F. Hansteen, A. V. Kimel, A. Kirilyuk, A. Tsukamoto, A. Itoh, and T. Rasing, "All-optical magnetic recording with circularly polarized light," Phys. Rev. Lett. **99**(4), 047601 (2007).
[290]S. A. Wolf, D. D. Awschalom, R. A. Buhrman, J. M. Daughton, v S. von Molnár, M. L. Roukes, A. Y. Chtchelkanova, and D. M. Treger, "Spintronics: A spin-based electronics vision for the future," Science **294**(5546), 1488–1495 (2001).
[291]J. Kuttruff, D. Garoli, J. Allerbeck, R. Krahne, A. De Luca, D. Brida, V. Caligiuri, and N. Maccaferri, "Ultrafast all-optical switching enabled by epsilon-near-zero-tailored absorption in metal-insulator nanocavities," Commun. Phys. **3**(1), 114 (2020).
[292]D. L. Sounas and A. Alu, "Non-reciprocal photonics based on time modulation," Nat. Photonics **11**(12), 774–783 (2017).
[293]G. Grinblat, R. Berté, M. P. Nielsen, Y. Li, R. F. Oulton, and S. A. Maier, "Sub-20 fs all-optical switching in a single Au-Clad Si nanodisk," Nano Lett. **18**(12), 7896–7900 (2018).
[294]M. Kataja, S. Pourjamal, N. Maccaferri, P. Vavassori, T. K. Hakala, M. J. Huttunen, P. Törmä, and S. van Dijken, "Hybrid plasmonic lattices with tunable magneto-optical activity," Opt. Express **24**(4), 3652 (2016).
[295]S. Pourjamal, M. Kataja, N. Maccaferri, P. Vavassori, and S. van Dijken, "Tunable magnetoplasmonics in lattices of Ni/SiO_2/Au dimers," Sci Rep **9**(1), 9907 (2019).
[296]A. López-Ortega, M. Zapata-Herrera, N. Maccaferri, M. Pancaldi, M. Garcia, A. Chuvilin, and P. Vavassori, "Enhanced magnetic modulation of light polarization exploiting hybridization with multipolar dark plasmons in magneto-plasmonic nanocavities," Light **9**(1), 49 (2020).
[297]N. Maccaferri, A. Berger, S. Bonetti, V. Bonanni, M. Kataja, Q. H. Qin, S. van Dijken, Z. Pirzadeh, A. Dmitriev, J. Nogués, J. Åkerman, and P. Vavassori, "Tuning the magneto-optical response of nanosize ferromagnetic Ni disks using the phase of localized plasmons," Phys. Rev. Lett. **111**(16), 167401 (2013).
[298]K. Lodewijks, N. Maccaferri, T. Pakizeh, R. K. Dumas, I. Zubritskaya, J. Åkerman, P. Vavassori, and A. Dmitriev, "Magnetoplasmonic design rules for active magneto-optics," Nano Lett. **14**(12), 7207–7214 (2014).
[299]N. Maccaferri, M. Kataja, V. Bonanni, S. Bonetti, Z. Pirzadeh, A. Dmitriev, S. van Dijken, J. Åkerman, and P. Vavassori, "Effects of a non-absorbing substrate on the magneto-optical Kerr response of plasmonic ferromagnetic nanodisks: Magneto-optical Kerr response of plasmonic ferromagnetic nanodisks," Phys. Status Solidi A **211**(5), 1067–1075 (2014).
[300]N. Maccaferri, X. Inchausti, A. García-Martín, J. C. Cuevas, D. Tripathy, A. O. Adeyeye, and P. Vavassori, "Resonant enhancement of magneto-optical activity induced by surface plasmon polariton modes coupling in 2D magnetoplasmonic crystals," ACS Photonics **2**(12), 1769–1779 (2015).
[301]N. Maccaferri, L. Bergamini, M. Pancaldi, M. K. Schmidt, M. Kataja, S. van Dijken, N. Zabala, J. Aizpurua, and P. Vavassori, "Anisotropic nanoantenna-based magnetoplasmonic crystals for highly enhanced and tunable magneto-optical activity," Nano Lett. **16**(4), 2533–2542 (2016).
[302]S. Schlauderer, C. Lange, S. Baierl, T. Ebnet, C. P. Schmid, D. C. Valovcin, A. K. Zvezdin, A. V. Kimel, R. V. Mikhaylovskiy, and R. Huber, "Temporal and spectral fingerprints of ultrafast all-coherent spin switching," Nature **569**(7756), 383–387 (2019).
[303]K. Mishra, R. M. Rowan-Robinson, A. Ciuciulkaite, C. S. Davies, A. Dmitriev, V. Kapaklis, A. V. Kimel, and A. Kirilyuk, "Ultrafast demagnetization control in magnetophotonic surface crystals," Nano Lett. **22**(23), 9773–9780 (2022).
[304]C. D. Stanciu, A. Tsukamoto, A. V. Kimel, F. Hansteen, A. Kirilyuk, A. Itoh, and T. Rasing, "Subpicosecond magnetization reversal across ferrimagnetic compensation points," Phys. Rev. Lett. **99**(21), 217204 (2007).
[305]C.-H. Lambert, S. Mangin, B. S. D. C. S. Varaprasad, Y. K. Takahashi, M. Hehn, M. Cinchetti, G. Malinowski, K. Hono, Y. Fainman, M. Aeschlimann, and E. E. Fullerton, "All-optical control of ferromagnetic thin films and nanostructures," Science **345**(6202), 1337–1340 (2014).
[306]S. Mangin, M. Gottwald, C.-H. Lambert, D. Steil, V. Uhlíř, L. Pang, M. Hehn, S. Alebrand, M. Cinchetti, G. Malinowski, Y. Fainman, M. Aeschlimann, and E. E. Fullerton, "Engineered materials for all-optical helicity-dependent magnetic switching," Nat. Mater. **13**(3), 286–292 (2014).
[307]T. A. Ostler, J. Barker, R. F. L. Evans, R. W. Chantrell, U. Atxitia, O. Chubykalo-Fesenko, S. El Moussaoui, L. Le Guyader, E. Mengotti, L. J. Heyderman, F. Nolting, A. Tsukamoto, A. Itoh, D. Afanasiev, B. A. Ivanov, A. M. Kalashnikova, K. Vahaplar, J. Mentink, A. Kirilyuk, Th. Rasing, and A. V. Kimel, "Ultrafast heating as a sufficient stimulus for magnetization reversal in a ferrimagnet," Nat. Commun. **3**(1), 666 (2012).
[308]M. Finazzi, M. Savoini, A. R. Khorsand, A. Tsukamoto, A. Itoh, L. Duo, A. Kirilyuk, T. Rasing, and M. Ezawa, "Laser-induced magnetic nanostructures with tunable topological properties," Phys. Rev. Lett. **110**(17), 177205 (2013).
[309]L. Le Guyader, S. El Moussaoui, M. Buzzi, R. V. Chopdekar, L. J. Heyderman, A. Tsukamoto, A. Itoh, A. Kirilyuk, T. Rasing, and A. V. Kimel, "Demonstration of laser induced magnetization reversal in GdFeCo nanostructures," Appl. Phys. Lett. **101**(2), 022410 (2012).
[310]L. Le Guyader, M. Savoini, S. El Moussaoui, M. Buzzi, A. Tsukamoto, A. Itoh, A. Kirilyuk, T. Rasing, A. V. Kimel, and F. Nolting, "Nanoscale sub-100 picosecond all-optical magnetization switching in GdFeCo microstructures," Nat. Commun. **6**(1), 5839 (2015).
[311]A. El-Ghazaly, B. Tran, A. Ceballos, C.-H. Lambert, A. Pattabi, S. Salahuddin, F. Hellman, and J. Bokor, "Ultrafast magnetization switching in nanoscale magnetic dots," Appl. Phys. Lett. **114**(23), 232407 (2019).
[312]T.-M. Liu, T. Wang, A. H. Reid, M. Savoini, X. Wu, B. Koene, P. Granitzka, C. E. Graves, D. J. Higley, Z. Chen, G. Razinskas, M. Hantschmann, A. Scherz, J. Stöhr, A. Tsukamoto, B. Hecht, A. V. Kimel, A. Kirilyuk, T. Rasing, and H. A. Dürr, "Nanoscale confinement of all-optical magnetic switching in TbFeCo—Competition with nanoscale heterogeneity," Nano Lett. **15**(10), 6862–6868 (2015).
[313]H. Xu, G. Hajisalem, G. M. Steeves, R. Gordon, and B. C. Choi, "Nanorod surface plasmon enhancement of laser-induced ultrafast demagnetization," Sci. Rep. **5**(1), 15933 (2015).
[314]M. Kataja, F. Freire-Fernández, J. P. Witteveen, T. K. Hakala, P. Törmä, and S. van Dijken, "Plasmon-induced demagnetization and magnetic switching in nickel nanoparticle arrays," Appl. Phys. Lett. **112**(7), 072406 (2018).
[315]J. P. van der Ziel, P. S. Pershan, and L. D. Malmstrom, "Optically-induced magnetization resulting from the inverse Faraday effect," Phys. Rev. Lett. **15**(5), 190–193 (1965).
[316]R. Hertel, "Theory of the inverse Faraday effect in metals," J. Magn. Magn. Mater. **303**(1), L1–L4 (2006).
[317]A. Nadarajah and M. T. Sheldon, "Optoelectronic phenomena in gold metal nanostructures due to the inverse Faraday effect," Opt. Express **25**(11), 12753 (2017).

[318]D. Popova, A. Bringer, and S. Blügel, "Theoretical investigation of the inverse Faraday effect via a stimulated Raman scattering process," Phys. Rev. B **85**(9), 094419 (2012).
[319]R. Mondal, M. Berritta, C. Paillard, S. Singh, B. Dkhil, P. M. Oppeneer, and L. Bellaiche, "Relativistic interaction Hamiltonian coupling the angular momentum of light and the electron spin," Phys. Rev. B **92**(10), 100402 (2015).
[320]M. Berritta, R. Mondal, K. Carva, and P. M. Oppeneer, "*Ab initio* theory of coherent laser-induced magnetization in metals," Phys. Rev. Lett. **117**(13), 137203 (2016).
[321]M. Battiato, G. Barbalinardo, and P. M. Oppeneer, "Quantum theory of the inverse Faraday effect," Phys. Rev. B **89**(1), 014413 (2014).
[322]N. I. Zheludev, P. J. Bennett, H. Loh, S. V. Popov, I. R. Shatwell, Yu. P. Svirko, V. E. Gusev, V. F. Kamalov, and E. V. Slobodchikov, "Cubic optical nonlinearity of free electrons in bulk gold," Opt. Lett. **20**(12), 1368 (1995).
[323]O. H.-C. Cheng, D. H. Son, and M. Sheldon, "Light-induced magnetism in plasmonic gold nanoparticles," Nat. Photonics **14**(6), 365–368 (2020).
[324]*Twisted Photons: Applications of Light with Orbital Angular Momentum*, edited by J. P. Torres and L. Torner (Wiley-VCH, Weinheim, Germany, 2011).
[325]L. Allen, S. M. Barnett, and M. J. Padgett, *Optical Angular Momentum* (CRC Press, 2016).
[326]D. Garoli, P. Zilio, Y. Gorodetski, F. Tantussi, and F. De Angelis, "Beaming of helical light from plasmonic vortices via adiabatically tapered nanotip," Nano Lett. **16**(10), 6636–6643 (2016).
[327]N. Maccaferri, Y. Gorodetski, A. Toma, P. Zilio, F. De Angelis, and D. Garoli, "Magnetoplasmonic control of plasmonic vortices," Appl. Phys. Lett. **111**(20), 201104 (2017).
[328]E. Prinz, M. Hartelt, G. Spektor, M. Orenstein, and M. Aeschlimann, "Orbital angular momentum in nanoplasmonic vortices," ACS Photonics **10**(2), 340–367 (2023).
[329]A. A. Sirenko, P. Marsik, C. Bernhard, T. N. Stanislavchuk, V. Kiryukhin, and S.-W. Cheong, "Terahertz vortex beam as a spectroscopic probe of magnetic excitations," Phys. Rev. Lett. **122**(23), 237401 (2019).
[330]M. Fanciulli, M. Pancaldi, E. Pedersoli, M. Vimal, D. Bresteau, M. Luttmann, D. De Angelis, P. R. Ribič, B. Rösner, C. David, C. Spezzani, M. Manfredda, R. Sousa, I.-L. Prejbeanu, L. Vila, B. Dieny, G. De Ninno, F. Capotondi, M. Sacchi, and T. Ruchon, "Observation of magnetic helicoidal dichroism with extreme ultraviolet light vortices," Phys. Rev. Lett. **128**(7), 077401 (2022).
[331]V. Karakhanyan, C. Eustache, Y. Lefier, and T. Grosjean, "Inverse Faraday effect from the orbital angular momentum of light," Phys. Rev. B **105**(4), 045406 (2022).
[332]E. Prinz, B. Stadtmüller, and M. Aeschlimann, "Twisted light affects ultrafast demagnetization," arXiv:2206.07502 (2022).
[333]A. Kazlou, A. L. Chekhov, A. I. Stognij, I. Razdolski, and A. Stupakiewicz, "Surface plasmon-enhanced photomagnetic excitation of spin dynamics in Au/YIG:Co magneto-plasmonic crystals," ACS Photonics **8**(8), 2197–2202 (2021).
[334]A. Kazlou, T. Kaihara, I. Razdolski, and A. Stupakiewicz, "Surface plasmon-assisted control of the phase of photo-induced spin precession," Appl. Phys. Lett. **120**(25), 251101 (2022).
[335]J. Lerme, M. Pellarin, E. Cottancin, M. Gaudry, M. Broyer, N. Del Fatti, F. Vallee, and C. Voisin, "Influence of lattice contraction on the optical properties and the electron dynamics in silver clusters," Eur. Phys. J. D-At., Mol., Opt. Plasma Phys. **17**(2), 213–220 (2001).
[336]M. van Exter and A. Lagendijk, "Ultrashort surface-plasmon and phonon dynamics," Phys. Rev. Lett. **60**(1), 49 (1988).
[337]M. E. Siemens, Q. Li, R. Yang, K. A. Nelson, E. H. Anderson, M. M. Murnane, and H. C. Kapteyn, "Quasi-ballistic thermal transport from nanoscale interfaces observed using ultrafast coherent soft x-ray beams," Nat. Mater. **9**(1), 26–30 (2010).
[338]J. Wang, J. Wu, and C. Guo, "Resolving dynamics of acoustic phonons by surface plasmons," Opt. Lett. **32**(6), 719–721 (2007).
[339]J. Wang and C. Guo, "Effect of electron heating on femtosecond laser-induced coherent acoustic phonons in noble metals," Phys. Rev. B **75**(18), 184304 (2007).
[340]M. Perner, S. Gresillon, J. März, G. Von Plessen, J. Feldmann, J. Porstendorfer, K.-J. Berg, and G. Berg, "Observation of hot-electron pressure in the vibration dynamics of metal nanoparticles," Phys. Rev. Lett. **85**(4), 792 (2000).
[341]W. M. Deacon, A. Lombardi, F. Benz, Y. del, V.-I. Redondo, R. Chikkaraddy, B. de Nijs, M.-E. Kleemann, J. Mertens, and J. J. Baumberg, "Interrogating nanojunctions using ultraconfined acoustoplasmonic coupling," Phys. Rev. Lett. **119**(2), 023901 (2017).
[342]P. Ruello, A. Ayouch, G. Vaudel, T. Pezeril, N. Delorme, S. Sato, K. Kimura, and V. E. Gusev, "Ultrafast acousto-plasmonics in gold nanoparticle superlattices," Phys. Rev. B **92**(17), 174304 (2015).
[343]V. V. Temnov, K. Nelson, G. Armelles, A. Cebollada, T. Thomay, A. Leitenstorfer, and R. Bratschitsch, "Femtosecond surface plasmon interferometry," Opt. Express **17**(10), 8423–8432 (2009).
[344]A. N. Koya, J. Cunha, K. A. Guerrero-Becerra, D. Garoli, T. Wang, S. Juodkazis, and R. Proietti Zaccaria, "Plasmomechanical systems: Principles and applications," Adv. Funct. Mater. **31**(41), 2103706 (2021).
[345]J. Cunha, T. Guo, G. Della Valle, A. N. Koya, R. Proietti Zaccaria, and A. Alabastri, "Controlling light, heat, and vibrations in plasmonics and phononics," Adv. Opt. Mater. **8**(24), 2001225 (2020).
[346]J. Cunha, T. Guo, A. N. Koya, A. Toma, M. Prato, G. Della Valle, A. Alabastri, and R. Proietti Zaccaria, "Photoinduced temperature gradients in sub-wavelength plasmonic structures: The thermoplasmonics of nanocones," Adv. Opt. Mater. **8**(18), 2000568 (2020).
[347]O. Kovalenko, V. Shalagatskyi, T. Pezeril, V. Gusev, D. Makarov, and V. V. Temnov, in *Ultrafast Magnetism I* (Springer, 2015), pp. 248–250.
[348]M. Pohl, V. I. Belotelov, I. A. Akimov, S. Kasture, A. S. Vengurlekar, A. V. Gopal, A. K. Zvezdin, D. R. Yakovlev, and M. Bayer, "Plasmonic crystals for ultrafast nanophotonics: Optical switching of surface plasmon polaritons," Phys. Rev. B **85**(8), 081401 (2012).
[349]G. Della Valle, F. Scotognella, A. R. S. Kandada, M. Zavelani-Rossi, H. Li, M. Conforti, S. Longhi, L. Manna, G. Lanzani, and F. Tassone, "Ultrafast optical mapping of nonlinear plasmon dynamics in $Cu_{2-x}Se$ nanoparticles," J. Phys. Chem. Lett. **4**(19), 3337–3344 (2013).
[350]M. Abb, Y. Wang, C. H. De Groot, and O. L. Muskens, "Hotspot-mediated ultrafast nonlinear control of multifrequency plasmonic nanoantennas," Nat. Commun. **5**(1), 4869 (2014).
[351]Q. Guo, Z. Qin, Z. Wang, Y.-X. Weng, X. Liu, G. Xie, and J. Qiu, "Broadly tunable plasmons in doped oxide nanoparticles for ultrafast and broadband mid-infrared all-optical switching," ACS Nano **12**(12), 12770–12777 (2018).
[352]X. Zhang, C. Huang, M. Wang, P. Huang, X. He, and Z. Wei, "Transient localized surface plasmon induced by femtosecond interband excitation in gold nanoparticles," Sci. Rep. **8**(1), 10499 (2018).
[353]J. Yang, Y. Fu, and X. Zhang, "A self-supported ultrathin plasmonic film for ultrafast optical switching," Nanoscale Adv. **4**(3), 943–951 (2022).
[354]Y. Lin, X. Zhang, X. Fang, and S. Liang, "A cross-stacked plasmonic nanowire network for high-contrast femtosecond optical switching," Nanoscale **8**(3), 1421–1429 (2016).
[355]Q. Guo, Y. Cui, Y. Yao, Y. Ye, Y. Yang, X. Liu, S. Zhang, X. Liu, J. Qiu, and H. Hosono, "A solution-processed ultrafast optical switch based on a nanostructured epsilon-near-zero medium," Adv. Mater. **29**(27), 1700754 (2017).
[356]P. Guo, R. D. Schaller, J. B. Ketterson, and R. P. Chang, "Ultrafast switching of tunable infrared plasmons in indium tin oxide nanorod arrays with large absolute amplitude," Nat. Photonics **10**(4), 267–273 (2016).
[357]M. Z. Alam, S. A. Schulz, J. Upham, I. De Leon, and R. W. Boyd, "Large optical nonlinearity of nanoantennas coupled to an epsilon-near-zero material," Nat. Photonics **12**(2), 79–83 (2018).
[358]M. Ren, B. Jia, J.-Y. Ou, E. Plum, J. Zhang, K. F. MacDonald, A. E. Nikolaenko, J. Xu, M. Gu, and N. I. Zheludev, "Nanostructured plasmonic medium for terahertz bandwidth all-optical switching," Adv. Mater. **23**(46), 5540–5544 (2011).
[359]G. Grinblat, H. Zhang, M. P. Nielsen, L. Krivitsky, R. Berté, Y. Li, B. Tilmann, E. Cortés, R. F. Oulton, and A. I. Kuznetsov, "Efficient ultrafast all-optical modulation in a nonlinear crystalline gallium phosphide nanodisk at the anapole excitation," Sci. Adv. **6**(34), eabb3123 (2020).
[360]P. Guo, R. D. Schaller, L. E. Ocola, B. T. Diroll, J. B. Ketterson, and R. P. Chang, "Large optical nonlinearity of ITO nanorods for sub-picosecond all-optical modulation of the full-visible spectrum," Nat. Commun. **7**(1), 12892 (2016).

[361]M. Ono, M. Hata, M. Tsunekawa, K. Nozaki, H. Sumikura, H. Chiba, and M. Notomi, "Ultrafast and energy-efficient all-optical switching with graphene-loaded deep-subwavelength plasmonic waveguides," Nat. Photonics **14**(1), 37–43 (2020).
[362]M. Z. Alam, I. De Leon, and R. W. Boyd, "Large optical nonlinearity of indium tin oxide in its epsilon-near-zero region," Science **352**(6287), 795–797 (2016).
[363]J. Bohn, T. S. Luk, C. Tollerton, S. W. Hutchings, I. Brener, S. Horsley, W. L. Barnes, and E. Hendry, "All-optical switching of an epsilon-near-zero plasmon resonance in indium tin oxide," Nat. Commun. **12**(1), 1017 (2021).
[364]E. Feigenbaum, K. Diest, and H. A. Atwater, "Unity-order index change in transparent conducting oxides at visible frequencies," Nano Lett. **10**(6), 2111–2116 (2010).
[365]A. Melikyan, N. Lindenmann, S. Walheim, P. M. Leufke, S. Ulrich, J. Ye, P. Vincze, H. Hahn, T. Schimmel, C. Koos, W. Freude, and J. Leuthold, "Surface plasmon polariton absorption modulator," Opt. Express **19**(9), 8855 (2011).
[366]G. Grinblat, "Nonlinear dielectric nanoantennas and metasurfaces: Frequency conversion and wavefront control," ACS Photonics **8**(12), 3406–3432 (2021).
[367]D. Ballarini, M. D. Giorgi, E. Cancellieri, R. Houdré, E. Giacobino, R. Cingolani, A. Bramati, G. Gigli, and D. Sanvitto, "All-optical polariton transistor," Nat. Commun. **4**(1), 1778 (2013).
[368]A. V. Zasedatelev, A. V. Baranikov, D. Urbonas, F. Scafirimuto, U. Scherf, T. Stöferle, R. F. Mahrt, and P. G. Lagoudakis, "A room-temperature organic polariton transistor," Nat. Photonics **13**(6), 378–383 (2019).
[369]W. Du, J. Zhao, W. Zhao, S. Zhang, H. Xu, and Q. Xiong, "Ultrafast modulation of exciton–plasmon coupling in a monolayer WS_2–Ag nanodisk hybrid system," ACS Photonics **6**(11), 2832–2840 (2019).
[370]A. Basiri, M. Z. E. Rafique, J. Bai, S. Choi, and Y. Yao, "Ultrafast low-pump fluence all-optical modulation based on graphene-metal hybrid metasurfaces," Light **11**(1), 1–14 (2022).
[371]S. Wu, S. Buckley, J. R. Schaibley, L. Feng, J. Yan, D. G. Mandrus, F. Hatami, W. Yao, J. Vučković, A. Majumdar, and X. Xu, "Monolayer semiconductor nanocavity lasers with ultralow thresholds," Nature **520**(7545), 69–72 (2015).
[372]S. Yamashita, "Nonlinear optics in carbon nanotube, graphene, and related 2D materials," APL Photonics **4**(3), 034301 (2019).
[373]C. Liu, J. Zheng, Y. Chen, T. Fryett, and A. Majumdar, "Van der Waals materials integrated nanophotonic devices [Invited]," Opt. Mater. Express **9**(2), 384 (2019).
[374]C. Jin, E. Y. Ma, O. Karni, E. C. Regan, F. Wang, and T. F. Heinz, "Ultrafast dynamics in van der Waals heterostructures," Nat. Nanotechnol. **13**(11), 994–1003 (2018).
[375]C. Trovatello, F. Katsch, N. J. Borys, M. Selig, K. Yao, R. Borrego-Varillas, F. Scotognella, I. Kriegel, A. Yan, A. Zettl, P. J. Schuck, A. Knorr, G. Cerullo, and S. D. Conte, "The ultrafast onset of exciton formation in 2D semiconductors," Nat. Commun. **11**(1), 5277 (2020).
[376]M. G. Burdanova, R. J. Kashtiban, Y. Zheng, R. Xiang, S. Chiashi, J. M. Woolley, M. Staniforth, E. Sakamoto-Rablah, X. Xie, M. Broome, J. Sloan, A. Anisimov, E. I. Kauppinen, S. Maruyama, and J. Lloyd-Hughes, "Ultrafast optoelectronic processes in 1D radial van der Waals heterostructures: Carbon, boron nitride, and MoS_2 nanotubes with coexisting excitons and highly mobile charges," Nano Lett. **20**(5), 3560–3567 (2020).
[377]C. Trovatello, H. P. C. Miranda, A. Molina-Sánchez, R. Borrego-Varillas, C. Manzoni, L. Moretti, L. Ganzer, M. Maiuri, J. Wang, D. Dumcenco, A. Kis, L. Wirtz, A. Marini, G. Soavi, A. C. Ferrari, G. Cerullo, D. Sangalli, and S. D. Conte, "Strongly coupled coherent phonons in single-layer MoS_2," ACS Nano **14**(5), 5700–5710 (2020).
[378]V. Smejkal, F. Libisch, A. Molina-Sanchez, C. Trovatello, L. Wirtz, and A. Marini, "Time-dependent screening explains the ultrafast excitonic signal rise in 2D semiconductors," ACS Nano **15**(1), 1179–1185 (2021).
[379]C. Trovatello, A. Marini, X. Xu, C. Lee, F. Liu, N. Curreli, C. Manzoni, S. D. Conte, K. Yao, A. Ciattoni, J. Hone, X. Zhu, P. J. Schuck, and G. Cerullo, "Optical parametric amplification by monolayer transition metal dichalcogenides," Nat. Photonics **15**(1), 6–10 (2020).
[380]E. A. A. Pogna, X. Jia, A. Principi, A. Block, L. Banszerus, J. Zhang, X. Liu, T. Sohier, S. Forti, K. Soundarapandian, B. Terrés, J. D. Mehew, C. Trovatello, C. Coletti, F. H. L. Koppens, M. Bonn, H. I. Wang, N. van Hulst, M. J. Verstraete, H. Peng, Z. Liu, C. Stampfer, G. Cerullo, and K.-J. Tielrooij, "Hot-carrier cooling in high-quality graphene is intrinsically limited by optical phonons," ACS Nano **15**(7), 11285–11295 (2021).
[381]X. Xu, C. Trovatello, F. Mooshammer, Y. Shao, S. Zhang, K. Yao, D. N. Basov, G. Cerullo, and P. J. Schuck, "Towards compact phase-matched and waveguided nonlinear optics in atomically layered semiconductors," Nat. Photonics **16**(10), 698–706 (2022).
[382]K. Nozaki, T. Tanabe, A. Shinya, S. Matsuo, T. Sato, H. Taniyama, and M. Notomi, "Sub-femtojoule all-optical switching using a photonic-crystal nanocavity," Nat. Photonics **4**(7), 477–483 (2010).
[383]J. Wang and W. J. Blau, "Inorganic and hybrid nanostructures for optical limiting," J. Opt. A **11**(2), 024001 (2009).
[384]P. Yin, X. Jiang, R. Huang, X. Wang, Y. Ge, C. Ma, and H. Zhang, "2D materials for nonlinear photonics and electro-optical applications," Adv. Mater. Interfaces **8**(14), 2100367 (2021).
[385]S. Yu, X. Wu, Y. Wang, X. Guo, and L. Tong, "2D materials for optical modulation: Challenges and opportunities," Adv. Mater. **29**(14), 1606128 (2017).
[386]A. V. Zasedatelev, A. V. Baranikov, D. Sannikov, D. Urbonas, F. Scafirimuto, V. Y. Shishkov, E. S. Andrianov, Y. E. Lozovik, U. Scherf, T. Stöferle, R. F. Mahrt, and P. G. Lagoudakis, "Single-photon nonlinearity at room temperature," Nature **597**(7877), 493–497 (2021).
[387]M. Burla, C. Hoessbacher, W. Heni, C. Haffner, Y. Fedoryshyn, D. Werner, T. Watanabe, H. Massler, D. L. Elder, L. R. Dalton, and J. Leuthold, "500 GHz plasmonic Mach-Zehnder modulator enabling sub-THz microwave photonics," APL Photonics **4**(5), 056106 (2019).
[388]Y. Salamin, I.-C. Benea-Chelmus, Y. Fedoryshyn, W. Heni, D. L. Elder, L. R. Dalton, J. Faist, and J. Leuthold, "Compact and ultra-efficient broadband plasmonic terahertz field detector," Nat. Commun. **10**(1), 5550 (2019).
[389]S. M. Koepfli, M. Eppenberger, M. S.-B. Hossain, M. Baumann, M. Doderer, M. Destraz, P. Habegger, E. De Leo, W. Heni, C. Hoessbacher, B. Baeuerle, Y. Fedoryshyn, and J. Leuthold, ">500 GHz bandwidth graphene photodetector enabling highest-capacity plasmonic-to-plasmonic links," in European Conference on Optical Communication, Th3B.5, 2022.
[390]N. Flöry, P. Ma, Y. Salamin, A. Emboras, T. Taniguchi, K. Watanabe, J. Leuthold, and L. Novotny, "Waveguide-integrated van der Waals heterostructure photodetector at telecom wavelengths with high speed and high responsivity," Nat. Nanotechnol. **15**(2), 118–124 (2020).
[391]Y. Ding, Z. Cheng, X. Zhu, K. Yvind, J. Dong, M. Galili, H. Hu, N. A. Mortensen, S. Xiao, and L. K. Oxenløwe, "Ultra-compact integrated graphene plasmonic photodetector with bandwidth above 110 GHz," Nanophotonics **9**(2), 317–325 (2020).
[392]S. Marconi, M. A. Giambra, A. Montanaro, V. Mišeikis, S. Soresi, S. Tirelli, P. Galli, F. Buchali, W. Templ, C. Coletti, V. Sorianello, and M. Romagnoli, "Photo thermal effect graphene detector featuring 105 Gbit s−1 NRZ and 120 Gbit s−1 PAM4 direct detection," Nat. Commun. **12**(1), 806 (2021).
[393]S. Cakmakyapan, P. K. Lu, A. Navabi, and M. Jarrahi, "Gold-patched graphene nano-stripes for high-responsivity and ultrafast photodetection from the visible to infrared regime," Light **7**(1), 20 (2018).
[394]P. Ma, Y. Salamin, B. Baeuerle, A. Josten, W. Heni, A. Emboras, and J. Leuthold, "Plasmonically enhanced graphene photodetector featuring 100 Gbit/s data reception, high responsivity, and compact size," ACS Photonics **6**(1), 154–161 (2019).
[395]S. Klimmer, O. Ghaebi, Z. Gan, A. George, A. Turchanin, G. Cerullo, and G. Soavi, "All-optical polarization and amplitude modulation of second-harmonic generation in atomically thin semiconductors," Nat. Photonics **15**(11), 837–842 (2021).
[396]T. Goswami, R. Rani, K. S. Hazra, and H. N. Ghosh, "Ultrafast carrier dynamics of the exciton and trion in MoS_2 monolayers followed by dissociation dynamics in Au@ MoS_2 2D heterointerfaces," J. Phys. Chem. Lett. **10**(11), 3057–3063 (2019).
[397]V. Krivenkov, P. Samokhvalov, I. S. Vasil'evskii, N. I. Kargin, and I. Nabiev, "Plasmon–exciton interaction strongly increases the efficiency of a quantum dot-based near-infrared photodetector operating in the two-photon absorption mode under normal conditions," Nanoscale **13**(47), 19929–19935 (2021).
[398]A. Genco and G. Cerullo, "Optical nonlinearity goes ultrafast in 2D semiconductor-based nanocavities," Light Sci. Appl. **11**, 127 (2022).
[399]H. Sun, J. Zhang, Y. Tang, H. Liu, J. Yang, and X. Zheng, "Ultrafast all-optical switching of dual-band plasmon-induced transparency in terahertz metamaterials," Chin. Opt. Lett. **20**(1), 013701 (2022).

[400]Y. Ding, C. Wei, H. Su, S. Sun, Z. Tang, Z. Wang, G. Li, D. Liu, S. Gwo, J. Dai, and J. Shi, "Second harmonic generation covering the entire visible range from a 2D material–plasmon hybrid metasurface," Adv. Opt. Mater. **9**(16), 2100625 (2021).
[401]G. Hajisalem, M. S. Shariatdoust, R. F. Ali, B. D. Gates, P. E. Barclay, and R. Gordon, "Single nanoflake hexagonal boron nitride harmonic generation with ultralow pump power," ACS Photonics **8**(7), 1922–1926 (2021).
[402]A. R. Echarri, J. D. Cox, R. Yu, and F. J. G. de Abajo, "Enhancement of nonlinear optical phenomena by localized resonances," ACS Photonics **5**(4), 1521–1527 (2018).
[403]X. Han, K. Wang, P. D. Persaud, X. Xing, W. Liu, H. Long, F. Li, B. Wang, M. R. Singh, and P. Lu, "Harmonic resonance enhanced second-harmonic generation in the monolayer WS_2-Ag nanocavity," ACS Photonics **7**(3), 562–568 (2020).
[404]S. Ren, Z. Chen, S. Li, S. Wang, Z. Zhao, Y. Zhao, R. Hu, J. Qu, and L. Liu, "Resonance-enhanced second harmonic generation via quantum dots integrated with Ag nanoarrays," Opt. Mater. Express **11**(9), 3223 (2021).
[405]Z. Wang, Z. Dong, H. Zhu, L. Jin, M.-H. Chiu, L.-J. Li, Q.-H. Xu, G. Eda, S. A. Maier, A. T. S. Wee, C.-W. Qiu, and J. K. W. Yang, "Selectively plasmon-enhanced second-harmonic generation from monolayer tungsten diselenide on flexible substrates," ACS Nano **12**(2), 1859–1867 (2018).
[406]D. Wang, N. Luo, W. Duan, and X. Zou, "High-temperature excitonic bose–einstein condensate in centrosymmetric two-dimensional semiconductors," J. Phys. Chem. Lett. **12**(23), 5479–5485 (2021).
[407]J. Zhao, R. Su, A. Fieramosca, W. Zhao, W. Du, X. Liu, C. Diederichs, D. Sanvitto, T. C. H. Liew, and Q. Xiong, "Ultralow threshold polariton condensate in a monolayer semiconductor microcavity at room temperature," Nano Lett. **21**(7), 3331–3339 (2021).
[408]A. Chernikov, T. C. Berkelbach, H. M. Hill, A. Rigosi, Y. Li, B. Aslan, D. R. Reichman, M. S. Hybertsen, and T. F. Heinz, "Exciton binding energy and nonhydrogenic rydberg series in monolayer WS_2," Phys. Rev. Lett. **113**(7), 076802 (2014).
[409]X. Gan, Y. Gao, K. F. Mak, X. Yao, R.-J. Shiue, A. van der Zande, M. E. Trusheim, F. Hatami, T. F. Heinz, J. Hone, and D. Englund, "Controlling the spontaneous emission rate of monolayer MoS_2 in a photonic crystal nanocavity," Appl. Phys. Lett. **103**(18), 181119 (2013).
[410]H. Shan, Z. Liu, X. Wang, F. Lin, Z. Liu, B. Shen, J. Lou, X. Zhu, P. M. Ajayan, and Z. Fang, "Spontaneous emission of plasmon-exciton polaritons revealed by ultrafast nonradiative decays," Laser Photonics Rev. **14**(12), 2000233 (2020).
[411]M. Klein, B. H. Badada, R. Binder, A. Alfrey, M. McKie, M. R. Koehler, D. G. Mandrus, T. Taniguchi, K. Watanabe, B. J. LeRoy, and J. R. Schaibley, "2D semiconductor nonlinear plasmonic modulators," Nat. Commun. **10**(1), 3264 (2019).
[412]M. Klein, R. Binder, M. R. Koehler, D. G. Mandrus, T. Taniguchi, K. Watanabe, and J. R. Schaibley, "Slow light in a 2D semiconductor plasmonic structure," Nat. Commun. **13**(1), 6216 (2022).
[413]T. Yang, I. Abdelwahab, H. Lin, Y. Bao, S. J. Rong Tan, S. Fraser, K. P. Loh, and B. Jia, "Anisotropic third-order nonlinearity in pristine and lithium hydride intercalated black phosphorus," ACS Photonics **5**(12), 4969–4977 (2018).
[414]J. W. You, S. R. Bongu, Q. Bao, and N. C. Panoiu, "Nonlinear optical properties and applications of 2D materials: Theoretical and experimental aspects," Nanophotonics **8**(1), 63–97 (2018).
[415]G. Scuri, Y. Zhou, A. A. High, D. S. Wild, C. Shu, K. De Greve, L. A. Jauregui, T. Taniguchi, K. Watanabe, P. Kim, M. D. Lukin, and H. Park, "Large excitonic reflectivity of monolayer $MoSe_2$ encapsulated in hexagonal boron nitride," Phys. Rev. Lett. **120**(3), 037402 (2018).
[416]S. Schönenberger, T. Stöferle, N. Moll, R. F. Mahrt, M. S. Dahlem, T. Wahlbrink, J. Bolten, T. Mollenhauer, H. Kurz, and B. J. Offrein, "Ultrafast all-optical modulator with femtojoule absorbed switching energy in silicon-on-insulator," Opt. Express **18**(21), 22485 (2010).
[417]Y. Tang, Y. Zhang, Q. Liu, K. Wei, X. Cheng, L. Shi, and T. Jiang, "Interacting plexcitons for designed ultrafast optical nonlinearity in a monolayer semiconductor," Light Sci. Appl. **11**, 94 (2022).
[418]M. P. Nielsen and A. Y. Elezzabi, "Ultrafast all-optical modulation in a silicon nanoplasmonic resonator," Opt. Express **21**(17), 20274 (2013).
[419]A. D. Neira, G. A. Wurtz, P. Ginzburg, and A. V. Zayats, "Ultrafast all-optical modulation with hyperbolic metamaterial integrated in Si photonic circuitry," Opt. Express **22**(9), 10987 (2014).
[420]M. Ono, M. Hata, M. Tsunekawa, K. Nozaki, H. Sumikura, and M. Notomi, "Ultrafast and energy-efficient all-optical modulator based on deep-subwavelength graphene-loaded plasmonic waveguides," in Conference on Lasers and Electro-Optics (CLEO), 2018.
[421]H. Shan, Y. Yu, X. Wang, Y. Luo, S. Zu, B. Du, T. Han, B. Li, Y. Li, J. Wu, F. Lin, K. Shi, B. K. Tay, Z. Liu, X. Zhu, and Z. Fang, "Direct observation of ultrafast plasmonic hot electron transfer in the strong coupling regime," Light: Sci. Appl. **8**, 9 (2019).
[422]X. Wen, W. Xu, W. Zhao, J. B. Khurgin, and Q. Xiong, "Plasmonic hot carriers-controlled second harmonic generation in WSe_2 bilayers," Nano Lett. **18**(3), 1686–1692 (2018).
[423]A. Y. Bykov, D. J. Roth, G. Sartorello, J. U. Salmón-Gamboa, and A. V. Zayats, "Dynamics of hot carriers in plasmonic heterostructures," Nanophotonics **10**(11), 2929–2938 (2021).
[424]M. Rahaman, M. A. Aslam, L. He, T. I. Madeira, and D. R. T. Zahn, "Plasmonic hot electron induced layer dependent anomalous Fröhlich interaction in InSe," Commun. Phys. **4**(1), 172 (2021).
[425]A. Kumar, P. Choudhary, K. Kumar, A. Kumar, and V. Krishnan, "Plasmon induced hot electron generation in two dimensional carbonaceous nanosheets decorated with Au nanostars: Enhanced photocatalytic activity under visible light," Mater. Chem. Front. **5**(3), 1448–1467 (2021).
[426]U. Sharma, S. Karazhanov, R. Jose, and S. Das, "Plasmonic hot-electron assisted phase transformation in 2D-MoS_2 for the hydrogen evolution reaction: Current status and future prospects," J. Mater. Chem. A **10**(16), 8626–8655 (2022).
[427]Y.-H. Chen, R. Tamming, K. Chen, Z. Zhang, F. Liu, Y. Zhang, J. Hodgkiss, R. Blaikie, B. Ding, and M. Qiu, "Bandgap control in two-dimensional semiconductors via coherent doping of plasmonic hot electrons," Nat. Commun. **12**, 4332 (2021).
[428]Y. Kang, S. Najmaei, Z. Liu, Y. Bao, Y. Wang, X. Zhu, N. J. Halas, P. Nordlander, P. M. Ajayan, J. Lou, and Z. Fang, "Plasmonic hot electron induced structural phase transition in a MoS_2 monolayer," Adv. Mater. **26**(37), 6467–6471 (2014).
[429]A. G. Milekhin, M. Rahaman, E. E. Rodyakina, A. V. Latyshev, V. M. Dzhagan, and D. R. T. Zahn, "Giant gap-plasmon tip-enhanced Raman scattering of MoS_2 monolayers on Au nanocluster arrays," Nanoscale **10**(6), 2755–2763 (2018).
[430]H. Yu, D. Talukdar, W. Xu, J. B. Khurgin, and Q. Xiong, "Charge-induced second-harmonic generation in bilayer WSe_2," Nano Lett. **15**(8), 5653–5657 (2015).
[431]M. Krüger, M. Schenk, and P. Hommelhoff, "Attosecond control of electrons emitted from a nanoscale metal tip," Nature **475**(7354), 78–81 (2011).
[432]F. Süßmann, L. Seiffert, S. Zherebtsov, V. Mondes, J. Stierle, M. Arbeiter, J. Plenge, P. Rupp, C. Peltz, A. Kessel, S. A. Trushin, B. Ahn, D. Kim, C. Graf, E. Rühl, M. F. Kling, and T. Fennel, "Field propagation-induced directionality of carrier-envelope phase-controlled photoemission from nanospheres," Nat. Commun. **6**(1), 7944 (2015).
[433]H. Y. Kim, M. Garg, S. Mandal, L. Seiffert, T. Fennel, and E. Goulielmakis, "Attosecond field emission," Nature **613**(7945), 662–666 (2023).
[434]T. Fennel, T. Döppner, J. Passig, C. Schaal, J. Tiggesbäumker, and K.-H. Meiwes-Broer, "Plasmon-enhanced electron acceleration in intense laser metal-cluster interactions," Phys. Rev. Lett. **98**(14), 143401 (2007).
[435]P. Dombi, S. E. Irvine, P. Rácz, M. Lenner, N. Kroó, G. Farkas, A. Mitrofanov, A. Baltuška, T. Fuji, F. Krausz, and A. Y. Elezzabi, "Observation of few-cycle, strong-field phenomena in surface plasmon fields," Opt. Express **18**(23), 24206 (2010).
[436]M. F. Ciappina, J. A. Pérez-Hernández, A. S. Landsman, W. A. Okell, S. Zherebtsov, B. Förg, J. Schötz, L. Seiffert, T. Fennel, T. Shaaran, T. Zimmermann, A. Chacón, R. Guichard, A. Zaïr, J. W. G. Tisch, J. P. Marangos, T. Witting, A. Braun, S. A. Maier, L. Roso, M. Krüger, P. Hommelhoff, M. F. Kling, F. Krausz, and M. Lewenstein, "Attosecond physics at the nanoscale," Rep. Prog. Phys. **80**(5), 054401 (2017).
[437]J. Hoffrogge, J. Paul Stein, M. Krüger, M. Förster, J. Hammer, D. Ehberger, P. Baum, and P. Hommelhoff, "Tip-based source of femtosecond electron pulses at 30 keV," J. Appl. Phys. **115**(9), 094506 (2014).

[438]Q. Liu, L. Seiffert, F. Süßmann, S. Zherebtsov, J. Passig, A. Kessel, S. A. Trushin, N. G. Kling, I. Ben-Itzhak, V. Mondes, C. Graf, E. Rühl, L. Veisz, S. Karsch, J. Rodríguez-Fernández, M. I. Stockman, J. Tiggesbäumker, K.-H. Meiwes-Broer, T. Fennel, and M. F. Kling, "Ionization-induced subcycle metallization of nanoparticles in few-cycle pulses," ACS Photonics **7**(11), 3207–3215 (2020).
[439]L. Veisz, "Contrast improvement of relativistic few-cycle light pulses" in *Coherence and Ultrashort Pulse Laser Emission*, edited by F. J. Duarte (InTech, 2010).
[440]L. Veisz "Optical parametric chirped-pulse amplification," in *Handbook of Laser Technology and Applications*, 2nd ed., edited by C. Guo (CRC Press, Taylor and Francis Group, 2020), ISBN: 978-1-138-19657-5.
[441]S. Sakabe, S. Shimizu, M. Hashida, F. Sato, T. Tsuyukushi, K. Nishihara, S. Okihara, T. Kagawa, Y. Izawa, K. Imasaki, and T. Iida, "Generation of high-energy protons from the Coulomb explosion of hydrogen clusters by intense femtosecond laser pulses," Phys. Rev. A **69**(2), 023203 (2004).
[442]T. Ditmire, J. W. G. Tisch, E. Springate, M. B. Mason, N. Hay, R. A. Smith, J. Marangos, and M. H. R. Hutchinson, "High-energy ions produced in explosions of superheated atomic clusters," Nature **386**(6620), 54–56 (1997).
[443]T. Ditmire, J. Zweiback, V. P. Yanovsky, T. E. Cowan, G. Hays, and K. B. Wharton, "Nuclear fusion from explosions of femtosecond laser-heated deuterium clusters," Nature **398**(6727), 489–492 (1999).
[444]X. Lavocat-Dubuis and J.-P. Matte, "Numerical simulation of harmonic generation by relativistic laser interaction with a grating," Phys. Rev. E **80**(5), 055401 (2009).
[445]M. Cerchez, A. L. Giesecke, C. Peth, M. Toncian, B. Albertazzi, J. Fuchs, O. Willi, and T. Toncian, "Generation of laser-driven higher harmonics from grating targets," Phys. Rev. Lett. **110**(6), 065003 (2013).
[446]L. Fedeli, A. Sgattoni, G. Cantono, D. Garzella, F. Réau, I. Prencipe, M. Passoni, M. Raynaud, M. Květoň, J. Proska, A. Macchi, and T. Ceccotti, "Electron acceleration by relativistic surface plasmons in laser-grating interaction," Phys. Rev. Lett. **116**(1), 015001 (2016).
[447]T. Ceccotti, V. Floquet, A. Sgattoni, A. Bigongiari, O. Klimo, M. Raynaud, C. Riconda, A. Heron, F. Baffigi, L. Labate, L. A. Gizzi, L. Vassura, J. Fuchs, M. Passoni, M. Květon, F. Novotny, M. Possolt, J. Prokůpek, J. Proška, J. Pšikal, L. Štolcová, A. Velyhan, M. Bougeard, P. D'Oliveira, O. Tcherbakoff, F. Réau, P. Martin, and A. Macchi, "Evidence of resonant surface-wave excitation in the relativistic regime through measurements of proton acceleration from grating targets," Phys. Rev. Lett. **111**(18), 185001 (2013).
[448]M. A. Purvis, V. N. Shlyaptsev, R. Hollinger, C. Bargsten, A. Pukhov, A. Prieto, Y. Wang, B. M. Luther, L. Yin, S. Wang, and J. J. Rocca, "Relativistic plasma nanophotonics for ultrahigh energy density physics," Nat. Photonics **7**(10), 796–800 (2013).
[449]A. Curtis, C. Calvi, J. Tinsley, R. Hollinger, V. Kaymak, A. Pukhov, S. Wang, A. Rockwood, Y. Wang, V. N. Shlyaptsev, and J. J. Rocca, "Micro-scale fusion in dense relativistic nanowire array plasmas," Nat. Commun. **9**(1), 1077 (2018).
[450]A. Curtis, R. Hollinger, C. Calvi, S. Wang, S. Huanyu, Y. Wang, A. Pukhov, V. Kaymak, C. Baumann, J. Tinsley, V. N. Shlyaptsev, and J. J. Rocca, "Ion acceleration and D-D fusion neutron generation in relativistically transparent deuterated nanowire arrays," Phys. Rev. Res. **3**(4), 043181 (2021).
[451]K. I. Popov, V. Yu. Bychenkov, W. Rozmus, R. D. Sydora, and S. S. Bulanov, "Vacuum electron acceleration by tightly focused laser pulses with nanoscale targets," Phys. Plasmas **16**(5), 053106 (2009).
[452]T. V. Liseykina, S. Pirner, and D. Bauer, "Relativistic attosecond electron bunches from laser-illuminated droplets," Phys. Rev. Lett. **104**(9), 095002 (2010).
[453]L. Di Lucchio and P. Gibbon, "Relativistic attosecond electron bunch emission from few-cycle laser irradiated nanoscale droplets," Phys. Rev. Spec. Top.-Accel. Beams **18**(2), 023402 (2015).
[454]D. E. Cardenas, T. M. Ostermayr, L. Di Lucchio, L. Hofmann, M. F. Kling, P. Gibbon, J. Schreiber, and L. Veisz, "Sub-cycle dynamics in relativistic nanoplasma acceleration," Sci. Rep. **9**(1), 7321 (2019).
[455]V. Horný and L. Veisz, "Generation of single attosecond relativistic electron bunch from intense laser interaction with a nanosphere," Plasma Phys. Controlled Fusion **63**(12), 125025 (2021).
[456]L. Di Lucchio, A. A. Andreev, and P. Gibbon, "Ion acceleration by intense, few-cycle laser pulses with nanodroplets," Phys. Plasmas **22**(5), 053114 (2015).
[457]A. Feist, G. Huang, G. Arend, Y. Yang, J.-W. Henke, A. S. Raja, F. J. Kappert, R. N. Wang, H. Lourenço-Martins, Z. Qiu, J. Liu, O. Kfir, T. J. Kippenberg, and C. Ropers, "Cavity-mediated electron-photon pairs," Science **377**(6607), 777–780 (2022).
[458]E. Cortés, F. J. Wendisch, L. Sortino, A. Mancini, S. Ezendam, S. Saris, L. de S. Menezes, A. Tittl, H. Ren, and S. A. Maier, "Optical metasurfaces for energy conversion," Chem. Rev. **122**(19), 15082–15176 (2022).
[459]J. A. Scholl, A. L. Koh, and J. A. Dionne, "Quantum plasmon resonances of individual metallic nanoparticles," Nature **483**(7390), 421–427 (2012).
[460]A. Rosławska, P. Merino, A. Grewal, C. C. Leon, K. Kuhnke, and K. Kern, "Atomic-Scale Structural Fluctuations of a Plasmonic Cavity," Nano Lett. **21**(17), 7221–7227 (2021).
[461]A. Emboras, J. Niegemann, P. Ma, C. Haffner, A. Pedersen, M. Luisier, C. Hafner, T. Schimmel, and J. Leuthold, "Atomic scale plasmonic switch," Nano Lett. **16**(1), 709–714 (2016).
[462]W. Zhu, R. Esteban, A. G. Borisov, J. J. Baumberg, P. Nordlander, H. J. Lezec, J. Aizpurua, and K. B. Crozier, "Quantum mechanical effects in plasmonic structures with subnanometre gaps," Nat. Commun. **7**(1), 11495 (2016).
[463]Y. Dai, Z. Zhou, A. Ghosh, R. S. K. Mong, A. Kubo, C.-B. Huang, and H. Petek, "Plasmonic topological quasiparticle on the nanometre and femtosecond scales," Nature **588**(7839), 616–619 (2020).
[464]J. J. Baumberg, "Picocavities: A Primer," Nano Lett. **22**(14), 5859–5865 (2022).
[465]D. Garoli, D. Mosconi, E. Miele, N. Maccaferri, M. Ardini, G. Giovannini, M. Dipalo, S. Agnoli, and F. De Angelis, "Hybrid plasmonic nanostructures based on controlled integration of MoS_2 flakes on metallic nanoholes," Nanoscale **10**(36), 17105–17111 (2018).
[466]W. Li, J. Zhou, N. Maccaferri, R. Krahne, K. Wang, and D. Garoli, "Enhanced optical spectroscopy for multiplexed DNA and protein-sequencing with plasmonic nanopores: Challenges and prospects," Anal. Chem. **94**(2), 503–514 (2022).